Supporting Information

Table of Contents

1. Experimental Section

1.1 General Method

All the reagents involved in this research were commercially available and used without further purification unless otherwise noted. Solvents were either employed as purchased or dried before use by standard laboratory procedures. Thin-layer chromatography (TLC) was carried out on 0.25 mm Leyan silica gel plates (60F-254). Column chromatography was performed on silica gel (200-300 mesh) as the stationary phase. ^{1}H, ^{13}C NMR, 2D NMR spectra were performed on Bruker Avance-500 NMR spectrometers. Chemical shifts are reported in ppm with residual solvents or TMS (tetramethylsilane) as the internal standards. The following abbreviations were used for signal multiplicities: s, singlet; d, doublet; dd, doublet of doublet; m, multiplet. Host-guest complexes were prepared by simply mixing the guests and hosts in 1: 1 stoichiometry in the corresponding solvent. Electrospray-ionization high-resolution mass spectrometry (ESI-HRMS) experiments were conducted on an applied Q-EXACTIVE mass spectrometry system. Circular Dichroism (CD) spectra were recorded on an Applied PhotoPhysics Chirascan CD spectropolarimeter, using a 1 cm quartz cuvette.

All titration experiments were repeated 3 times, and the averaged values and standard deviations are given.

1.2 Synthetic Procedures of Chiral Naphthotubes

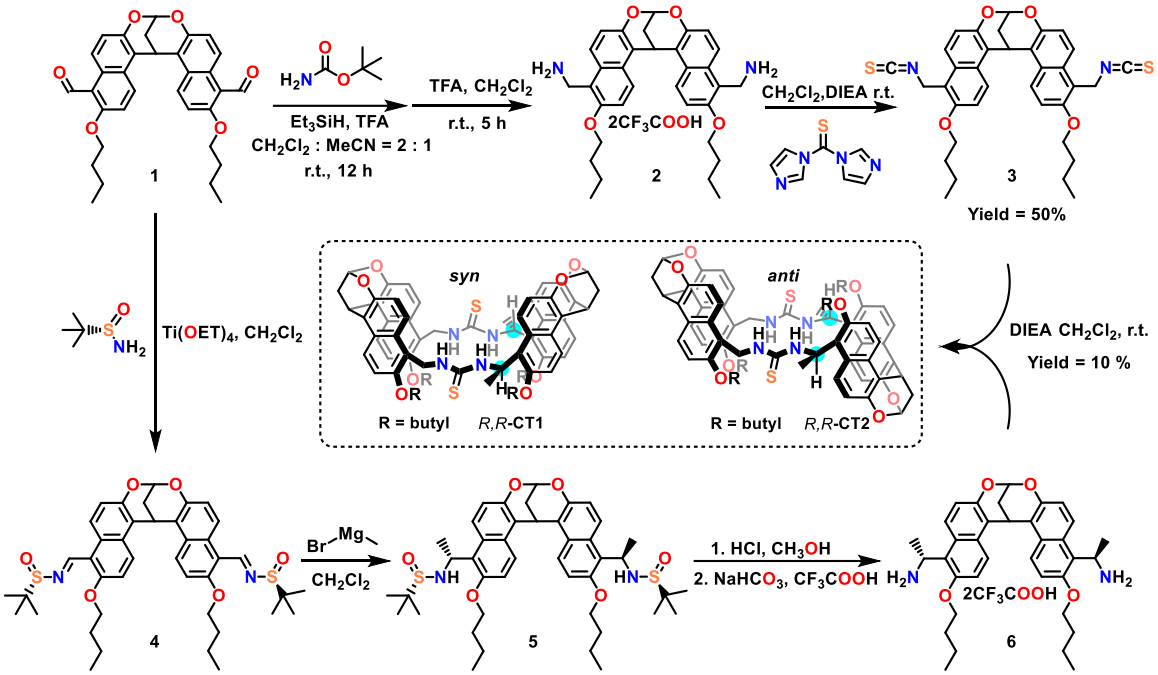

Scheme S1. Synthetic procedures of naphthotubes *R,R*-**CT1** and *R,R*-**CT2**. The other pair of enantiomeric chiral macrocyclic compounds *S,S*-**CT1**, and *S,S*-**CT2** can be synthesized by similar methods.

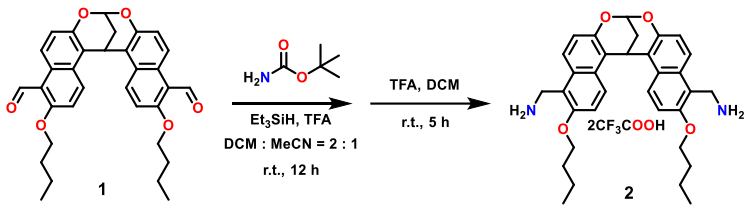

The synthesis of dialdehyde-substituted bis-naphthalene cleft **1** has been reported previously.[1] **1** (5.0 g, 10 mmol, 1.0 equiv.) and *t*-Butyl carbamate (7.03 g, 60 mmol, 7.0 equiv.) were dissolved in the mixture of acetonitrile (60 mL) and dichloromethane (120 mL) in a 1 L two-neck flask under Ar atmosphere. To this solution, triethyl silane (9 mL) and trifluoroacetic acid (7.6 mL) were added through syringes. The resulting mixture was stirred at room temperature for another 12 h. The solvents were removed under reduced pressure. The crude product was dissolved in the mixture of dichloromethane (30 mL) and trifluoroacetic acid (15 mL). The solution was stirred at room temperature for 6 h. The solvents were removed under reduced pressure, and the residue was washed by ether to afford pure **2** as a white powder (6 g, yield 80%).

2: ^{1}H NMR (500 MHz, DMSO-d_6, 298K) δ [ppm] = 8.88 (d, J = 9.6 Hz, 2H), 8.17 (s, 6H), 7.88 (d, J = 9.3 Hz, 2H), 7.54 (d, J = 9.5 Hz, 2H), 7.22 (d, J = 9.2 Hz, 2H), 6.42 (q, J = 1.9 Hz, 1H), 5.70 (d, J = 3.6 Hz, 1H), 4.40 (s, 4H), 4.18 (ddt, J = 27.0, 9.3, 6.5 Hz, 4H), 2.47 (t, J = 2.5 Hz, 2H), 1.80 (dq, J = 9.0, 6.6 Hz, 4H), 1.54-1.47 (m, 4H), 0.98 (t, J = 7.4 Hz, 6H).

^{13}C NMR (126 MHz, DMSO-d_6, 298K) δ [ppm] = 159.03, 153.95, 148.77, 128.83, 126.98, 126.46, 123.46, 120.20, 119.71, 115.36, 114.46, 91.46, 68.97, 33.14, 31.43, 26.58, 22.15, 19.21, 14.28.

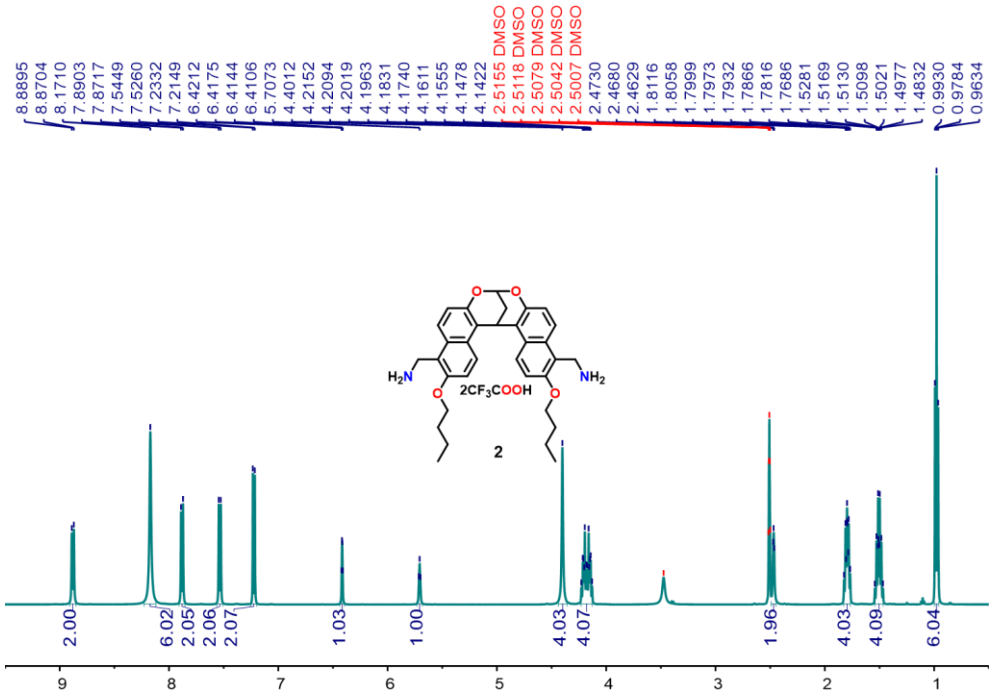

^{1}H NMR spectrum (500 MHz, DMSO-d_6, 298 K) of **2**.

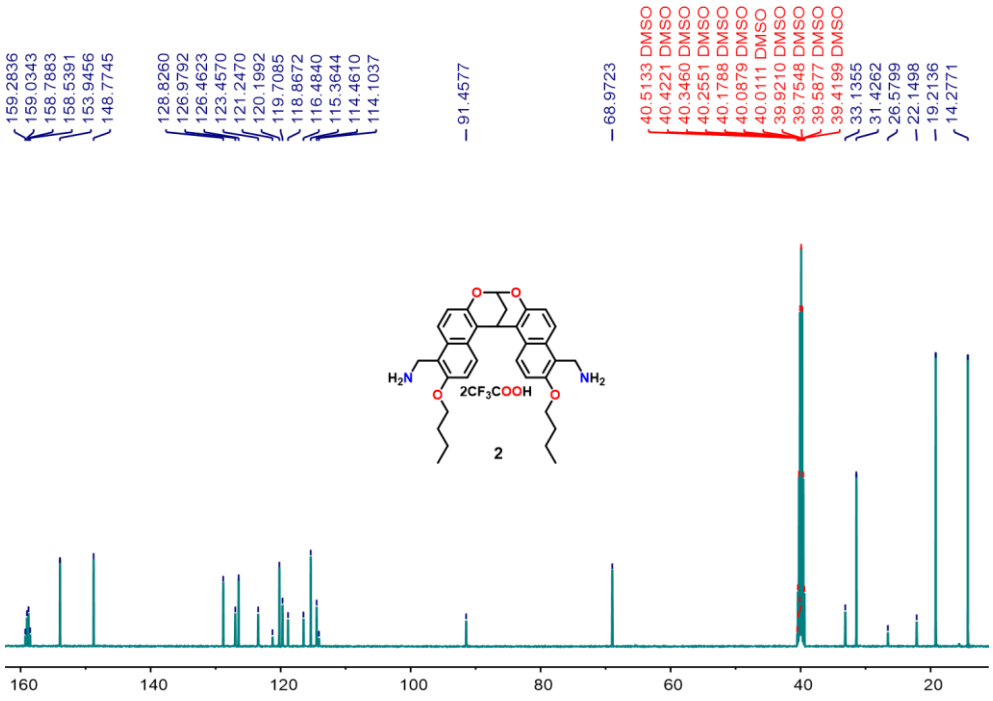

^{13}C NMR spectrum (126 MHz, DMSO-d_6, 298 K) of **2**.

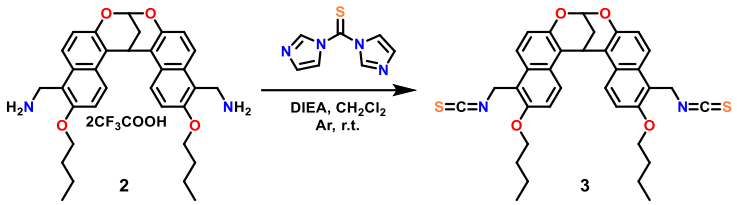

To the solution of 1, 1'-Thiocarbonyldiimidazole (5.2 g, 30 mmol) in CH_2Cl_2 (400 mL), added compound **2** (5.3 g, 10 mmol) and Hünig's base (2.6 g, 20 mmol) were added dropwise during 30 min. The resulting mixture was stirred at room temperature for 3 h. The solvent was removed under vacuum, and the residue was purified by column chromatography (SiO_2, Hexane / CH_2Cl_2 = 1 / 1) to give the compound **3** as a yellow solid (5.6 g, 92 %).

3: ^{1}H NMR (400 MHz, $CDCl_3$, 298K) δ [ppm] = 8.56 (d, *J* = 9.4 Hz, 2H), 7.69 (d, *J* = 9.2 Hz, 2H), 7.34 (d, *J* = 9.4 Hz, 2H), 7.28 (s, 1H), 7.26 (s, 1H), 5.35-5.27 (m, 1H), 5.11-4.92 (m, 4H), 4.14 (qt, *J* = 9.1, 6.5 Hz, 4H), 2.45 (dd, *J* = 3.1, 2.1 Hz, 2H), 1.90-1.78 (m, 4H), 1.54 (ddd, *J* = 9.5, 6.5, 5.1 Hz, 5H), 1.01 (t, *J* = 7.4 Hz, 6H).

^{13}C NMR (126 MHz, $CDCl_3$, 298K) δ 152.91, 148.85, 131.03, 128.72, 126.53, 125.25, 122.67, 120.32, 119.08, 116.03, 114.23, 91.37, 69.30, 39.26, 31.56, 26.87, 22.99, 19.36, 13.93.

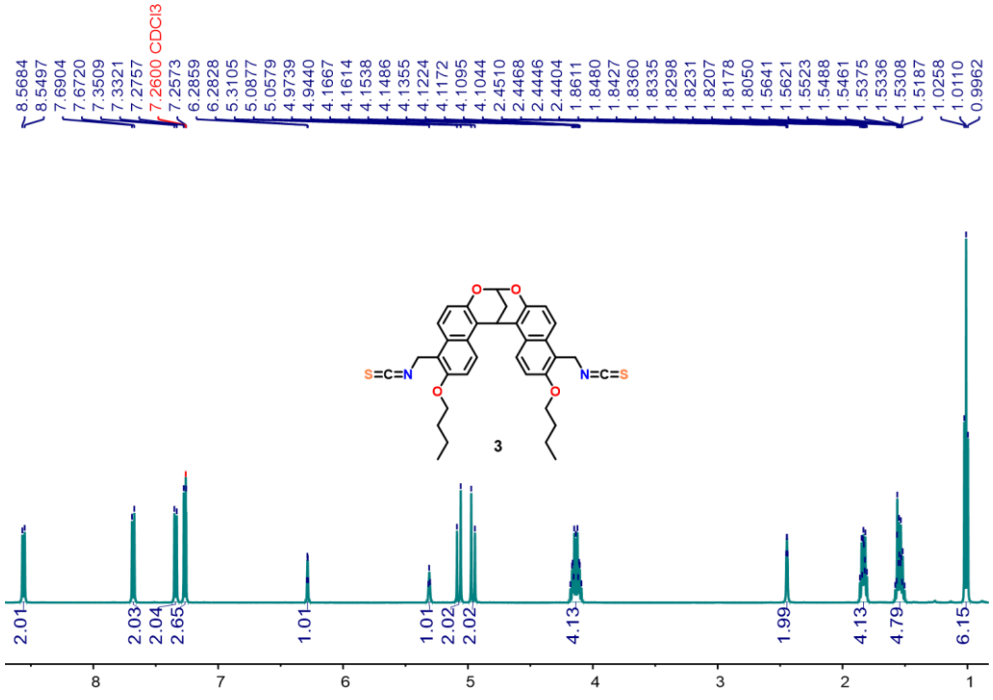

^{1}H NMR spectrum (500 MHz, $CDCl_3$, 298 K) of **3**.

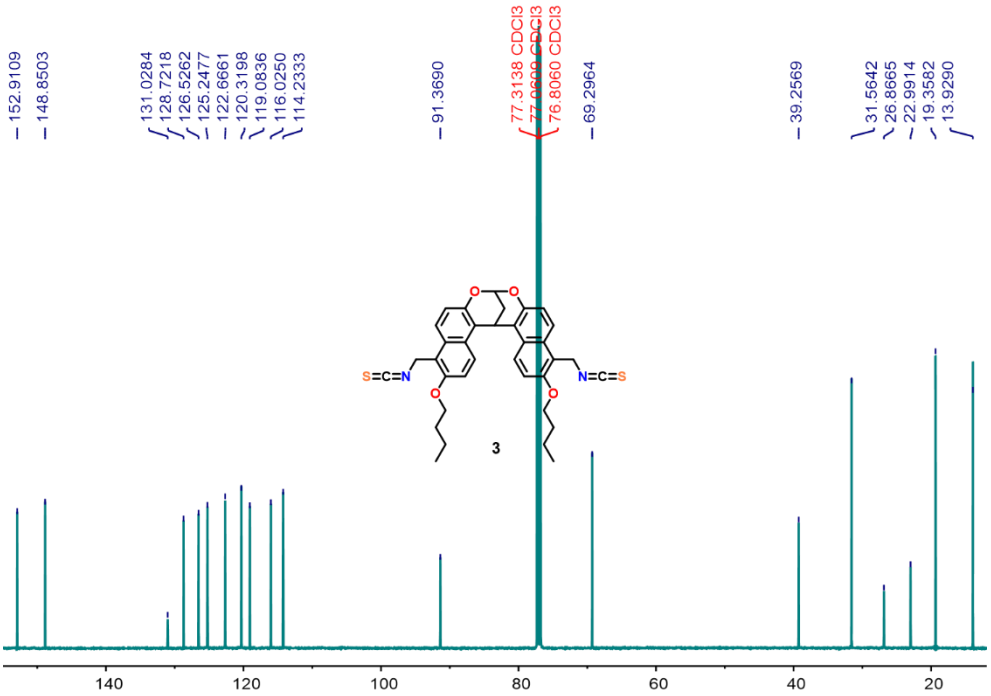

^{13}C NMR spectrum (126 MHz, $CDCl_3$, 298 K) of **3**.

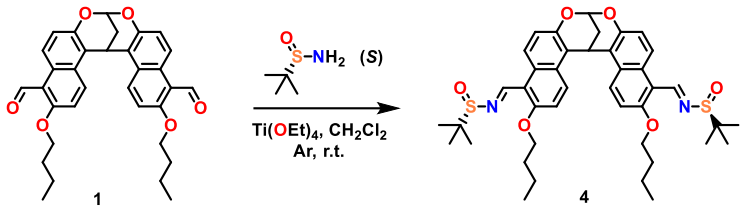

To a solution of **1** (1.05 g, 2 mmol) and *tert*-butanesulfinamide (1.45 g, 12 mmol) in CH_2Cl_2 (dry, 80 mL), titanium ethoxide (2.5 mL, 12 mmol) was added under Ar at 0 °C. After stirring at 0 °C for 1 h, the resulting mixture was warmed to room temperature and stirred for another 12 h. The solution was then poured into ice water. The resulting suspension was extracted with CH_2Cl_2 (100 mL × 3). The combined organic phase was washed consecutively with H_2O (100 mL) and then dried over anhydrous Na_2SO_4. After removing the CH_2Cl_2, the solid was washed with n-hexane and the **4** (1.4 g, yield 97%, yellow solid) was obtained.

4: ^{1}H NMR (500 MHz, $CDCl_3$, 298K) δ[ppm] = 9.40 (d, *J* = 2.7 Hz, 2H), 9.17 (dd, *J* = 17.5, 9.4 Hz, 2H), 8.66 (d, *J* = 9.5 Hz, 2H), 7.36 (dd, *J* = 9.5, 2.8 Hz, 2H), 7.24 (dd, *J* = 9.4, 1.5 Hz, 2H), 6.27 (q, *J* = 1.8 Hz, 1H), 5.30 (d, *J* = 3.2 Hz, 1H), 4.17 (dtq, *J* = 12.7, 6.5, 2.9 Hz, 4H), 2.45 (t, *J* = 2.6 Hz, 2H), 1.87 – 1.81 (m, 4H), 1.55 – 1.49 (m, 4H), 1.28 (s, 6H), 1.21 (d, *J* = 1.8 Hz, 12H), 0.97 (td, *J* = 7.5, 2.4 Hz, 6H).

^{13}C NMR (126 MHz, $CDCl_3$, 298K) δ[ppm] = 160.23, 160.10, 158.27 (d, *J* = 6.3 Hz), 149.07, 128.90 (d, *J* = 6.0 Hz), 128.29, 126.50, 126.39, 125.90 (d, *J* = 12.5 Hz), 120.97

(d, *J* = 1.7 Hz), 118.82, 118.75, 116.18, 114.08 (d, *J* = 5.0 Hz), 91.23, 69.62 (d, *J* = 1.9 Hz), 57.19 (d, *J* = 5.0 Hz), 31.33, 26.96, 23.02, 22.60, 22.50, 22.13, 19.22, 13.86.

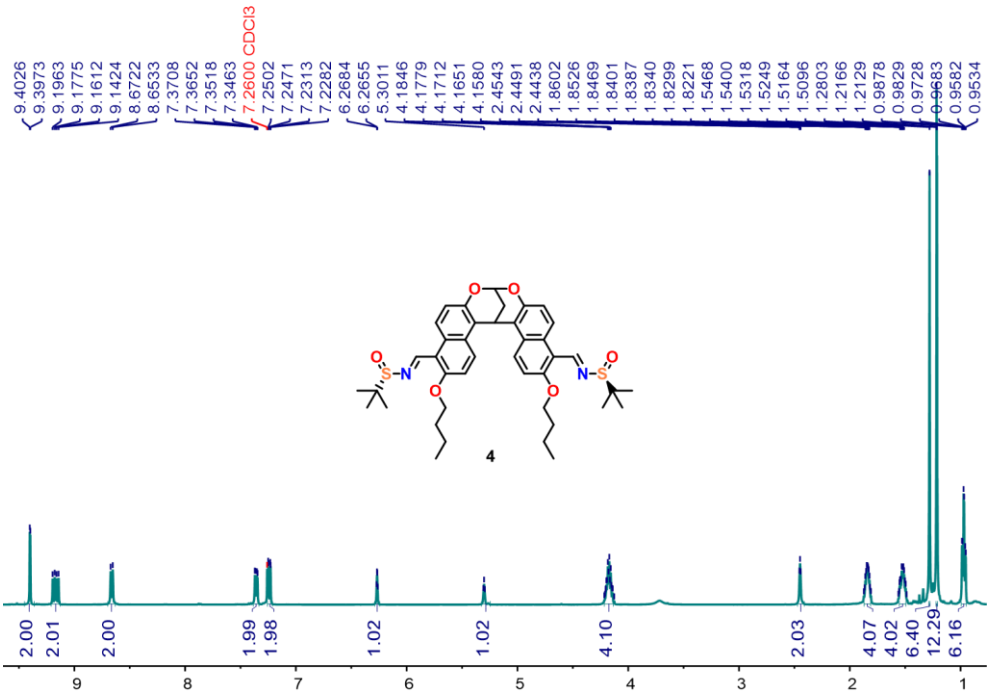

^{1}H NMR spectrum (500 MHz, $CDCl_3$, 298 K) of **4**.

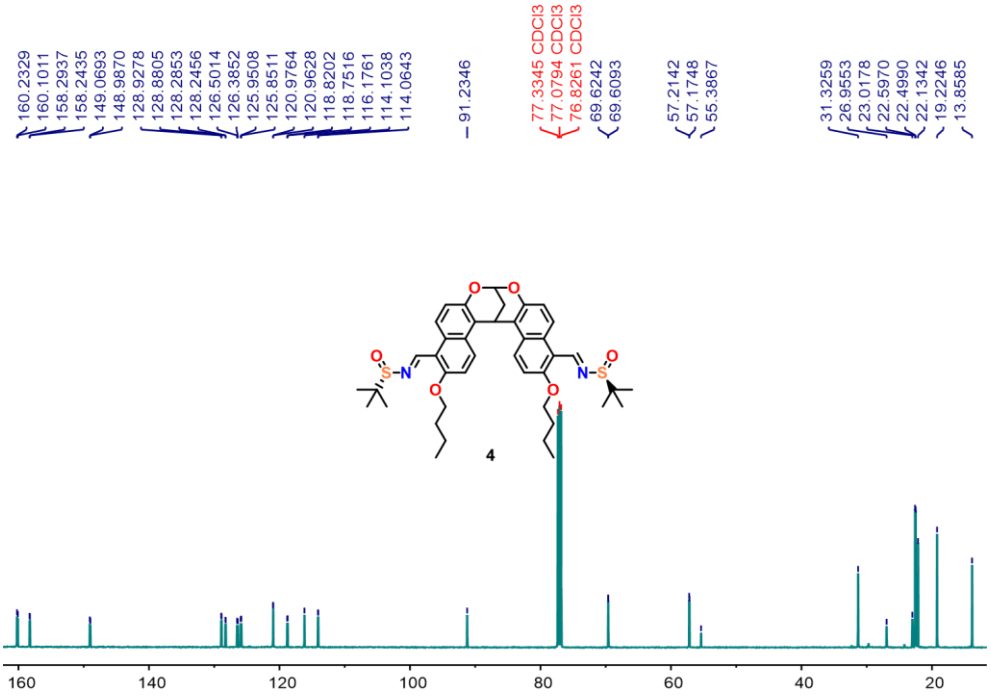

^{13}C NMR spectrum (126 MHz, $CDCl_3$, 298 K) of **4**.

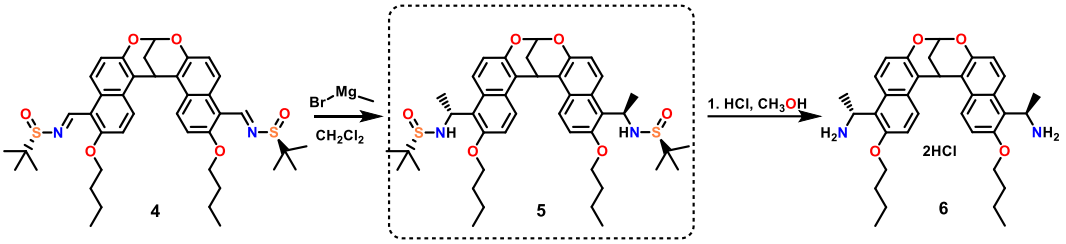

To a solution of **4** (2.92 g, 4 mmol) in dry CH_2Cl_2 (200 mL) at 0°C was added methyl magnesium bromide (40 mL of a 1.0 M THF solution) dropwise under Ar. The reaction mixture was stirred at 0°C for 2 h, the reaction was continued overnight at room temperature. A saturated ammonium chloride solution was added to the reaction mixture after cooling in an ice bath. The reaction mixture was stirred for 30 min, and then the resulting suspension was extracted with CH_2Cl_2 (100 mL × 3). The combined organic phase was washed consecutively with H_2O (100 mL×3) and then dried over anhydrous Na_2SO_4. After removing the CH_2Cl_2, the solid was washed with n-hexane to provide **5** (3.04 g, yield 99%, pale white solid), then **5** was used directly for the next step without further purification. To a solution of **5** (0.97 g, 1.3 mmol) in 20 mL of MeOH was added 0.5 mL (6 mmol) of 12 M HCl solution at room temperature, and the mixture was stirred for 30 min. After removing MeOH, the solid was washed with diethyl ether (20 mL×3), and the **6** (0.64 g, yield 91%, pale white solid) was obtained.

6: ^{1}H NMR (500 MHz, DMSO-d_6, 298K) δ [ppm] = ^{1}H NMR (500 MHz, DMSO-d_6) δ 8.90 – 8.79 (m, 2H), 8.44 (s, 2H), 8.35 (s, 1H), 7.92 (d, *J* = 9.4 Hz, 1H), 7.87 (d, *J* = 9.2 Hz, 1H), 7.53 (dd, *J* = 21.0, 9.5 Hz, 2H), 7.21 (dd, *J* = 9.3, 5.8 Hz, 2H), 6.41 (s, 1H), 5.72 (s, 1H), 5.15 (p, *J* = 6.1 Hz, 1H), 5.12 – 5.06 (m, 1H), 4.25 (t, *J* = 7.0 Hz, 3H), 4.21 – 4.14 (m, 1H), 2.45 (s, 2H), 1.87 – 1.78 (m, 5H), 1.62 (d, *J* = 6.8 Hz, 3H), 1.54 (d, *J* = 6.8 Hz, 3H), 1.46 (tq, *J* = 15.8, 7.9, 7.3 Hz, 6H), 0.97 (q, *J* = 7.4 Hz, 8H).

^{13}C NMR (126 MHz, DMSO-d_6) δ 153.12, 148.73, 148.53, 127.72, 127.63, 126.79, 126.60, 126.36, 122.72 (d, *J* = 30.2 Hz), 120.35, 120.23, 119.59 (dd, *J* = 51.9, 17.6 Hz), 114.75, 91.37, 68.84 (d, *J* = 15.2 Hz), 31.09 (d, *J* = 5.0 Hz), 26.58, 23.28, 22.20, 19.28, 19.12, 18.96, 14.31 (d, *J* = 2.3 Hz).

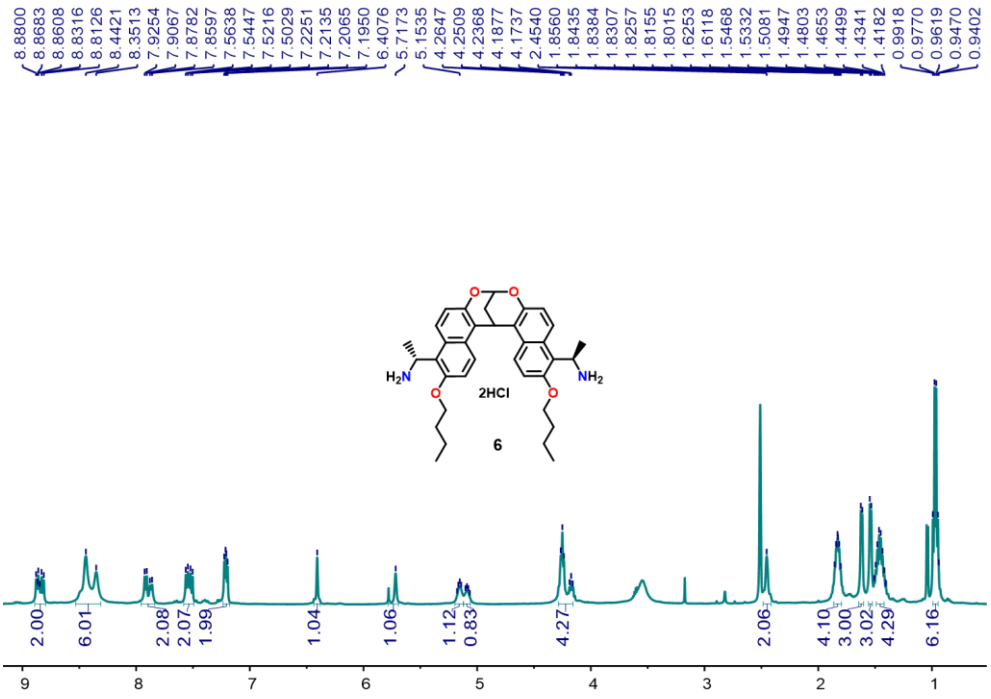

^{1}H NMR spectrum (500 MHz, DMSO-d_6, 298 K) of **6**.

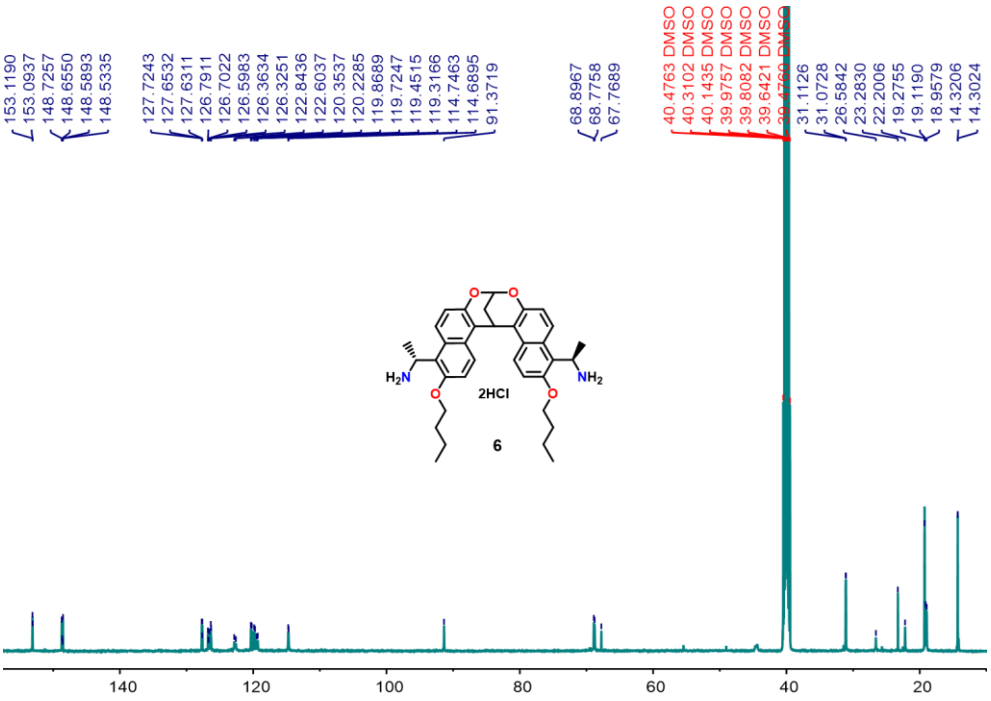

^{13}C NMR spectrum (126 MHz, $CDCl_3$, 298 K) of **6**.

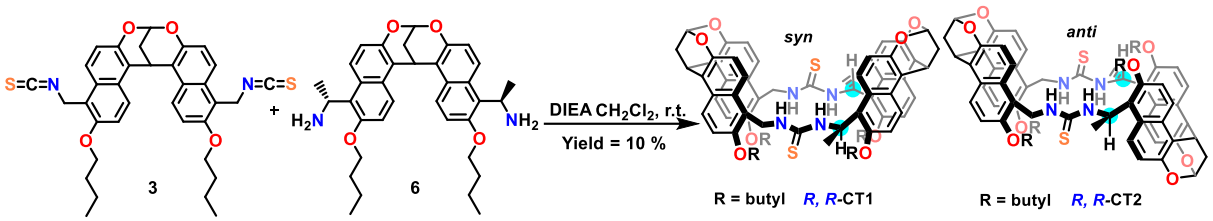

The solutions of compounds **3** (483 mg, 0.92 mmol; in 60 mL CH_2Cl_2) and **6** (560 mg, 0.92 mmol; in 60 mL CH_2Cl_2) in two separate syringes were added dropwise via a double-channel syringe pump to the solution of Hünig's base (545 mg, 5.0 mmol) in CH_2Cl_2 (400 mL) during the course of 10 h. The resulting mixture was stirred at room temperature for 24 h. The solvent was removed in vacuum, and the residue was purified by column chromatography (SiO_2, CH_2Cl_2: MeOH = 1000 / 5) to give the compound *R*,*R*-**CT1** and *R*,*R*-**CT2** as a white solid (54mg, 5.0 %, 55mg, 5.1 %).

R,*R*-**CT1**: ^{1}H NMR (500 MHz, Toluene-d_8, 298 K) δ [ppm] = 8.65 (d, *J* = 9.2 Hz, 1H), 8.39 (d, *J* = 9.3 Hz, 2H), 8.34 (d, *J* = 9.4 Hz, 1H), 8.27 (dd, *J* = 12.3, 9.4 Hz, 2H), 7.74 (d, *J* = 9.3 Hz, 1H), 7.29 (dd, *J* = 9.2, 6.0 Hz, 2H), 7.16 (d, *J* = 9.1 Hz, 2H), 7.13 – 7.10 (m, 2H), 6.98 (d, *J* = 9.1 Hz, 1H), 6.93 (dd, *J* = 9.3, 5.8 Hz, 3H), 6.49 (d, *J* = 8.9 Hz, 2H), 6.20 (dd, *J* = 13.7, 5.8 Hz, 1H), 5.92 – 5.85 (m, 2H), 5.57 (s, 1H), 5.16 (d, *J* = 8.9 Hz, 1H), 4.98 – 4.94 (m, 2H), 4.89 (s, 1H), 4.68 (d, *J* = 14.0 Hz, 1H), 4.49 (d, *J* = 13.6 Hz, 1H), 3.92 – 3.83 (m, 2H), 3.76 – 3.61 (m, 4H), 3.52 (dt, *J* = 9.1, 6.6 Hz, 1H), 3.37 (dt, *J* = 9.0, 6.7 Hz, 1H), 1.99 (ddd, *J* = 12.5, 3.8, 1.8 Hz, 1H), 1.89 – 1.17 (m, 24H), 0.98 (t, *J* = 7.4 Hz, 3H), 0.92 (d, *J* = 7.4 Hz, 3H), 0.85 (t, *J* = 7.4 Hz, 3H), 0.73 (t, *J* = 7.4 Hz, 3H).

^{13}C NMR (126 MHz, Toluene-d_8, 298 K) δ [ppm] = 183.56, 181.47, 153.05, 152.97, 152.59, 151.61, 150.17, 149.95, 148.30, 147.85, 137.12, 129.76, 129.42, 128.70, 128.51, 128.32, 127.89, 127.79, 127.60, 127.41, 126.76, 126.40, 124.96, 124.76, 124.57, 123.96, 123.63, 123.50, 123.42, 121.69, 120.75, 120.49, 120.46, 120.07, 119.78, 118.91, 118.81, 118.24, 117.99, 115.39, 114.53, 113.42, 113.16, 91.33, 91.08, 70.07, 69.30, 68.67, 67.78, 65.55, 48.20, 46.67, 39.12, 39.09, 31.71, 31.59, 31.23, 26.71, 26.24, 23.19, 22.82, 21.03, 20.52, 20.37, 20.21, 20.06, 19.91, 19.76, 19.60, 19.34, 19.26, 19.25, 19.22, 15.19, 13.72, 13.69, 13.61, 13.35.

R,*R*-**CT1**: ^{1}H NMR (500 MHz, DMSO-d_6, 298 K) δ [ppm] = 8.83 (d, *J* = 9.4 Hz, 1H), 8.75 (d, *J* = 9.4 Hz, 1H), 8.42 (d, *J* = 9.5 Hz, 1H), 8.24 (d, *J* = 9.4 Hz, 1H), 7.88 (d, *J* = 9.6 Hz, 1H), 7.71 (d, *J* = 9.3 Hz, 2H), 7.54 (dd, *J* = 9.1, 4.3 Hz, 2H), 7.50 (d, *J* = 9.3 Hz, 2H), 7.20 (d, *J* = 9.2 Hz, 2H), 7.12 (dd, *J* = 8.9, 5.1 Hz, 2H), 7.06 (d, *J* = 9.3 Hz, 2H),

6.96 (d, *J* = 9.2 Hz, 1H), 6.92 (d, *J* = 4.9 Hz, 1H), 6.88 – 6.85 (m, 1H), 6.38 (p, *J* = 6.9 Hz, 1H), 6.34 – 6.27 (m, 2H), 6.21 – 6.12 (m, 1H), 5.61 – 5.55 (m, 1H), 5.51 (d, *J* = 24.7 Hz, 2H), 5.25 (dd, *J* = 13.3, 4.1 Hz, 1H), 4.52 (d, *J* = 13.3 Hz, 1H), 4.16 (t, *J* = 6.3 Hz, 2H), 4.11 (t, *J* = 6.4 Hz, 2H), 4.01 – 3.91 (m, 2H), 3.84 (ddt, *J* = 16.0, 9.2, 6.2 Hz, 2H), 2.57 – 2.52 (m, 2H), 2.32 – 2.19 (m, 2H), 1.76 – 1.40 (m, 22H), 0.98 – 0.85 (m, 12H).

^{13}C NMR (126 MHz, DMSO-d_6, 298 K) δ [ppm] = 153.48, 153.21, 152.50, 150.95, 149.97, 149.90, 147.42, 146.91, 127.83, 127.41, 127.38, 127.27, 126.54, 125.60, 125.43, 125.13, 124.71, 124.59, 124.44, 124.05, 123.14, 121.22, 120.82, 120.38, 120.18, 119.30, 119.17, 118.81, 117.64, 115.82, 115.13, 115.03, 113.99, 91.66, 91.51, 69.39, 69.15, 69.08, 68.16, 65.41, 47.08, 45.77, 38.22, 31.63, 31.61, 31.51, 31.42, 26.97, 26.72, 22.54, 22.17, 21.30, 19.93, 19.37, 19.26, 19.21, 19.13, 15.66, 14.27, 14.23, 14.14.

ESI-HRMS: m/z calculated for *R*,*R*-**CT1** $[M + H]^+$ $C_{70}H_{77}N_4O_8S_2$: 1165.5178, found 1165.5173 (error = -0.4 ppm).

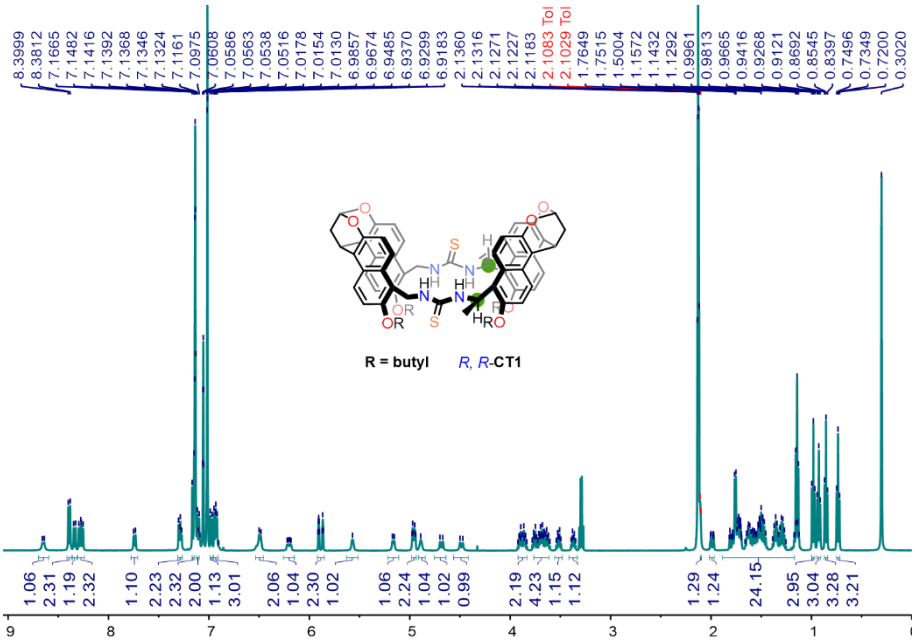

^{1}H NMR spectrum (500 MHz, Toluene-d_8, 298 K) of *R*,*R*-**CT1**.

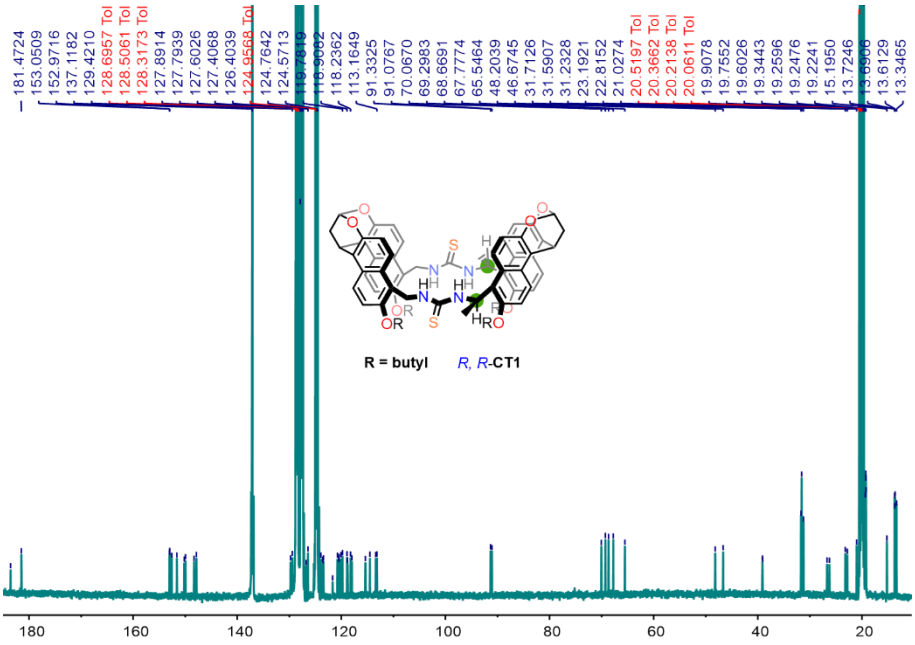

^{13}C NMR spectrum (126 MHz, Toluene-d_8, 298 K) of *R*,*R*-**CT1**.

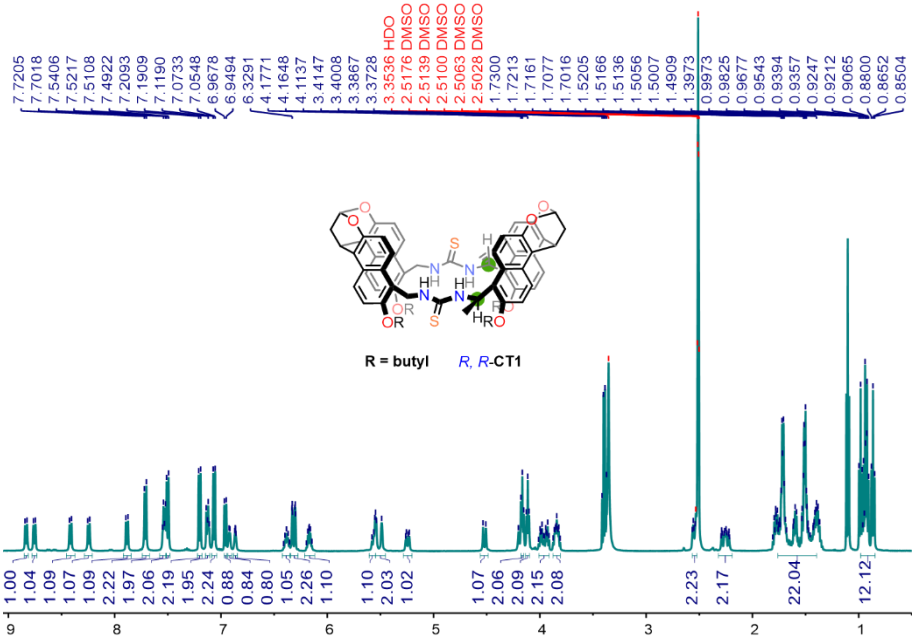

^{1}H NMR spectrum (500 MHz, DMSO-d_6, 298 K) of *R*,*R*-**CT1**.

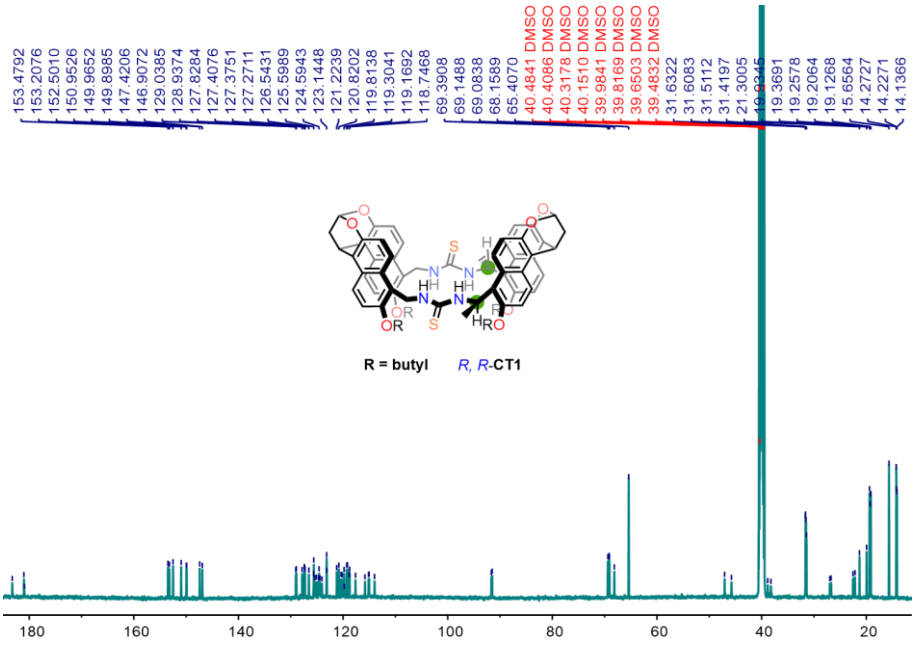

^{13}C NMR spectrum (126 MHz, DMSO-d_6, 298 K) of *R*,*R*-**CT1**.

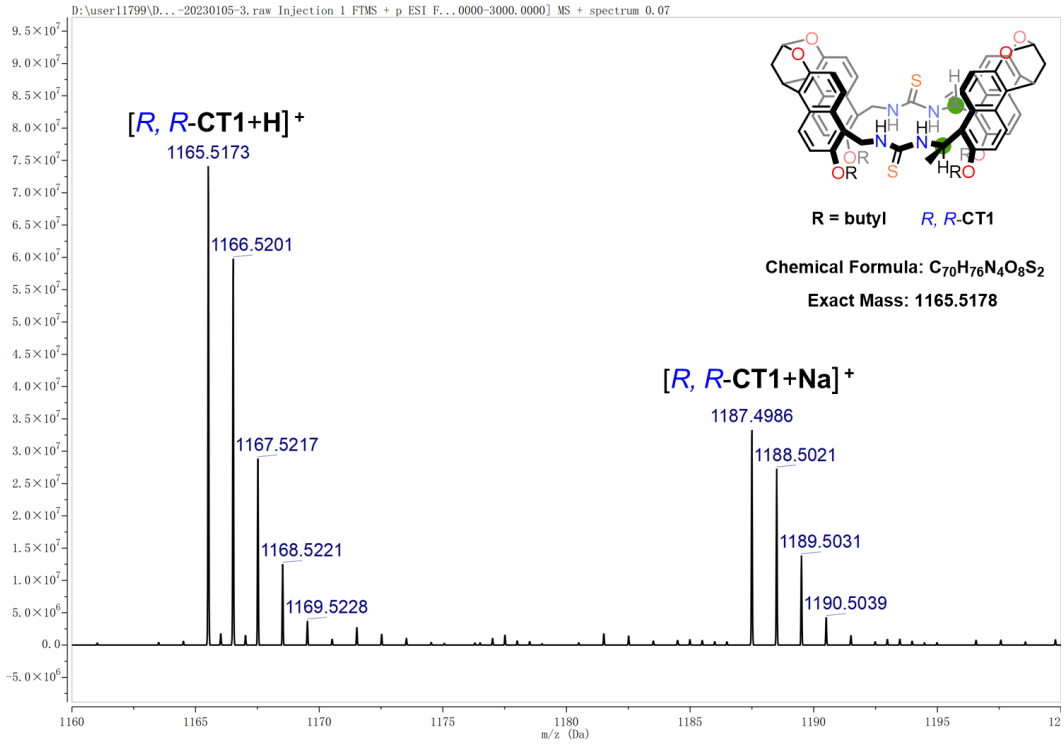

ESI mass spectrum of *R*,*R*-**CT1**.

R,*R*-**CT2**: ^{1}H NMR (500 MHz, CD_2Cl_2, 298K) δ [ppm] = 8.30 (t, *J* = 10.1 Hz, 3H), 8.13 (d, *J* = 9.4 Hz, 1H), 7.86 – 7.65 (m, 4H), 7.26 – 7.08 (m, 3H), 7.06 – 7.00 (m, 2H), 6.98 (s, 1H), 6.97 – 6.92 (m, 2H), 6.41 (s, 1H), 6.13 – 6.07 (m, 2H), 5.72 – 5.64 (m, 1H), 5.51 (s, 1H), 5.18 (d, *J* = 7.9 Hz, 1H), 5.12 (dd, *J* = 5.7, 3.1 Hz, 2H), 4.49 (d, *J* = 13.8 Hz, 1H), 3.93 (hept, *J* = 16.8, 15.9 Hz, 9H), 2.40 – 2.18 (m, 4H), 1.73 (dq, *J* = 19.6, 6.3 Hz, 9H), 1.61 (t, *J* = 7.5 Hz, 2H), 1.47 (d, *J* = 2.6 Hz, 9H), 1.34 (q, *J* = 7.5 Hz, 2H), 0.92 (ddd, *J* = 9.5, 7.3, 2.0 Hz, 9H), 0.85 (t, *J* = 7.4 Hz, 3H).

^{13}C NMR (126 MHz, CD_2Cl_2, 298K) δ [ppm] = 124.22, 124.05, 123.98, 123.65, 123.46, 119.39, 119.23, 119.17, 118.35, 115.88, 114.03, 113.89, 91.71, 91.60, 70.19, 69.42, 68.88, 68.68, 53.89, 53.68, 53.46, 53.25, 53.03, 48.35, 46.67, 39.15, 31.73, 31.67, 31.51, 27.05, 26.79, 23.21, 22.95, 20.66, 20.06, 19.60, 19.39, 19.34, 19.29, 13.74, 13.65.

ESI-HRMS: m/z calculated for *R*,*R*-**CT2** $[M + H]^+$ $C_{70}H_{77}N_4O_8S_2$: 1165.5178, found 1165.5178 (no error).

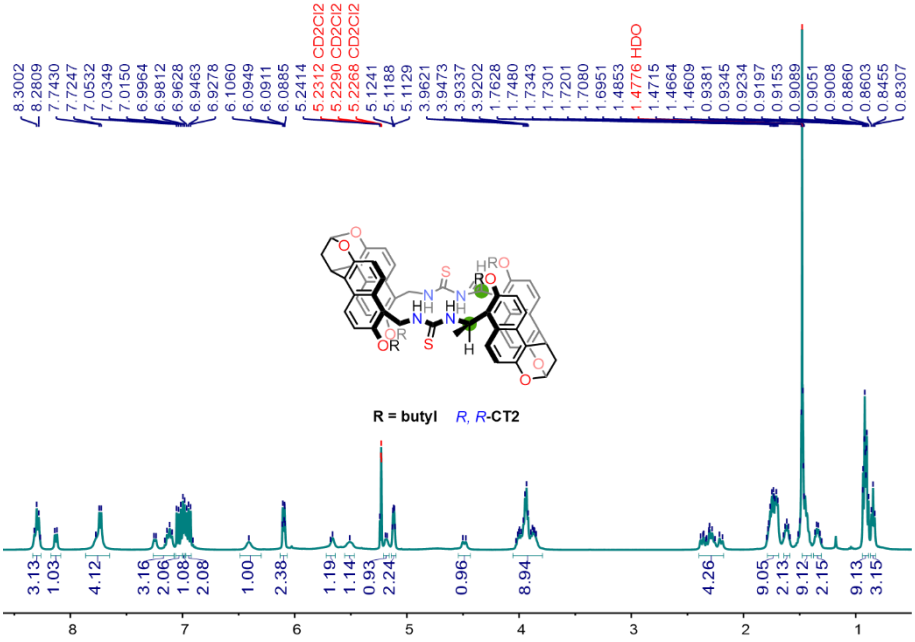

^{1}H NMR spectrum (500 MHz, CD_2Cl_2, 298 K) of *R*,*R*-**CT2**.

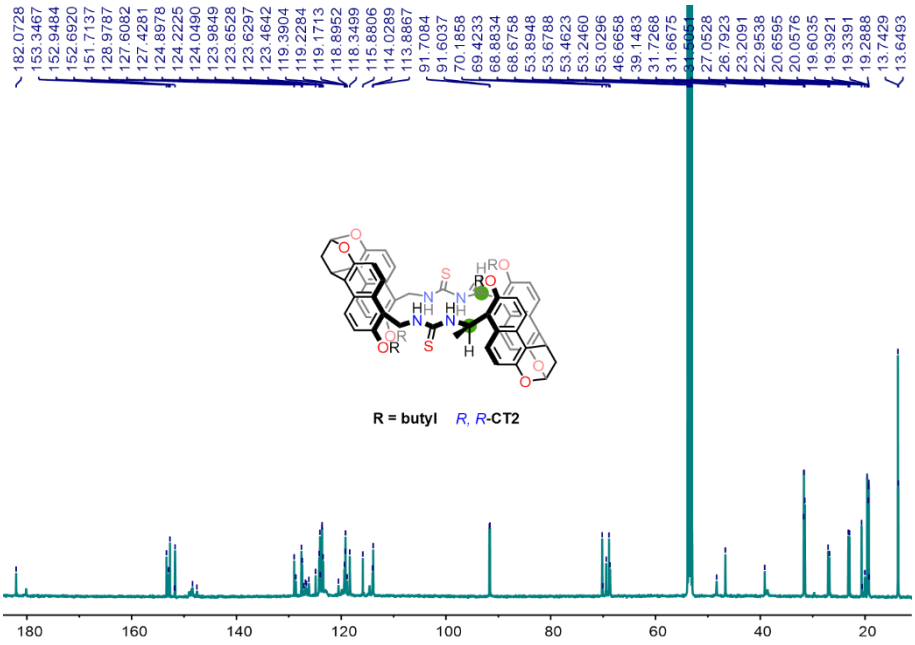

^{13}C NMR spectrum (126 MHz, CD_2Cl_2, 298 K) of *R*,*R*-**CT2**.

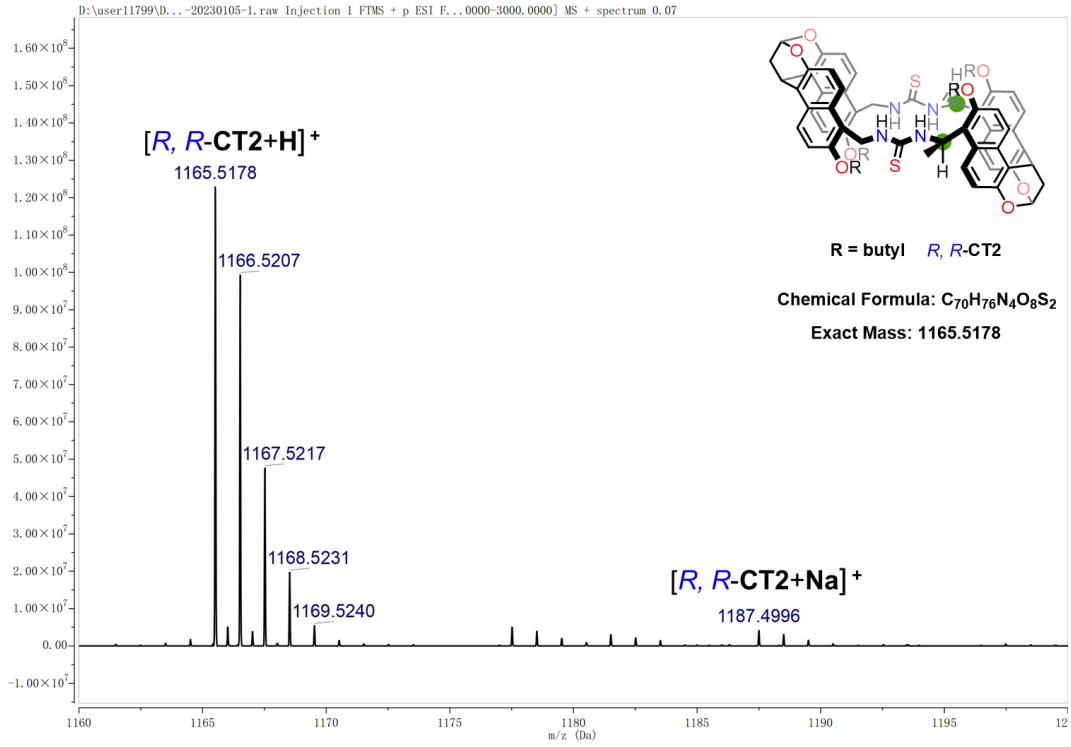

ESI mass spectrum of *R*,*R*-**CT2**.

The NMR spectra of enantiomers including *S,S*-**CT1** and *S,S*-**CT2** are consistent with *R,R*-**CT1** and *R,R*-**CT2** respectively. **ESI-HRMS:** m/z calcd for *S,S*-**CT1** $[M + H]^+$ $C_{70}H_{77}N_4O_8S_2$: 1165.5178, found 1165.5175 (error = -0.3 ppm). m/z calcd for *S,S*-**CT2** $[M + H]^+$ $C_{70}H_{77}N_4O_8S_2$: 1165.5178, found 1165.5173 (error = -0.4 ppm).

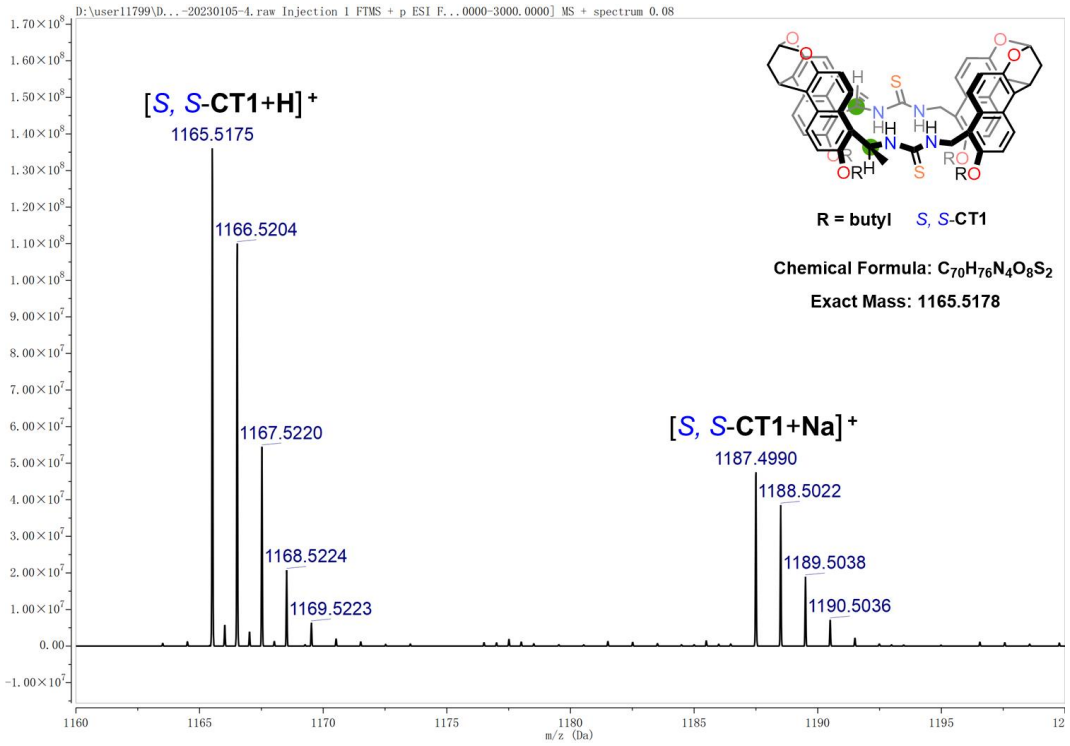

ESI mass spectrum of *S,S*-**CT1**.

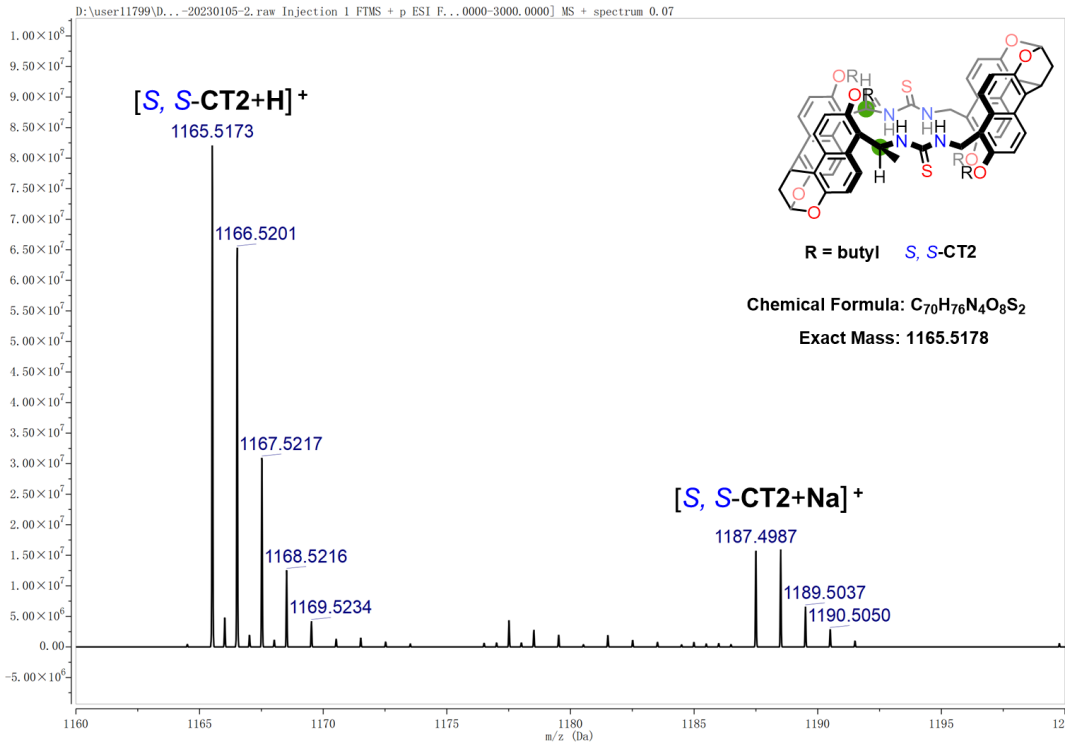

ESI mass spectrum of *S,S*-**CT2**.

2. Configurational Assignments of Chiral Naphthotubes (2D NMR)

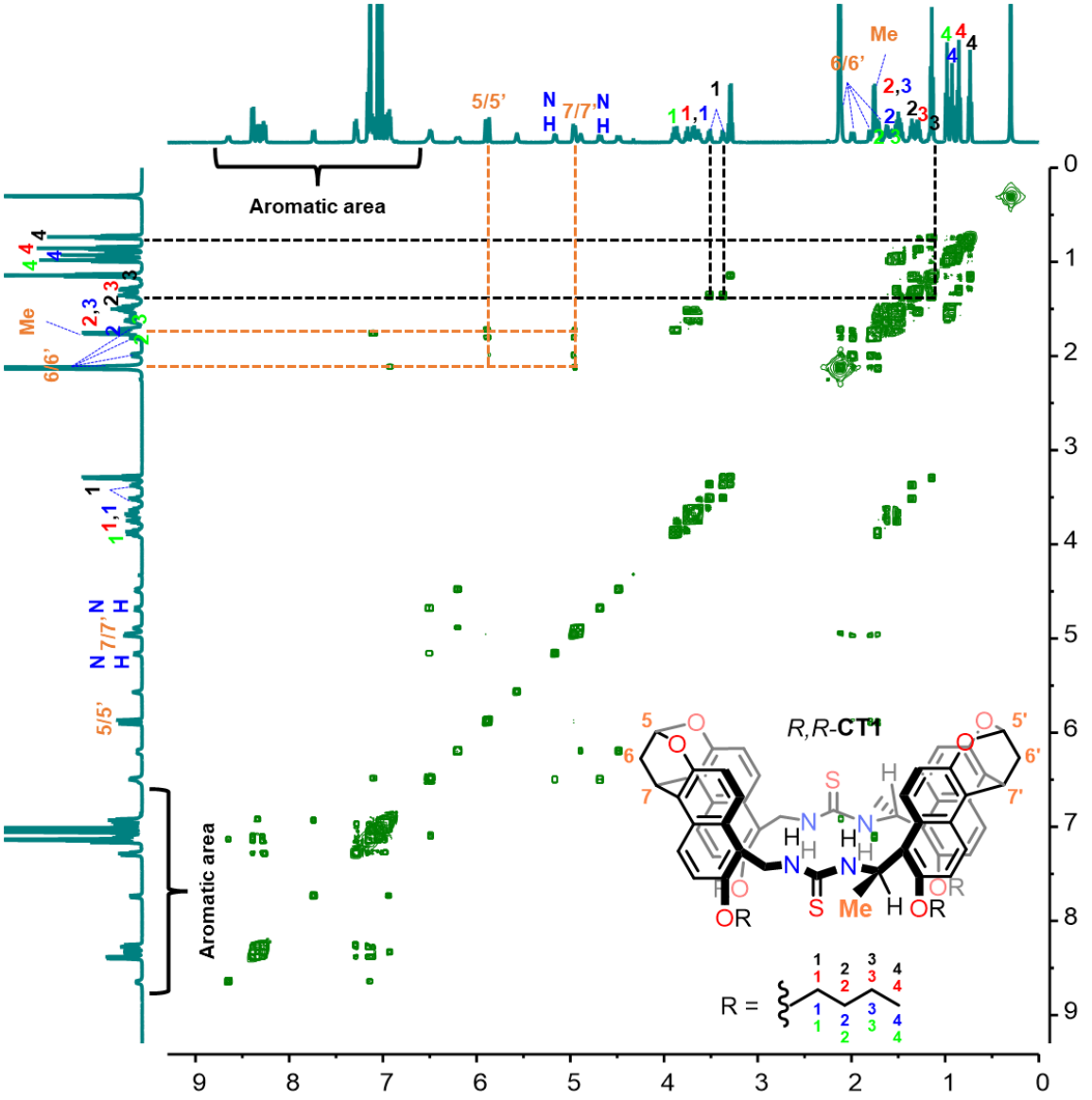

Figure *S1.* ^{1}H,^{1}H-COSY NMR spectrum of *R,R*-**CT1** (500 MHz, Toluene-d$_8$, 298 K), the introduction of a chiral center reduces the symmetry of the naphthotube, and the protons on the four side chains are clearly distinguished. The 2D NMR spectra of *S,S*-**CT1** are consistent with *R,R*-**CT1**.

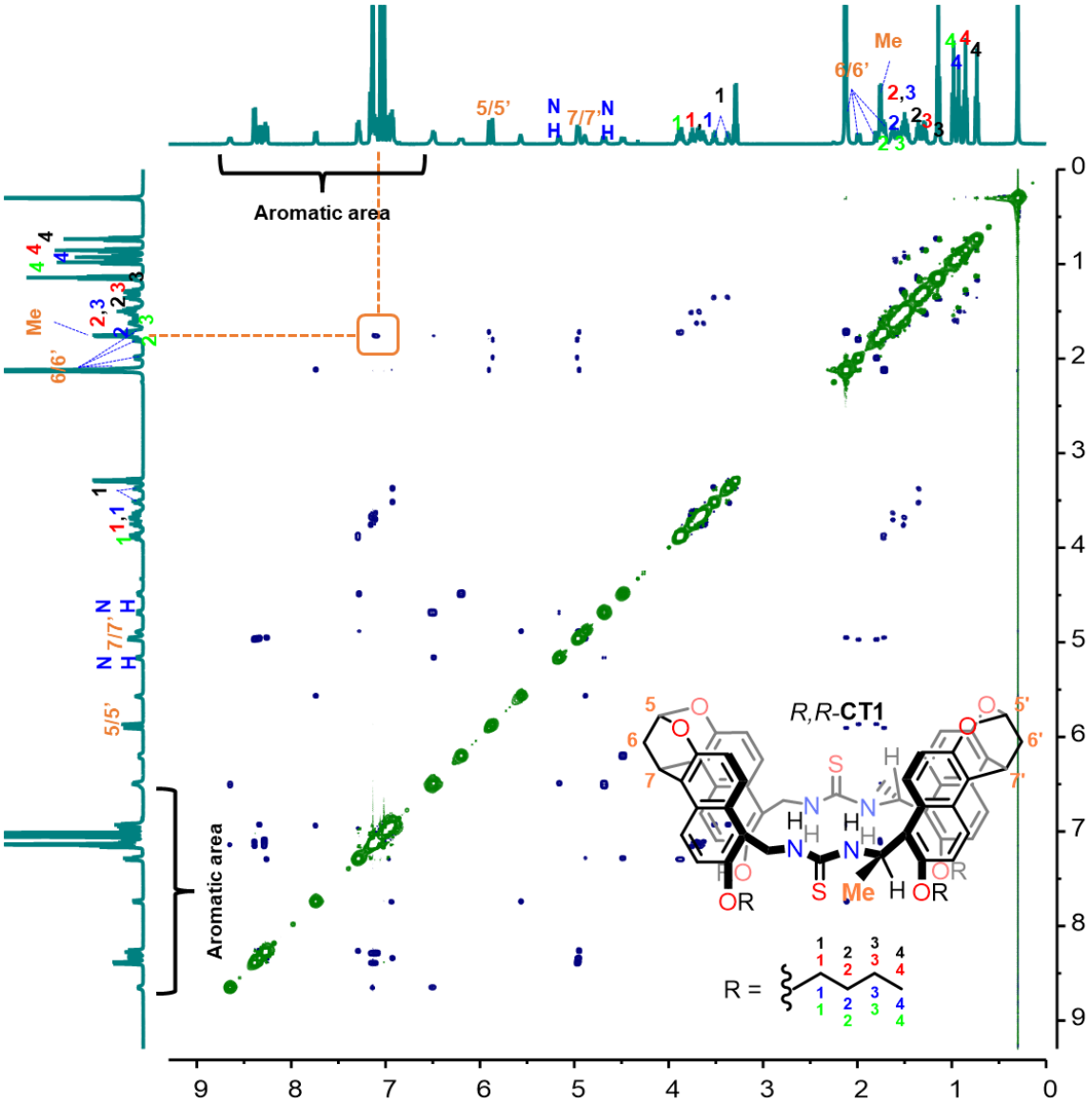

Figure *S2.* ^{1}H,^{1}H-ROESY NMR spectrum of *R,R*-**CT1** (500 MHz, Toluene-d$_8$, 298 K). The NOE signal between one of two methyl groups in chiral centers and aromatic protons, as shown by the orange box, indicating that the methyl group is close to the bis-naphthalene cleft. The 2D NMR spectra of *S,S*-**CT1** are consistent with *R,R*-**CT1**.

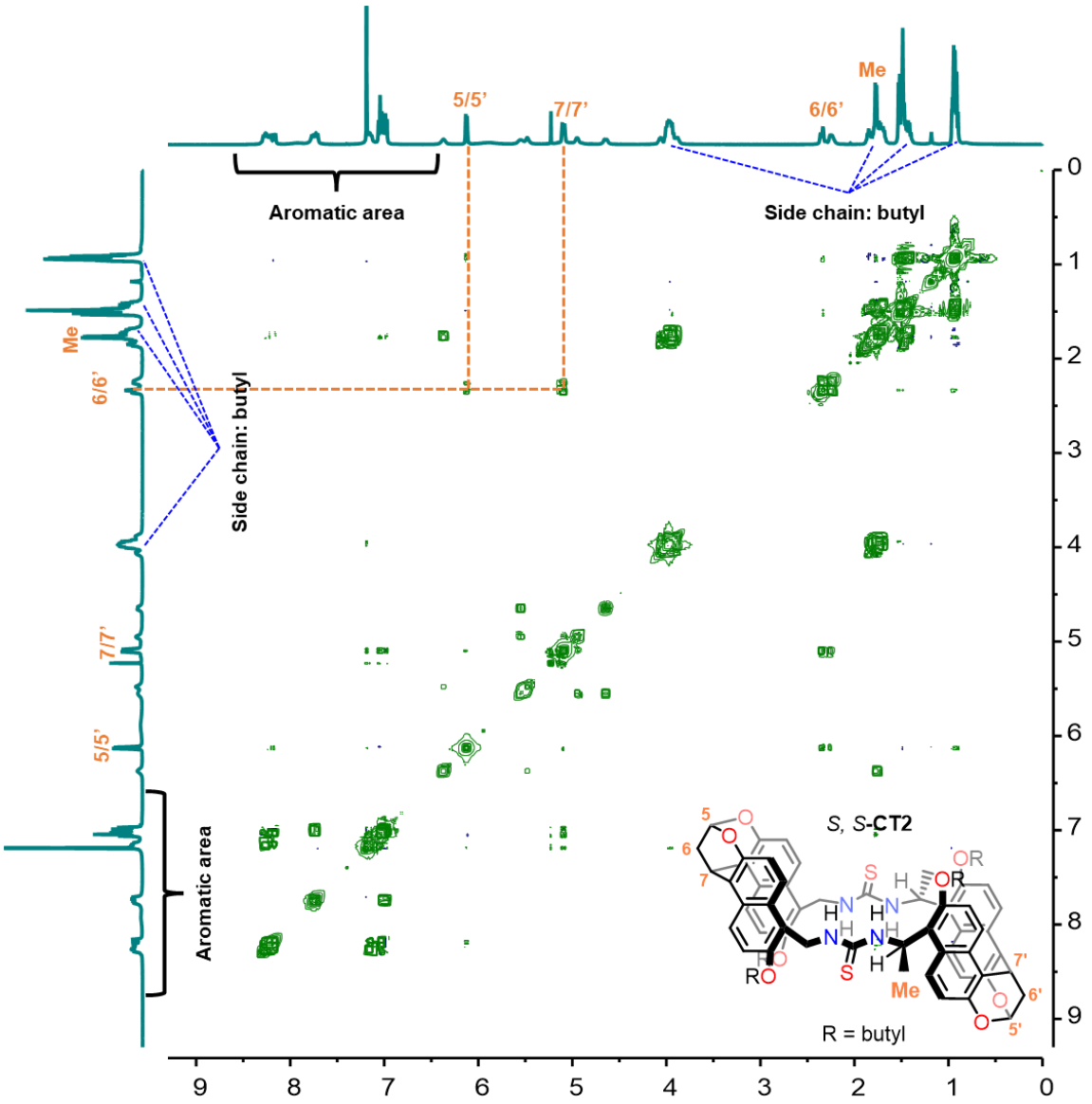

Figure *S3.* ^{1}H,^{1}H-COSY NMR spectrum of *S,S*-**CT2** (500 MHz, $CDCl_3$, 298 K). The 2D NMR spectra of *R,R*-**CT2** are consistent with *S,S*-**CT2**.

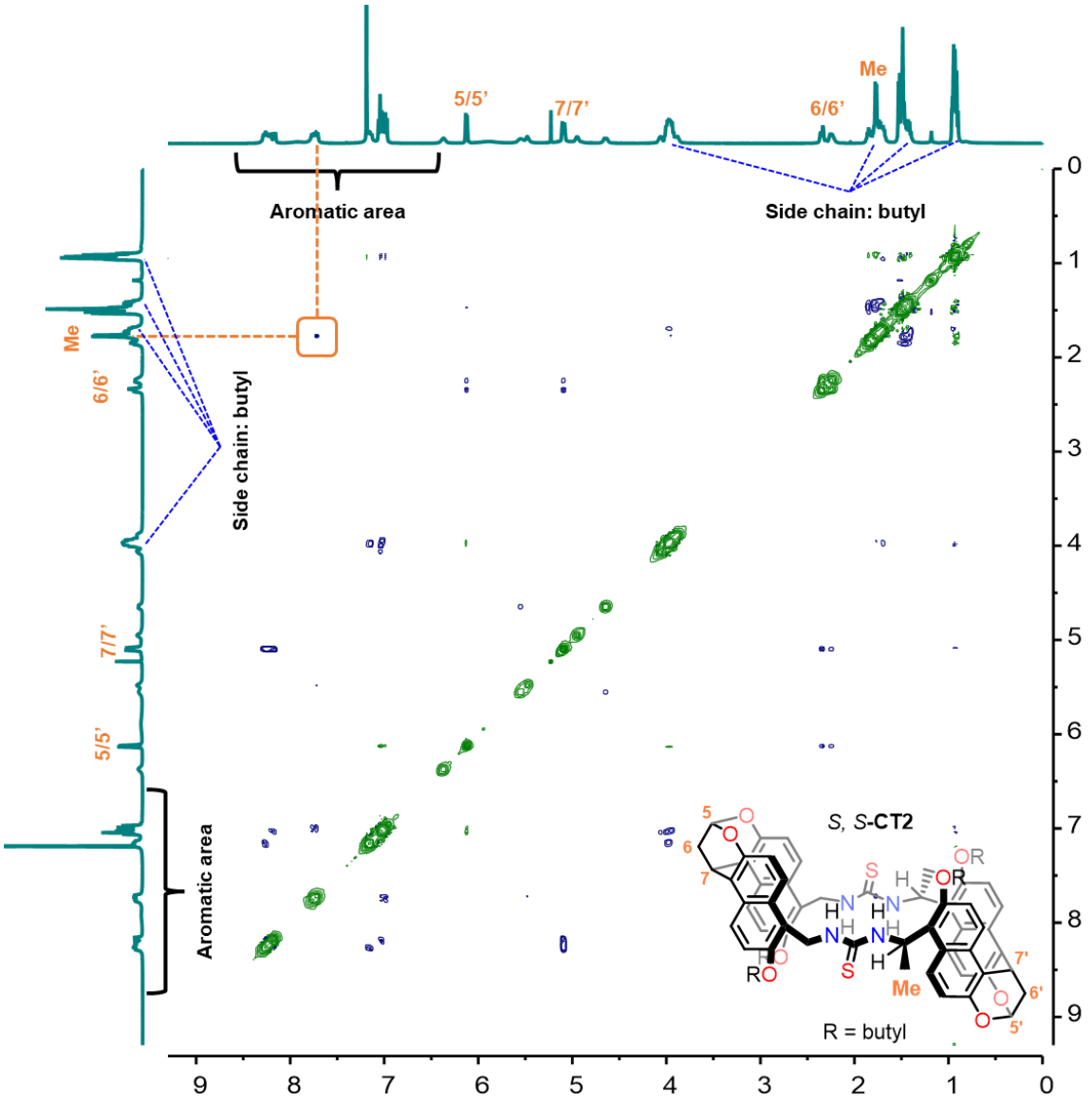

Figure *S4.* ^{1}H,^{1}H-ROESY NMR spectrum of *S,S*-**CT2** (500 MHz, $CDCl_3$, 298 K). The NOE signal between one of two methyl groups in chiral centers and aromatic protons, as shown by the orange box, indicating that the methyl group is close to the bis-naphthalene cleft. The 2D NMR spectra of *R,R*-**CT2** are consistent with *S,S*-**CT2**.

3. Dihedral Angles of Bis-Naphthalene Clefts in Naphthotubes

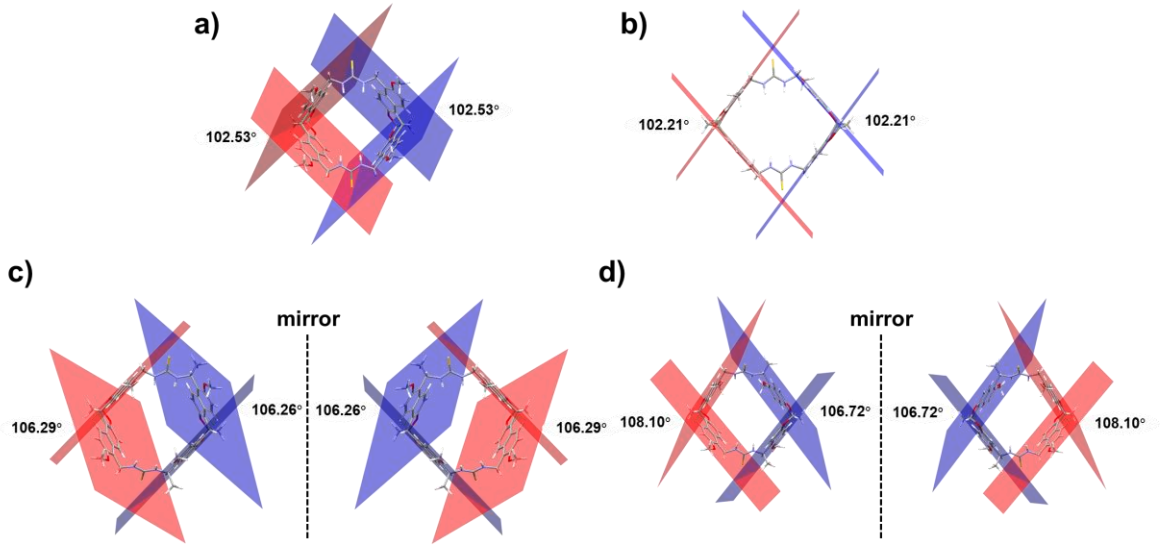

Figure *S5*. Dihedral angles of bridged bis-naphthalene groups in macrocycles. a) Achiral *syn*-naphthotube (102.53°, 102.53°); b) Achiral *anti*-naphthotube (102.21°, 102.21°), c) *R,R*-**CT1** and *S,S*-**CT1** (106.29°, 106.26°), d) *R,R*-**CT2** and *S,S*-**CT2** (108.10°, 106.72°). All planes are calculated using 10 carbon atoms of naphthalene, butoxys are replaced with methoxys for clarity. Energy minimized structures obtained by DFT (B3LYP/6-31G* with D3)[2] calculations with the PCM solution model[3] in chloroform at 298 K.

4. HPLC of Chiral naphthotubes on Chiral Column

Column :	CHIRALPAK® IK-3 (IK30CE-CM026)
Column size	0.46 cm I.D. × 25 cm L × 3 μm
Injection	1μl Mobile
Phase	n-Hexane / Ethanol / Trifluoroacetic acid = 60/40/0.1(v/v/v)
Flow rate	1.0 mL/min
Wavelength	UV 220 nm
Temperature	35 °C
Sample solution	1 mg/ml in MeOH 50% DCM 50%
HPLC equipment	Shimadzu LC 20A QA&QC-HPLC-12

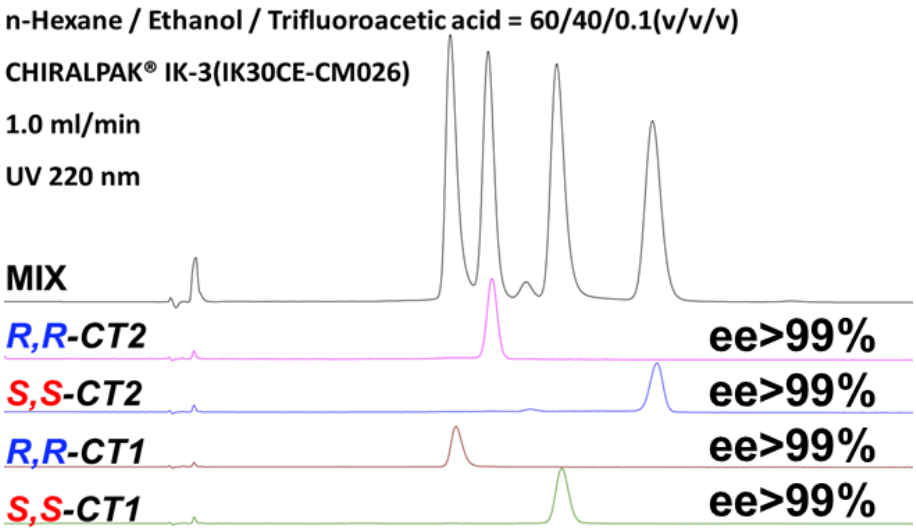

Figure *S6*. Chiral HPLC stack spectra of four macrocycles (*R,R*-**CT1**, *S,S*-**CT1**, *R,R*-**CT2** and *S,S*-**CT2**).

5. ^{1}H NMR Spectra of the 1: 1 Host-Guest Complexes

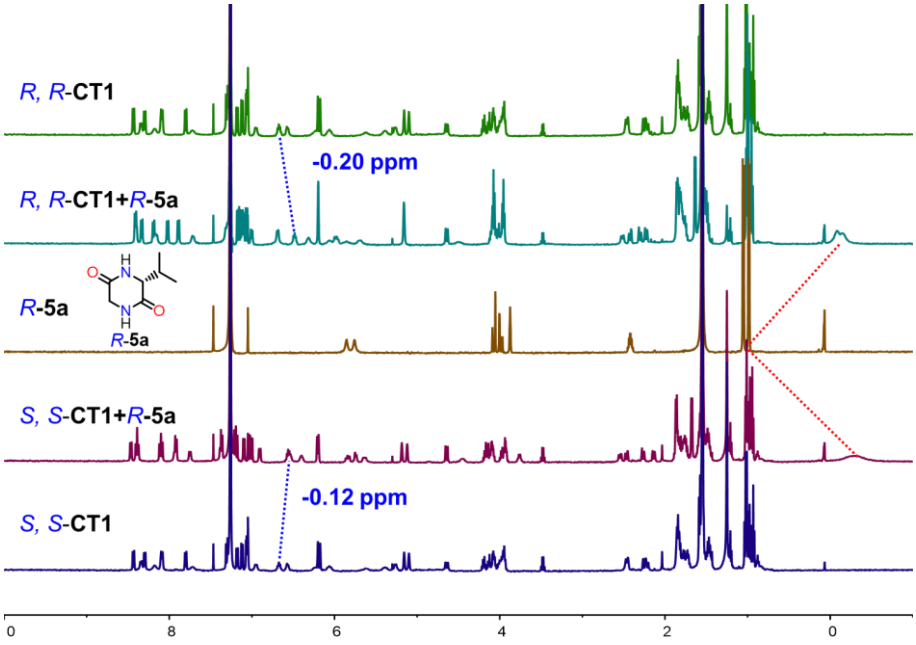

Figure *S7*. ^{1}H NMR spectra of host-guest 1: 1 complexes (500 MHz, $CDCl_3$, 0.5 mM, 298 K). The blue dashed line marks the signal change of host chemical shift, The red dashed line marks the signal change of guest chemical shift.

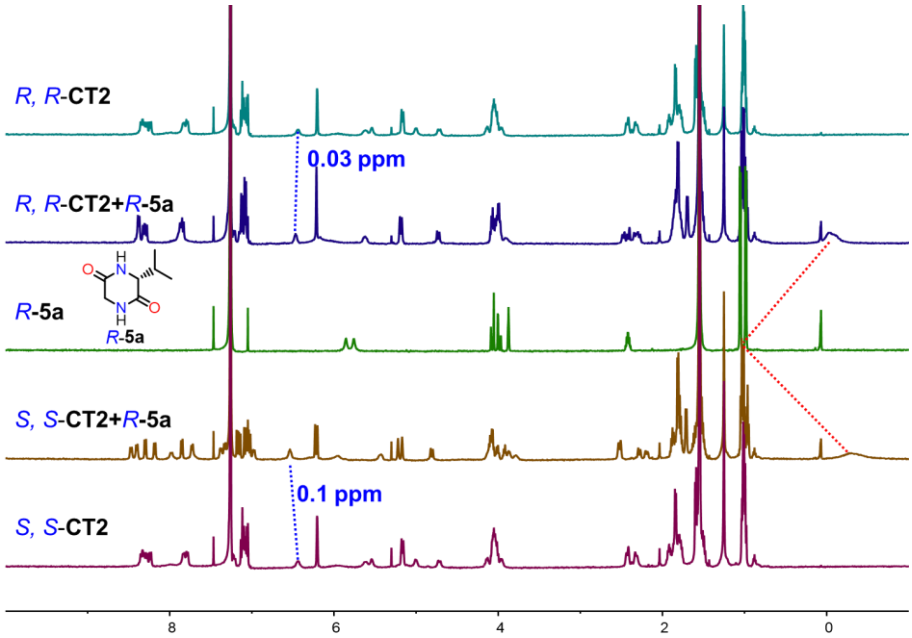

Figure *S8*. ^{1}H NMR spectra of host-guest 1: 1 complexes (500 MHz, $CDCl_3$, 0.5 mM, 298 K). The blue dashed line marks the signal change of host chemical shift, The red dashed line marks the signal change of guest chemical shift.

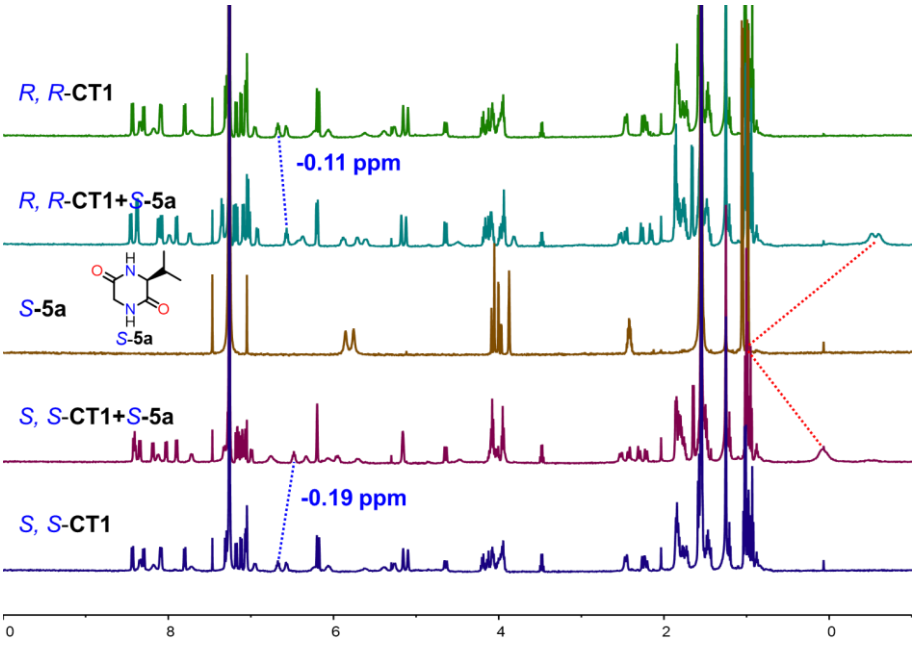

Figure *S9*. ^{1}H NMR spectra of host-guest 1: 1 complexes (500 MHz, $CDCl_3$, 0.5 mM, 298 K). The blue dashed line marks the signal change of host chemical shift, The red dashed line marks the signal change of guest chemical shift.

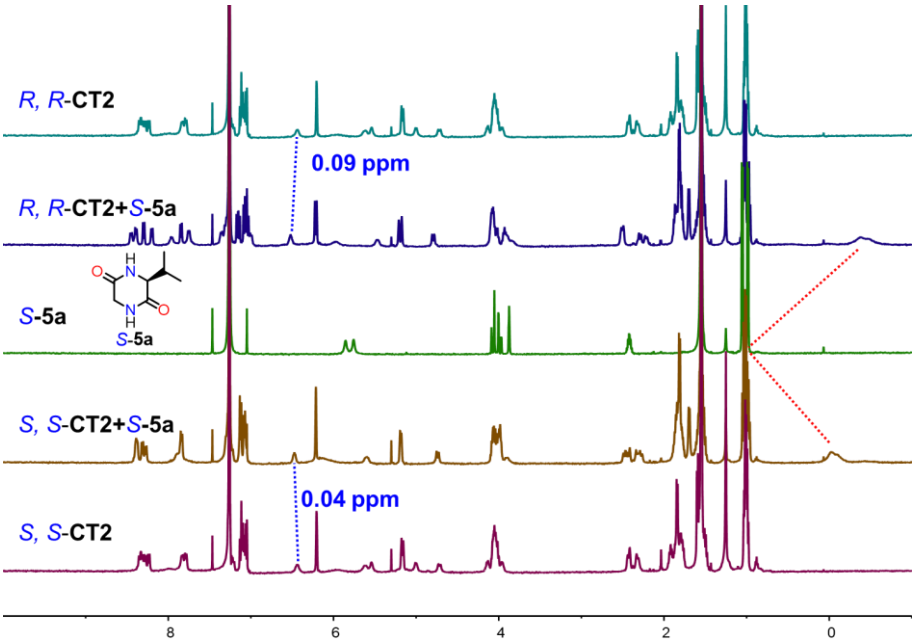

Figure *S10*. ^{1}H NMR spectra of host-guest 1: 1 complexes (500 MHz, $CDCl_3$, 0.5 mM, 298 K). The blue dashed line marks the signal change of host chemical shift, The red dashed line marks the signal change of guest chemical shift.

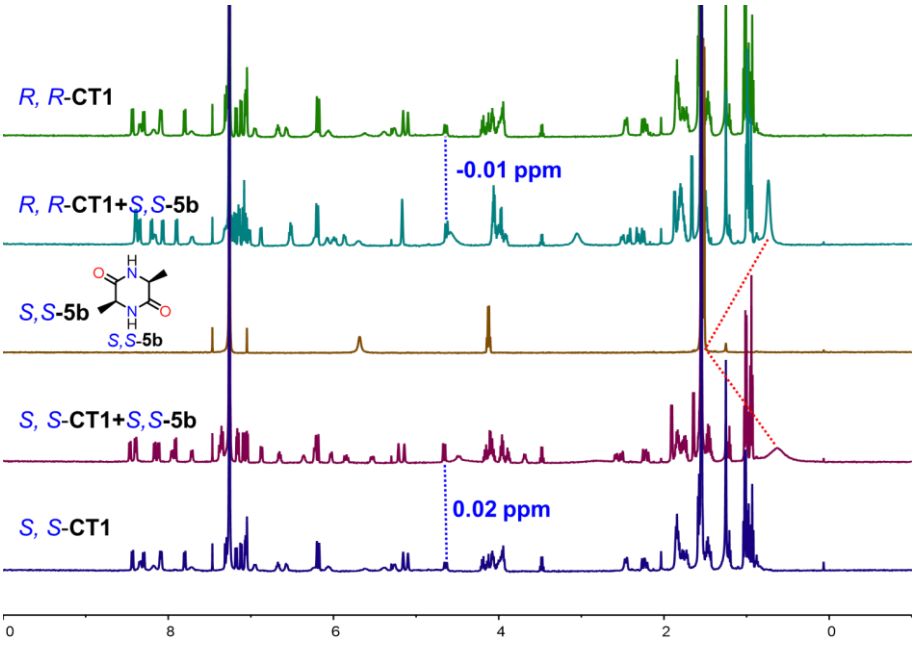

Figure *S11*. ^{1}H NMR spectra of host-guest 1: 1 complexes (500 MHz, $CDCl_3$, 0.5 mM, 298 K). The blue dashed line marks the signal change of host chemical shift, The red dashed line marks the signal change of guest chemical shift.

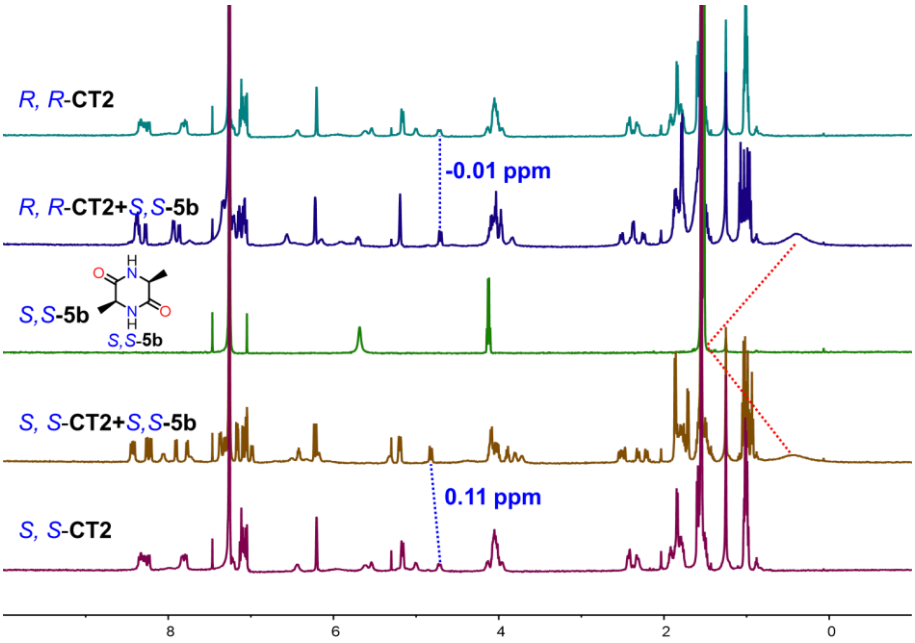

Figure *S12*. ^{1}H NMR spectra of host-guest 1: 1 complexes (500 MHz, $CDCl_3$, 0.5 mM, 298 K). The blue dashed line marks the signal change of host chemical shift, The red dashed line marks the signal change of guest chemical shift.

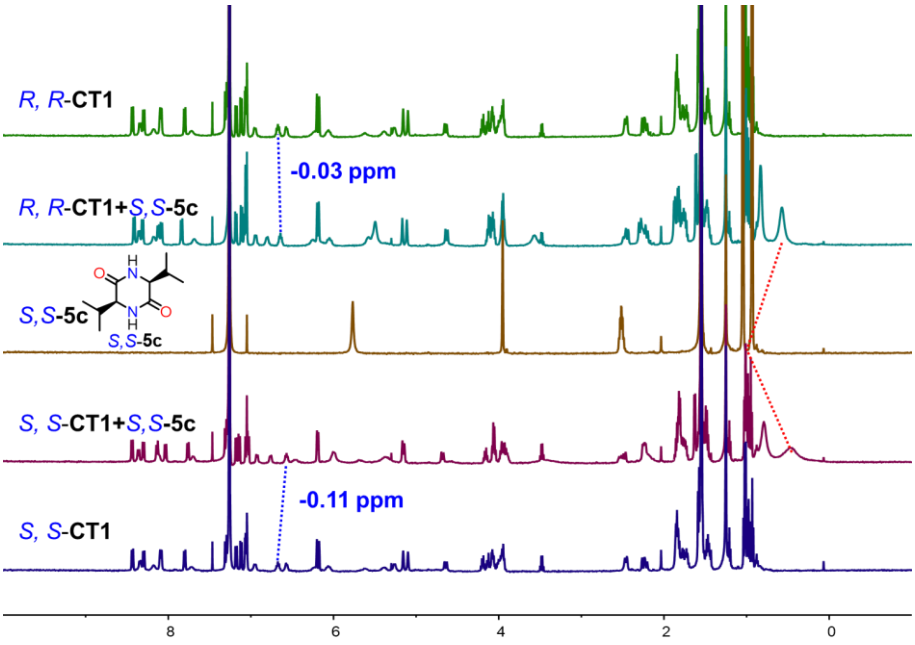

Figure *S13*. ^{1}H NMR spectra of host-guest 1: 1 complexes (500 MHz, $CDCl_3$, 0.5 mM, 298 K). The blue dashed line marks the signal change of host chemical shift, The red dashed line marks the signal change of guest chemical shift.

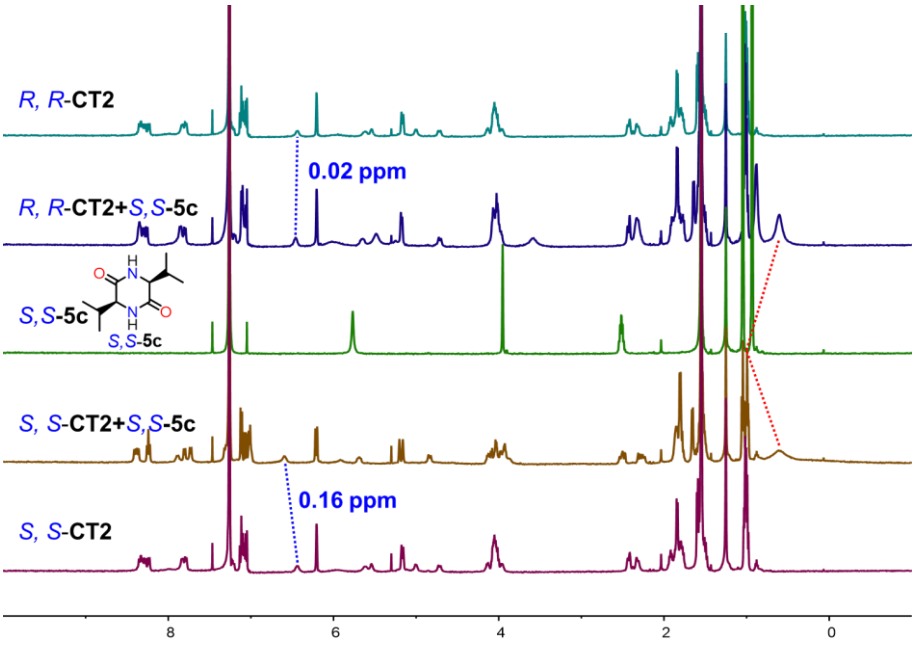

Figure *S14*. ^{1}H NMR spectra of host-guest 1: 1 complexes (500 MHz, $CDCl_3$, 0.5 mM, 298 K). The blue dashed line marks the signal change of host chemical shift, The red dashed line marks the signal change of guest chemical shift.

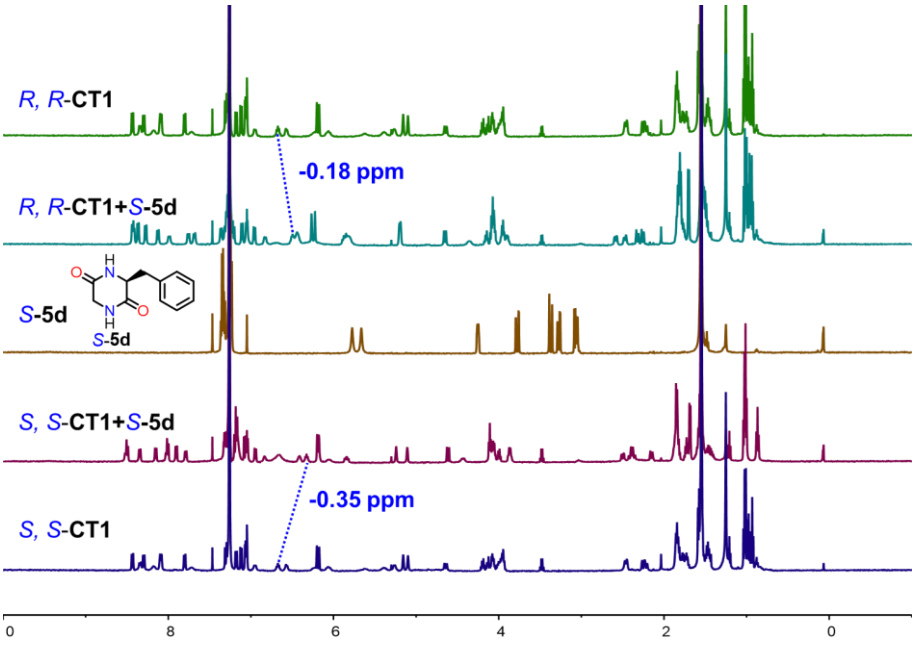

Figure *S15*. ^{1}H NMR spectra of host-guest 1: 1 complexes (500 MHz, $CDCl_3$, 0.5 mM, 298 K). The blue dashed line marks the signal change of host chemical shift, The red dashed line marks the signal change of guest chemical shift.

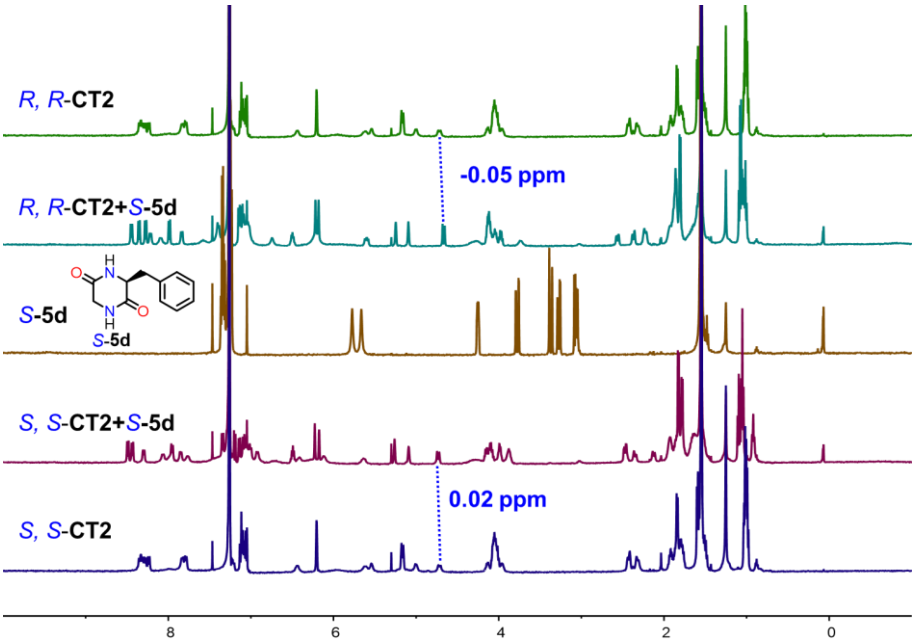

Figure *S16*. ^{1}H NMR spectra of host-guest 1: 1 complexes (500 MHz, $CDCl_3$, 0.5 mM, 298 K). The blue dashed line marks the signal change of the host chemical shift.

6. Job's Plot of Host and Guest

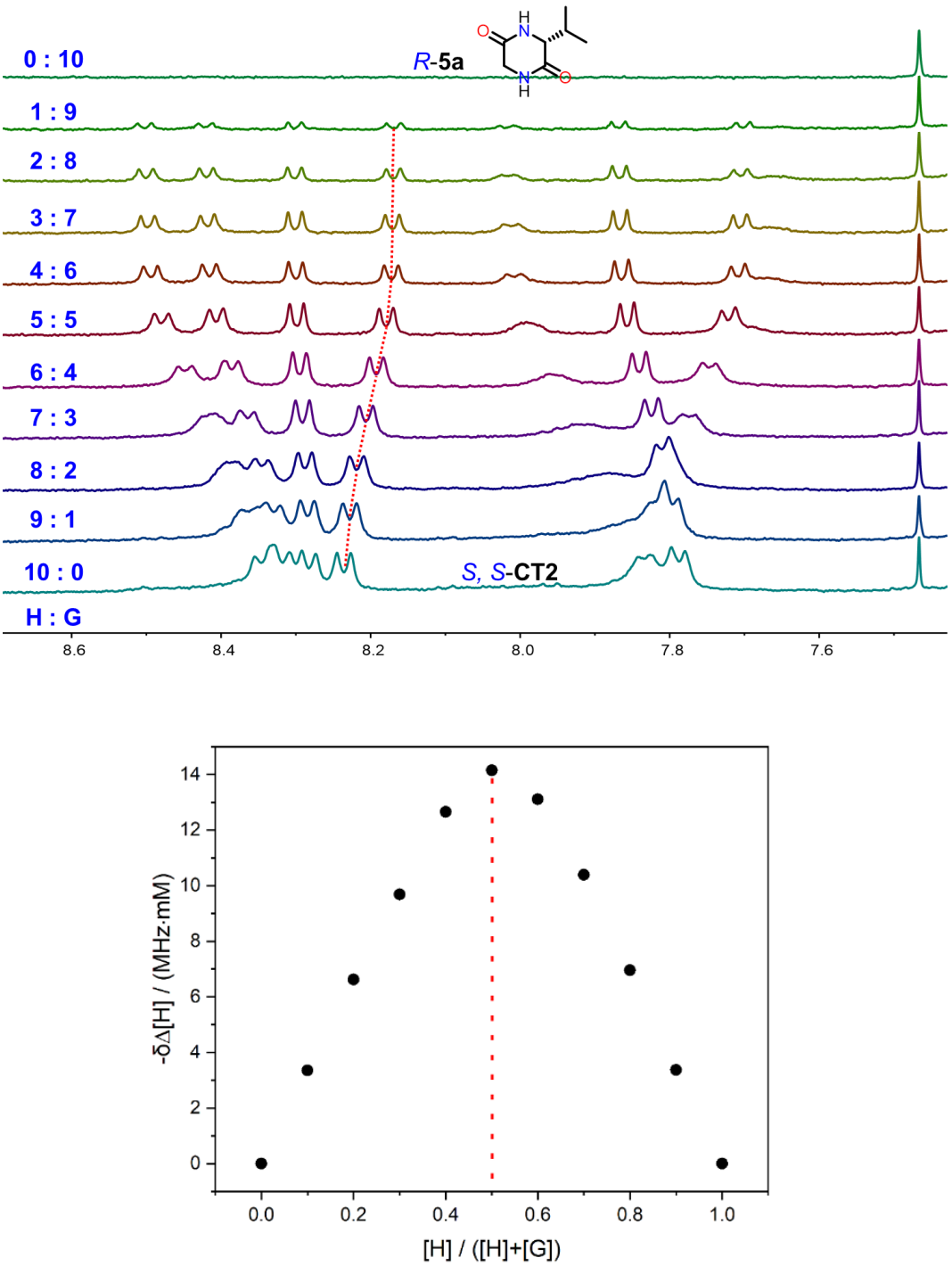

Figure *S17*. Job's plot was obtained by plotting the chemical shift change (Δδ) of the *S,S*-**CT2**'s proton (Ar-H) in ^{1}H NMR spectra by varying the ratio of the *S,S*-**CT2** and *R*-**5a** against the mole fraction of *S,S*-**CT2** and *R*-**5a**. The total concentration of the host and the guest is fixed: [Host] + [Guest] = 0.5 mM. This experiment supports a 1: 1 binding stoichiometry between *R*-**5a** and *S,S*-**CT2** in $CDCl_3$.

7. ESI-HRMS for Host-Guest Complexes

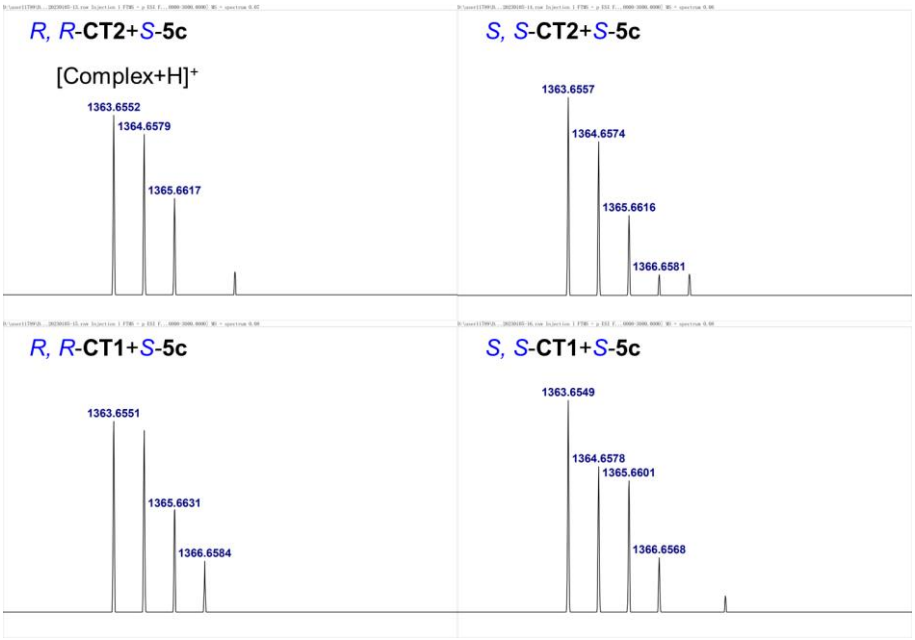

Figure *S18.* ESI mass spectra of the solution of Hosts (*R,R*-**CT1**, *S,S*-**CT1**, *R,R*-**CT2**, *S,S*-**CT2**) in the presence of one equivalent of *S*-**5c**. The results support a 1: 1 binding stoichiometry.

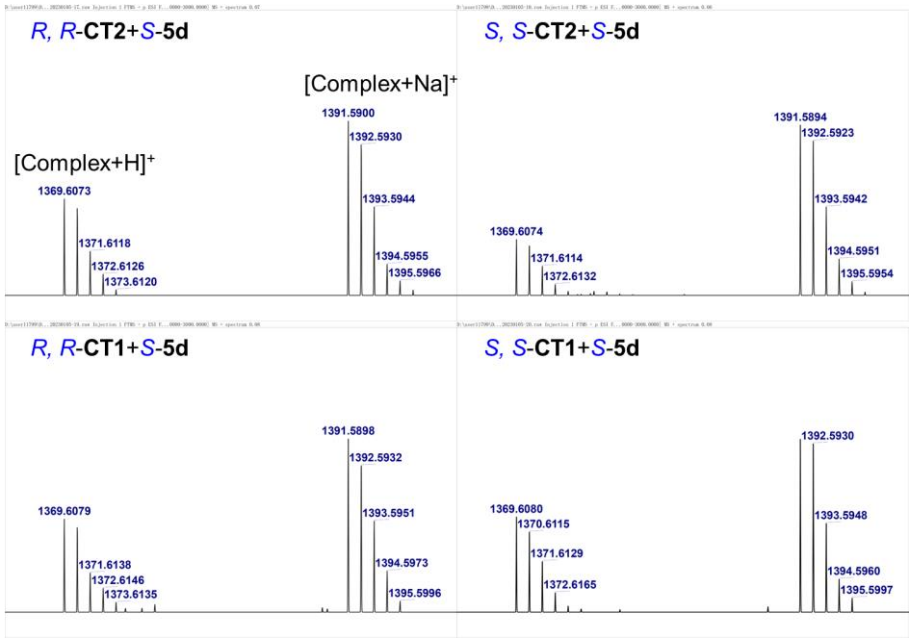

Figure *S19.* ESI mass spectra of the solution of hosts (*R,R*-**CT1**, *S,S*-**CT1**, *R,R*-**CT2**, *S,S*-**CT2**) in the presence of one equivalent of *S*-**5d**. The results support a 1: 1 binding stoichiometry.

8. Determination of Association Constants of Hosts and Guests

- The association constants for the complexes of **CT**s with most guests (except *S,S*-**CT2** with *S*-**5d**) are small (< 10^5 M^{-1}) and the chemical exchange is fast at the NMR timescale. Thus, we used direct NMR titrations to determine their association constants.

- For the cases (*S,S*-**CT2** complex with *S*-**5d**) with large association constants (> 10^5 M^{-1}) and fast exchange kinetics, the binding affinities were determined by competitive NMR titrations and using guest *S*-**5a** (binding constant with *S,S*-**CT2** is 1.2×10^4 M^{-1}) as the outgoing guest. The data from competitive titrations was nonlinearly fitted[4] according to the equations developed by Prof. Werner Nau (available from their website, http://www.jacobs-university.de/ses/wnau).

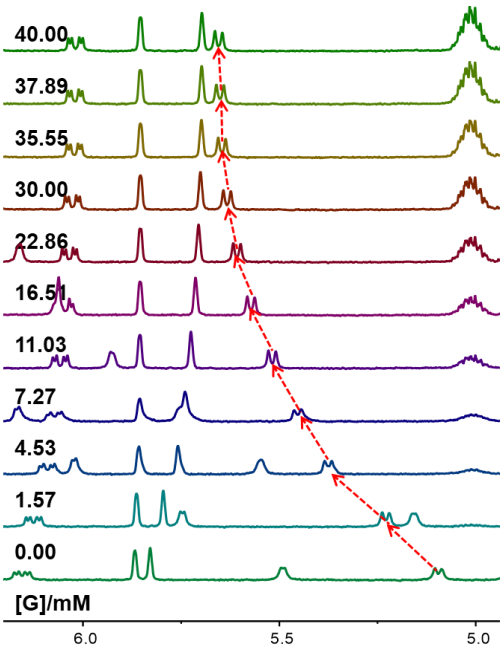

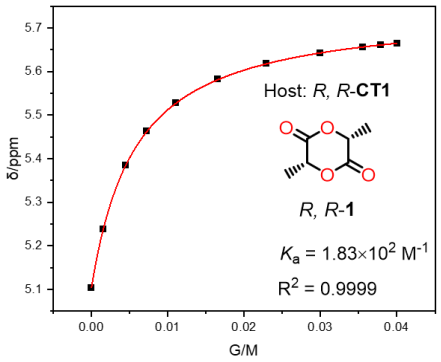

	K_a /M^{-1}	R^2
Titration-1	1.83×10^2	0.9999
Titration-2	1.70×10^2	0.9992
Titration-3	1.83×10^2	0.9998
Average	(1.8±0.1)×10^2	

Figure *S20*. *Left*: Partial ^{1}H NMR spectra (500 MHz, Toluene-d$_8$, 298 K) of *R,R*-**CT1** (0.5 mM) titrated by *R,R*-**1**. From bottom to top, the concentration range of 1 is 0 ~ 40.00 mM. *Right*: Nonlinear curve fitting for the complexation between *R,R*-**CT1** and *R,R*-**1** based on the NMR data.

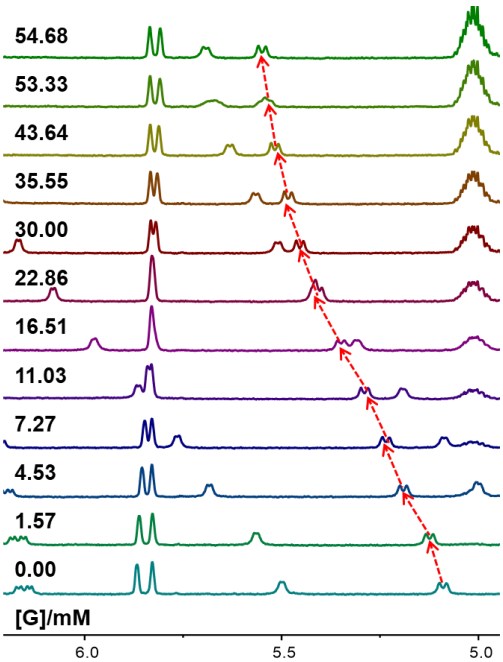

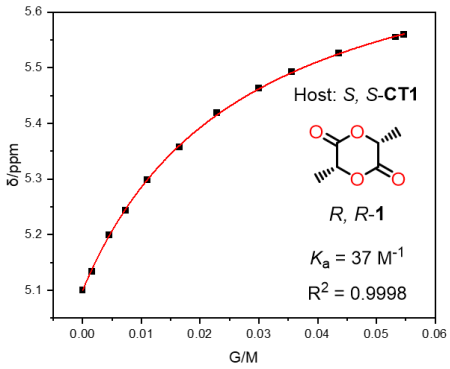

	K_a /M^{-1}	R^2
Titration-1	37	0.9998
Titration-2	36	0.9991
Titration-3	38	0.9994
Average	37±1	

Figure *S21*. *Left*: Partial ^{1}H NMR spectra (500 MHz, Toluene-d$_8$, 298 K) of *S,S*-**CT1** (0.5 mM) titrated by *R,R*-**1**. From bottom to top, the concentration range of 1 is 0 ~ 54.68 mM. *Right*: Nonlinear curve fitting for the complexation between *S,S*-**CT1** and *R,R*-**1** based on the NMR data.

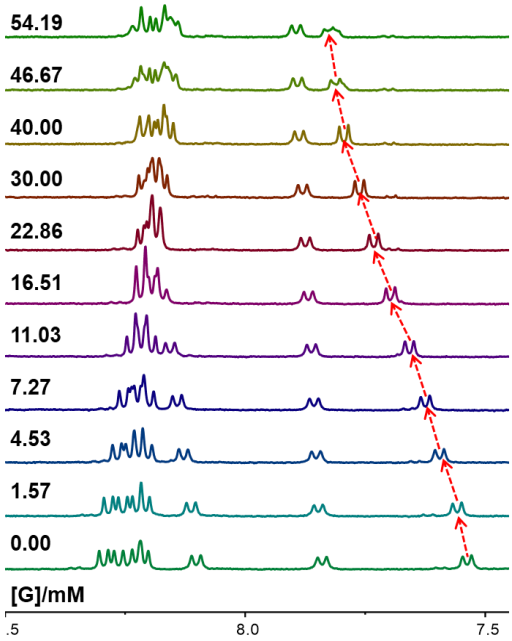

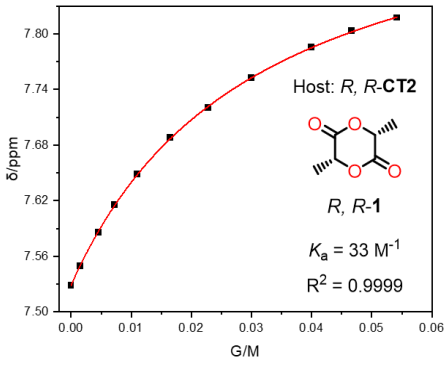

	K_a /M^{-1}	R^2
Titration-1	33	0.9999
Titration-2	32	0.9999
Titration-3	41	0.9991
Average	35±4	

Figure *S22*. *Left*: Partial ^{1}H NMR spectra (500 MHz, Toluene-d_8, 298 K) of *R,R*-**CT2** (0.5 mM) titrated by *R,R*-**1**. From bottom to top, the concentration range of 1 is 0 ~ 54.19 mM. *Right*: Nonlinear curve fitting for the complexation between *R,R*-**CT2** and *R,R*-**1** based on the NMR data.

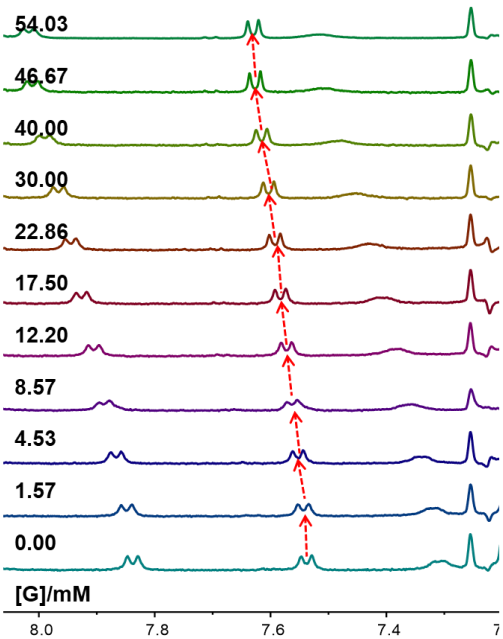

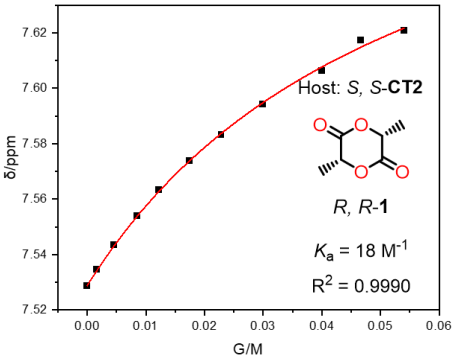

	K_a /M^{-1}	R^2
Titration-1	18	0.9990
Titration-2	18	0.9999
Titration-3	19	0.9998
Average	18±1	

Figure *S23*. *Left*: Partial ^{1}H NMR spectra (500 MHz, Toluene-d_8, 298 K) of *S,S*-**CT2** (0.5 mM) titrated by *R,R*-**1**. From bottom to top, the concentration range of 1 is 0 ~ 54.03 mM. *Right*: Nonlinear curve fitting for the complexation between *S,S*-**CT2** and *R,R*-**1** based on the NMR data.

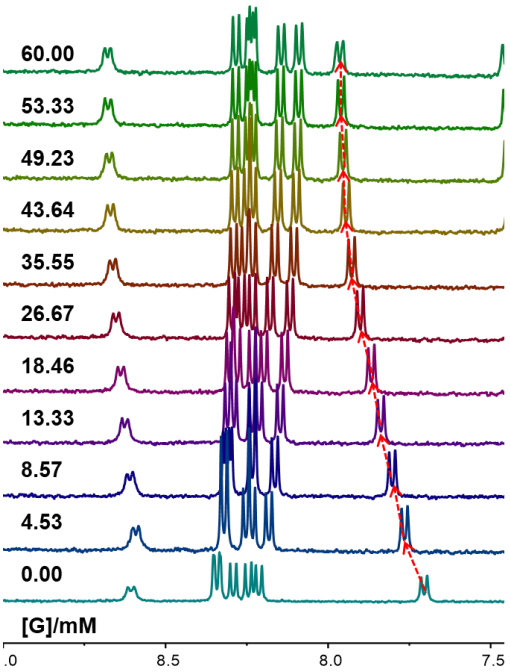

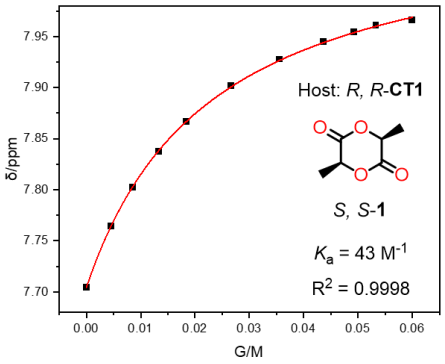

	K_a /M^{-1}	R^2
Titration-1	44	0.9998
Titration-2	43	0.9990
Titration-3	45	0.9998
Average	41±1	

Figure *S24*. *Left*: Partial ^{1}H NMR spectra (500 MHz, Toluene-d_8, 298 K) of *R,R*-**CT2**(0.5 mM) titrated by *R,R*-**1**. From bottom to top, the concentration range of 1 is 0 ~ 60.00 mM. *Right*: Nonlinear curve fitting for the complexation between *R,R*-**CT2** and *R,R*-**1** based on the NMR data.

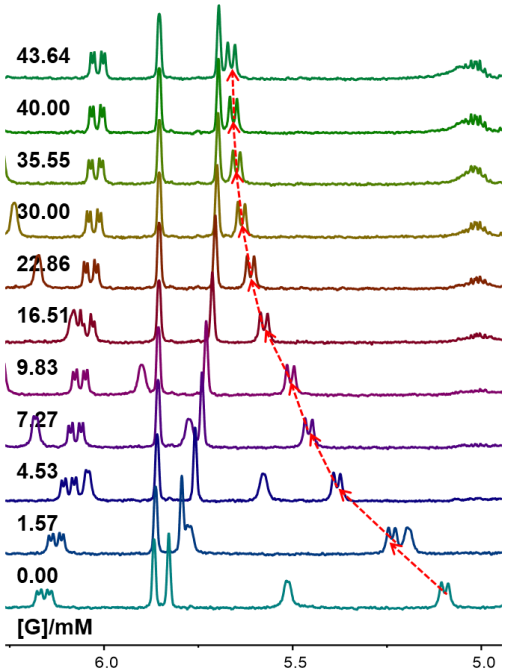

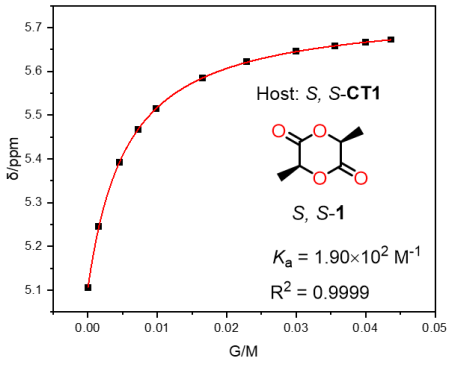

	K_a /M^{-1}	R^2
Titration-1	1.90×10^2	0.9999
Titration-2	1.76×10^2	0.9990
Titration-3	2.00×10^2	0.9998
Average	(1.9±0.1)×10^2	

Figure *S25*. *Left*: Partial ^{1}H NMR spectra (500 MHz, Toluene-d_8, 298 K) of *S,S*-**CT2** (0.5 mM) titrated by *R,R*-**1**. From bottom to top, the concentration range of 1 is 0 ~ 43.64 mM. *Right*: Nonlinear curve fitting for the complexation between *S,S*-**CT2** and *R,R*-**1** based on the NMR data.

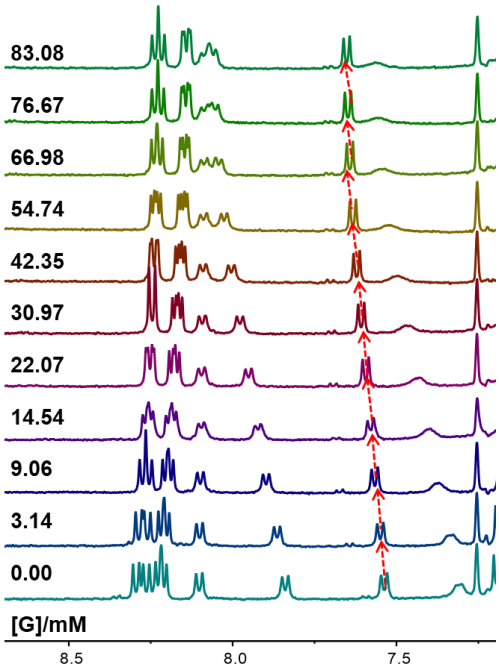

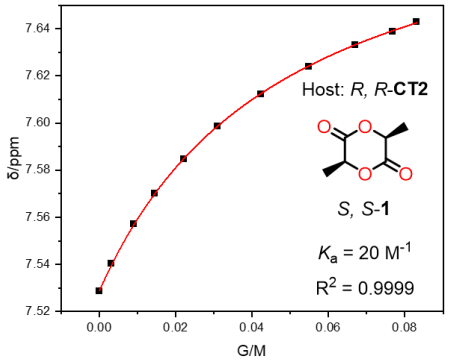

	K_a /M^{-1}	R^2
Titration-1	20	0.9999
Titration-2	21	0.9996
Titration-3	23	0.9998
Average	21±1	

Figure *S26*. *Left*: Partial ^{1}H NMR spectra (500 MHz, Toluene-d_8, 298 K) of *R,R*-**CT1** (0.5 mM) titrated by *R,R*-**1**. From bottom to top, the concentration range of 1 is 0 ~ 83.03 mM. *Right*: Nonlinear curve fitting for the complexation between *R,R*-**CT1** and *R,R*-**1** based on the NMR data.

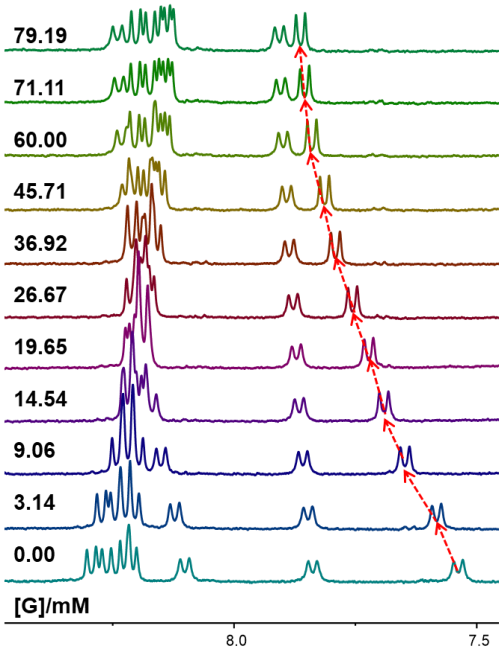

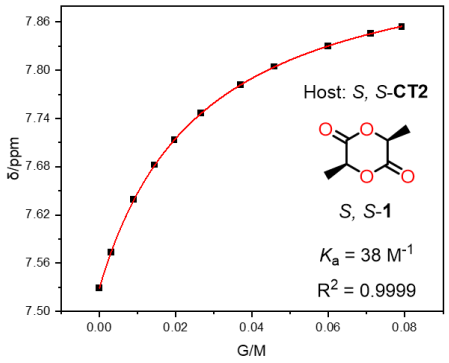

	K_a /M^{-1}	R^2
Titration-1	38	0.9999
Titration-2	42	0.9997
Titration-2	43	0.9979
Average	41±2	

Figure *S27*. *Left*: Partial ^{1}H NMR spectra (500 MHz, Toluene-d_8, 298 K) of *S,S*-**CT1** (0.5 mM) titrated by *R,R*-**1**. From bottom to top, the concentration range of 1 is 0 ~ 79.19 mM. *Right*: Nonlinear curve fitting for the complexation between *S,S*-**CT1** and *R,R*-**1** based on the NMR data.

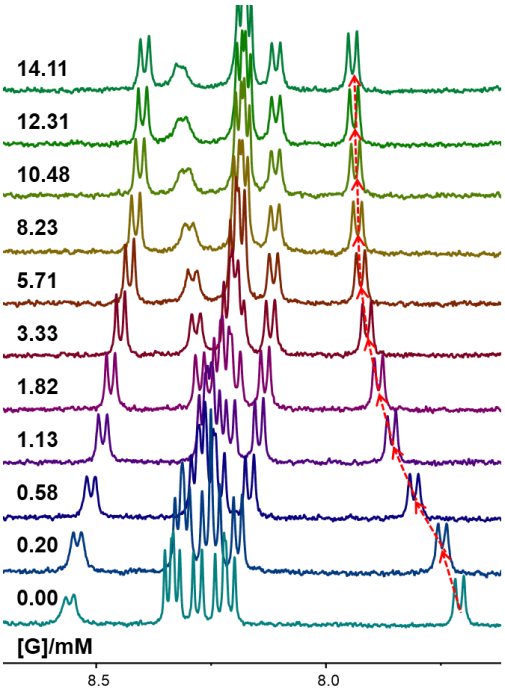

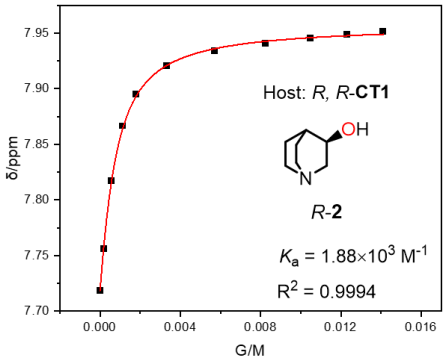

	K_a /M^{-1}	R^2
Titration-1	1.88×10^3	0.9994
Titration-2	1.67×10^3	0.9996
Titration-3	1.77×10^3	0.9991
Average	(1.7±0.1)×10^3	

Figure *S28*. *Left*: Partial ^{1}H NMR spectra (500 MHz, Toluene-d$_8$, 298 K) of *R,R*-**CT1** (0.5 mM) titrated by *R*-**2**. From bottom to top, the concentration range of 1 is 0 ~ 14.11 mM. *Right*: Nonlinear curve fitting for the complexation between *R,R*-**CT1** and *R*-**2** based on the NMR data.

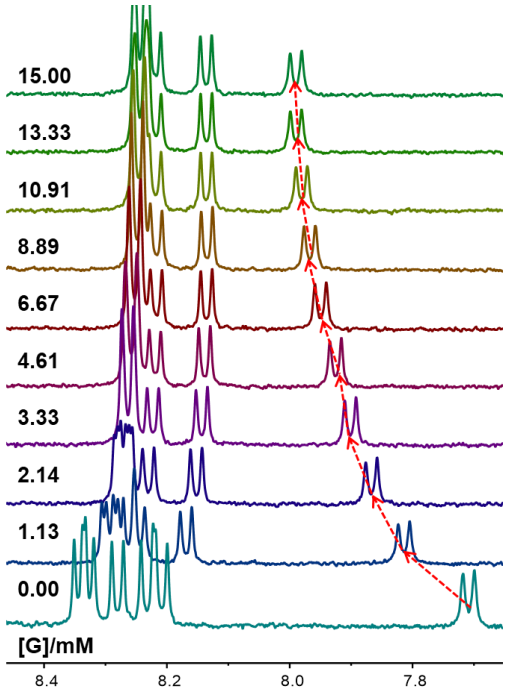

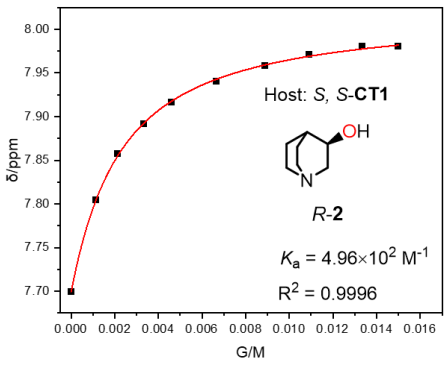

	K_a /M^{-1}	R^2
Titration-1	4.96×10^2	0.9996
Titration-2	4.93×10^2	0.9994
Titration-3	5.21×10^2	0.9995
Average	(5.0±0.1)×10^2	

Figure *S29*. *Left*: Partial ^{1}H NMR spectra (500 MHz, Toluene-d$_8$, 298 K) of *S,S*-**CT1** (0.5 mM) titrated by *R*-**2**. From bottom to top, the concentration range of 1 is 0 ~ 16.00 mM. *Right*: Nonlinear curve fitting for the complexation between *S,S*-**CT1** and *R*-**2** based on the NMR data.

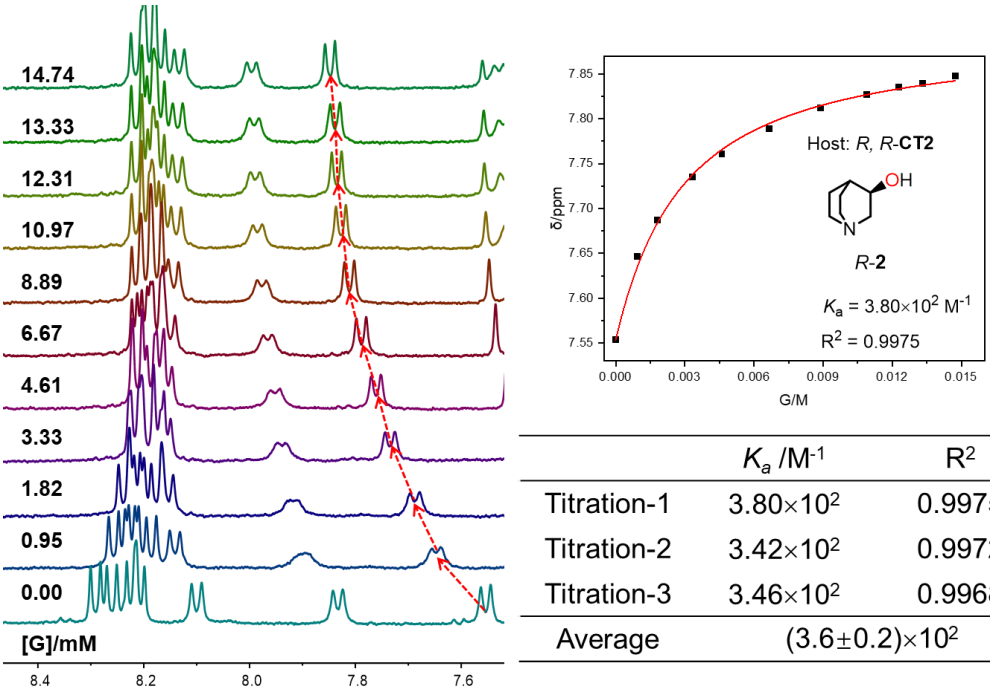

	K_a /M^{-1}	R^2
Titration-1	3.80×10^2	0.9975
Titration-2	3.42×10^2	0.9972
Titration-3	3.46×10^2	0.9968
Average	$(3.6\pm0.2)\times10^2$	

Figure *S30*. *Left*: Partial ^{1}H NMR spectra (500 MHz, Toluene-d$_8$, 298 K) of *R,R*-**CT2** (0.5 mM) titrated by *R*-**2**. From bottom to top, the concentration range of 1 is 0 ~ 14.74 mM. *Right*: Nonlinear curve fitting for the complexation between *R,R*-**CT2** and *R*-**2** based on the NMR data.

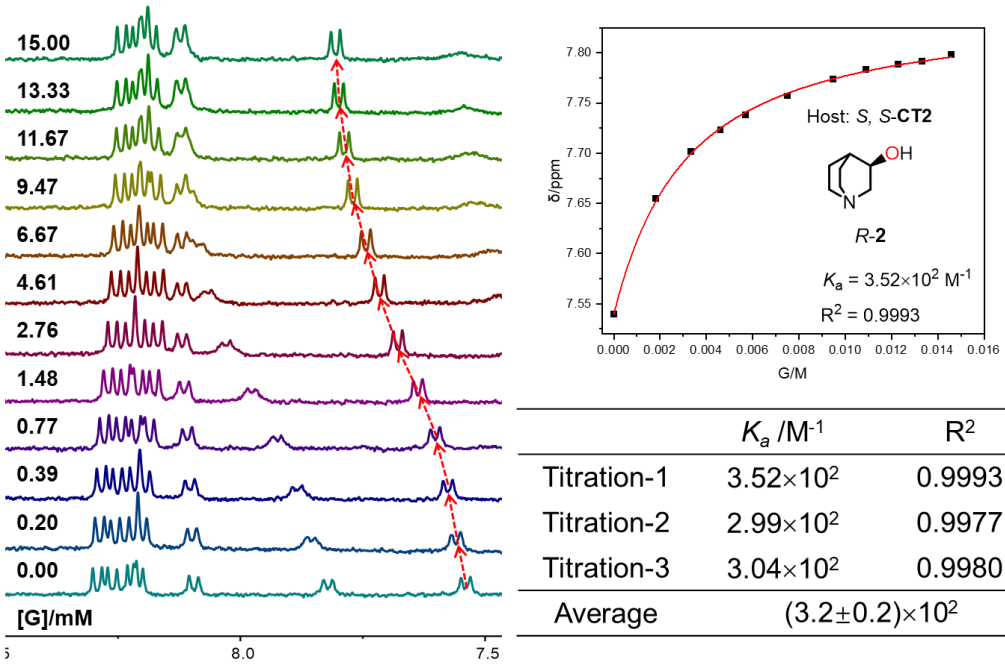

	K_a /M^{-1}	R^2
Titration-1	3.52×10^2	0.9993
Titration-2	2.99×10^2	0.9977
Titration-3	3.04×10^2	0.9980
Average	$(3.2\pm0.2)\times10^2$	

Figure *S31*. *Left*: Partial ^{1}H NMR spectra (500 MHz, Toluene-d$_8$, 298 K) of *S,S*-**CT2** (0.5 mM) titrated by *R*-**2**. From bottom to top, the concentration range of 1 is 0 ~ 15.00 mM. *Right*: Nonlinear curve fitting for the complexation between *S,S*-**CT2** and *R*-**2** based on the NMR data.

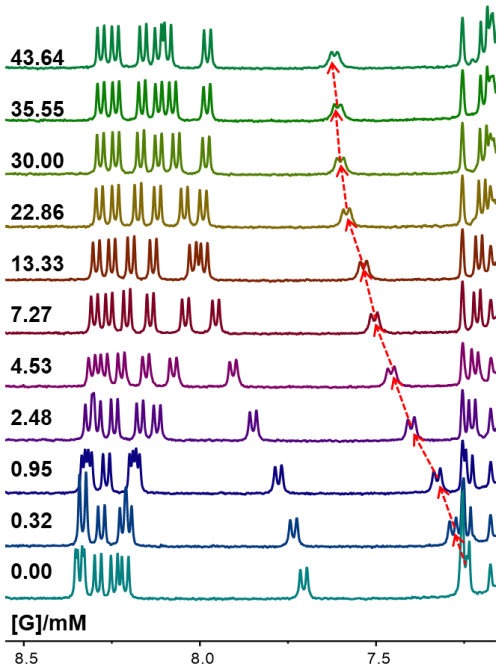

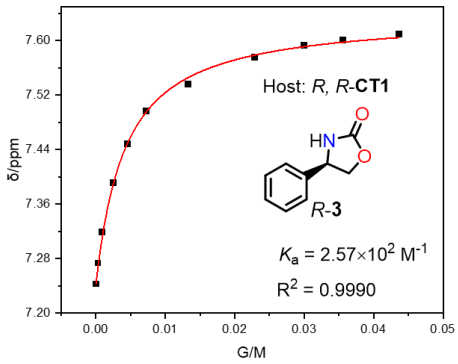

	K_a /M^{-1}	R^2
Titration-1	2.57×10^2	0.9990
Titration-2	2.18×10^2	0.9990
Titration-3	2.11×10^2	0.9993
Average	(2.3±0.2)×10^2	

Figure *S32*. *Left*: Partial ^{1}H NMR spectra (500 MHz, Toluene-d$_8$, 298 K) of *R,R*-**CT1** (0.5 mM) titrated by *R*-**3**. From bottom to top, the concentration range of 1 is 0 ~ 43.64 mM. *Right*: Nonlinear curve fitting for the complexation between *R,R*-**CT1** and *R*-**3** based on the NMR data.

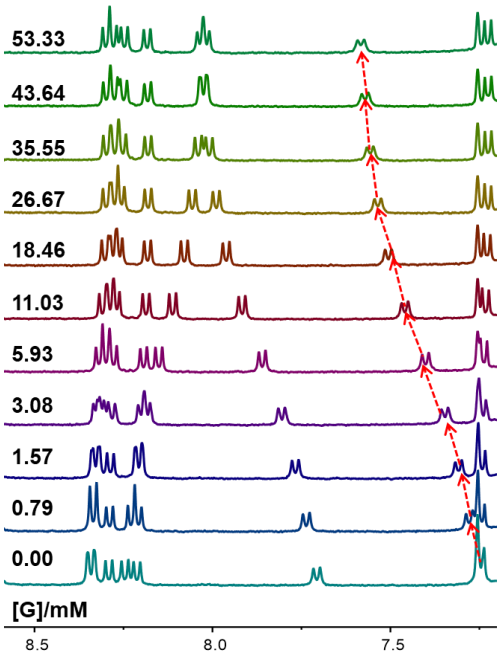

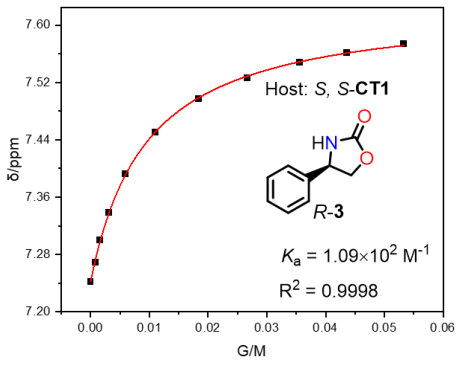

	K_a /M^{-1}	R^2
Titration-1	1.09×10^2	0.9998
Titration-2	1.06×10^2	0.9986
Titration-3	1.28×10^2	0.991
Average	(1.1±0.1)×10^2	

Figure *S33*. *Left*: Partial ^{1}H NMR spectra (500 MHz, Toluene-d$_8$, 298 K) of *S,S*-**CT1** (0.5 mM) titrated by *R*-**3**. From bottom to top, the concentration range of 1 is 0 ~ 53.33 mM. *Right*: Nonlinear curve fitting for the complexation between *S,S*-**CT1** and *R*-**3** based on the NMR data.

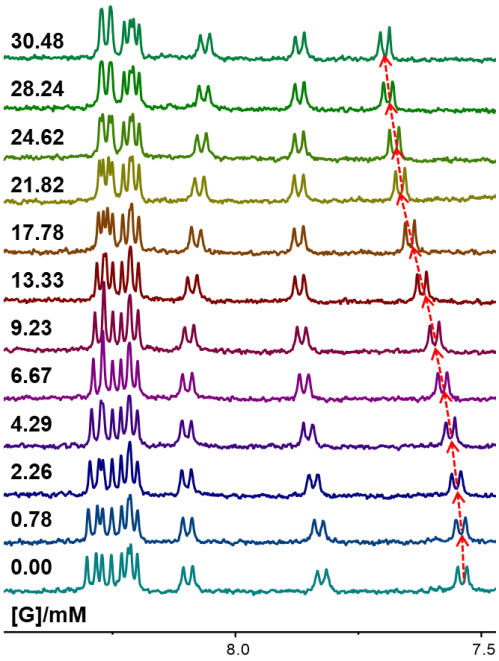

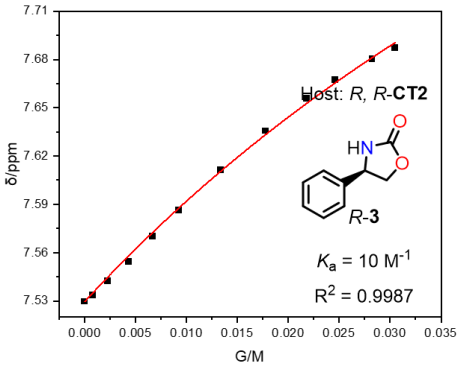

	K_a /M^{-1}	R^2
Titration-1	10	0.9987
Titration-2	9	0.9982
Titration-3	10	0.9983
Average	9±1	

Figure *S34*. *Left*: Partial ^{1}H NMR spectra (500 MHz, Toluene-d$_8$, 298 K) of *R,R*-**CT2** (0.5 mM) titrated by *R*-**3**. From bottom to top, the concentration range of 1 is 0 ~ 30.48 mM. *Right*: Nonlinear curve fitting for the complexation between *R,R*-**CT2** and *R*-**3** based on the NMR data.

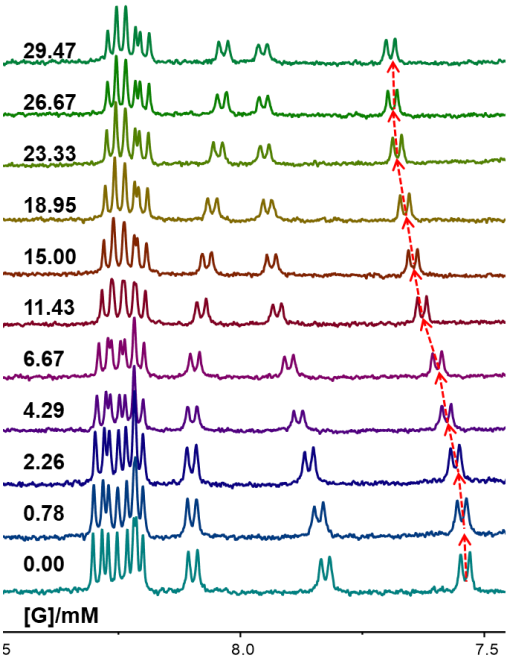

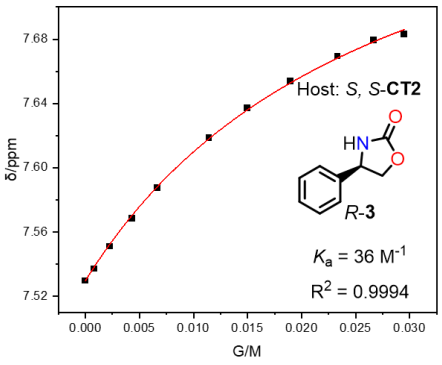

	K_a /M^{-1}	R^2
Titration-1	36	0.9994
Titration-2	37	0.9994
Titration-3	35	0.9995
Average	36±1	

Figure *S35*. *Left*: Partial ^{1}H NMR spectra (500 MHz, Toluene-d$_8$, 298 K) of *S,S*-**CT2** (0.5 mM) titrated by *R*-**3**. From bottom to top, the concentration range of 1 is 0 ~ 29.47 mM. *Right*: Nonlinear curve fitting for the complexation between *S,S*-**CT2** and *R*-**3** based on the NMR data.

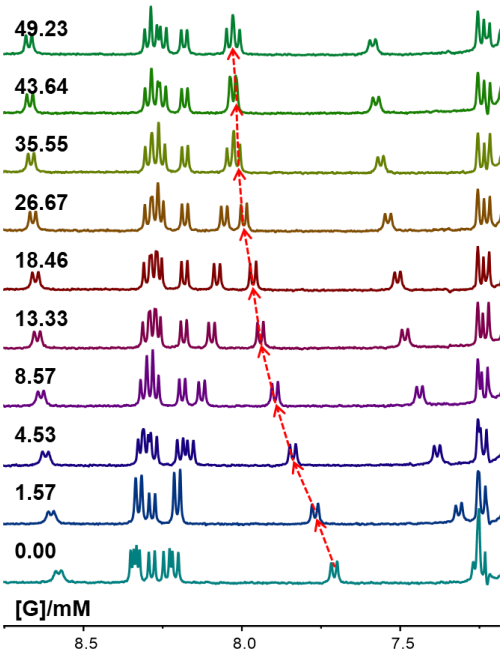

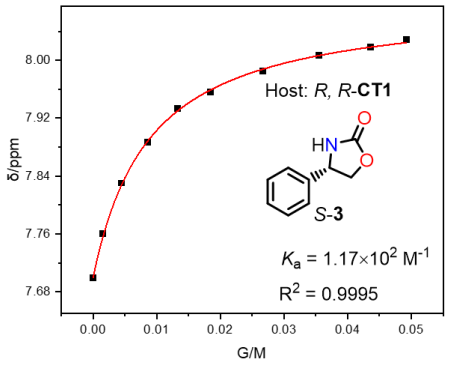

	K_a /M^{-1}	R^2
Titration-1	1.17×10^2	0.9995
Titration-2	1.11×10^2	0.9993
Titration-3	1.06×10^2	0.9997
Average	(1.1±0.1)×10^2	

Figure *S36*. *Left*: Partial ^{1}H NMR spectra (500 MHz, Toluene-d$_8$, 298 K) of *R,R*-**CT1** (0.5 mM) titrated by *S*-**3**. From bottom to top, the concentration range of 1 is 0 ~ 49.23 mM. *Right*: Nonlinear curve fitting for the complexation between *R,R*-**CT1** and *S*-**3** based on the NMR data.

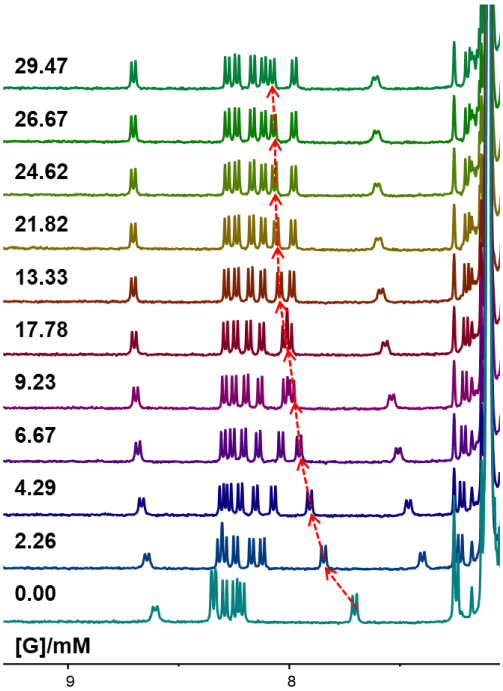

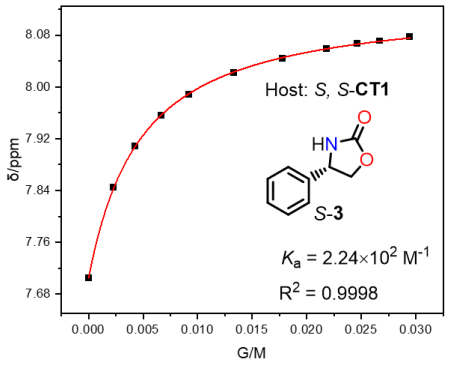

	K_a /M^{-1}	R^2
Titration-1	2.24×10^2	0.9998
Titration-2	2.47×10^2	0.9996
Titration-3	2.26×10^2	0.9998
Average	(2.3±0.1)×10^2	

Figure *S37*. *Left*: Partial ^{1}H NMR spectra (500 MHz, Toluene-d$_8$, 298 K) of *S,S*-**CT1** (0.5 mM) titrated by *S*-**3**. From bottom to top, the concentration range of 1 is 0 ~ 29.47 mM. *Right*: Nonlinear curve fitting for the complexation between *S,S*-**CT1** and *S*-**3** based on the NMR data.

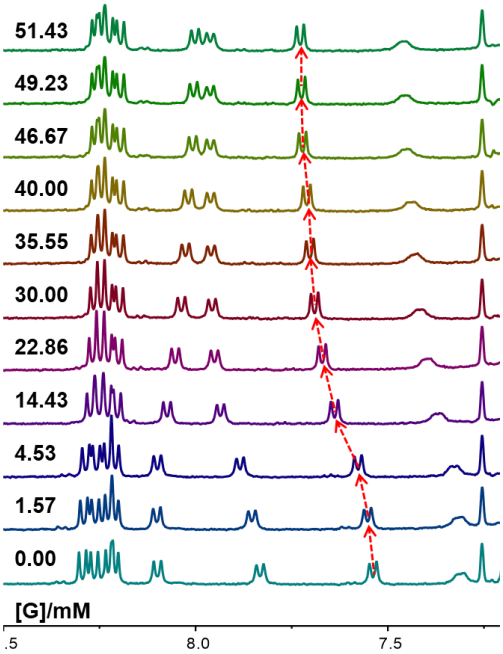

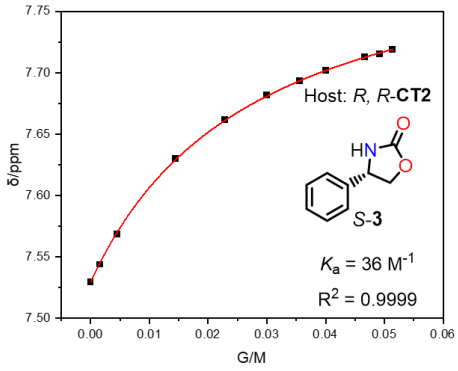

	K_a /M^{-1}	R^2
Titration-1	36	0.9999
Titration-2	37	0.9999
Titration-3	33	0.9998
Average	35±2	

Figure *S38*. *Left*: Partial ^{1}H NMR spectra (500 MHz, Toluene-d$_8$, 298 K) of *R,R*-**CT2** (0.5 mM) titrated by *S*-**3**. From bottom to top, the concentration range of 1 is 0 ~ 51.43 mM. *Right*: Nonlinear curve fitting for the complexation between *R,R*-**CT2** and *S*-**3** based on the NMR data.

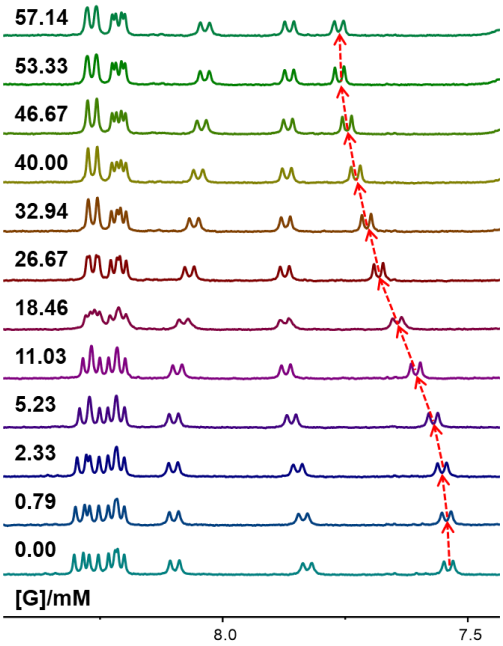

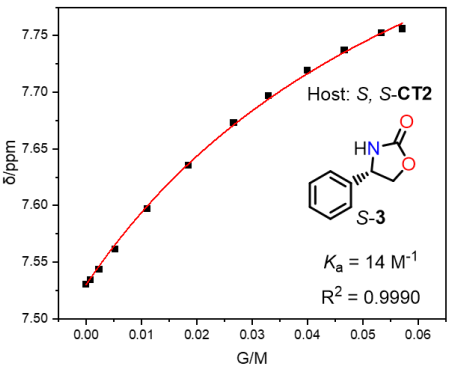

	K_a /M^{-1}	R^2
Titration-1	14	0.9990
Titration-2	13	0.9973
Titration-3	13	0.9994
Average	13±1	

Figure *S39*. *Left*: Partial ^{1}H NMR spectra (500 MHz, Toluene-d$_8$, 298 K) of *S,S*-**CT2** (0.5 mM) titrated by *S*-**3**. From bottom to top, the concentration range of 1 is 0 ~ 57.14 mM. *Right*: Nonlinear curve fitting for the complexation between *S,S*-**CT2** and *S*-**3** based on the NMR data.

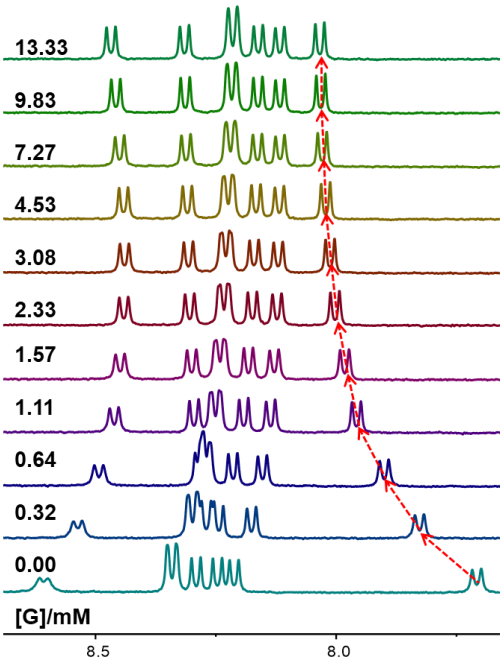

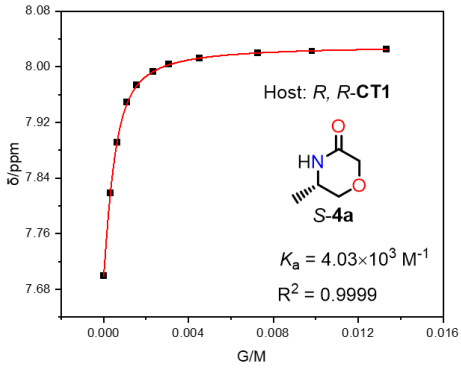

	K_a /M^{-1}	R^2
Titration-1	4.03×10^3	0.9999
Titration-2	3.79×10^3	0.9998
Titration-3	4.43×10^3	0.9997
Average	(4.1±0.3)×10^3	

Figure *S40*. *Left*: Partial ^{1}H NMR spectra (500 MHz, Toluene-d$_8$, 298 K) of *R,R*-**CT1** (0.5 mM) titrated by *S*-**4a**. From bottom to top, the concentration range of 1 is 0 ~ 13.33 mM. *Right*: Nonlinear curve fitting for the complexation between *R,R*-**CT1** and *S*-**4a** based on the NMR data.

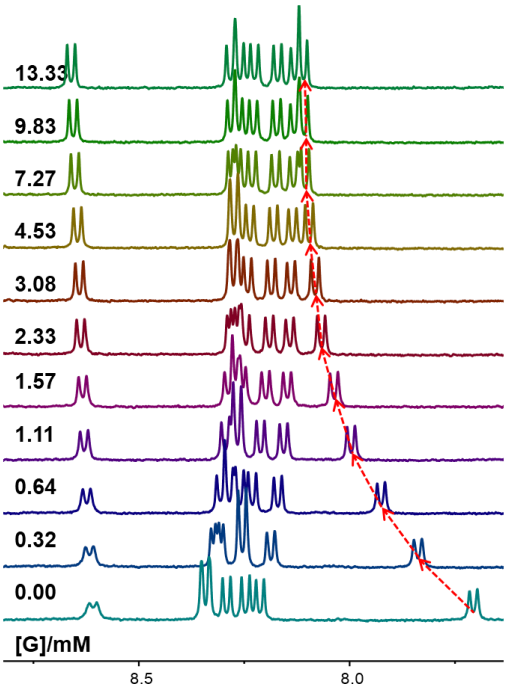

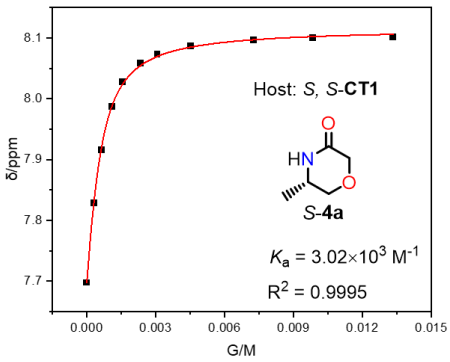

	K_a /M^{-1}	R^2
Titration-1	3.02×10^3	0.9995
Titration-2	3.29×10^3	0.9994
Titration-3	3.36×10^3	0.9997
Average	(3.2±0.1)×10^3	

Figure *S41*. *Left*: Partial ^{1}H NMR spectra (500 MHz, Toluene-d$_8$, 298 K) of *S,S*-**CT1** (0.5 mM) titrated by *S*-**4a**. From bottom to top, the concentration range of 1 is 0 ~ 1.33 mM. *Right*: Nonlinear curve fitting for the complexation between *S,S*-**CT1** and *S*-**4a** based on the NMR data.

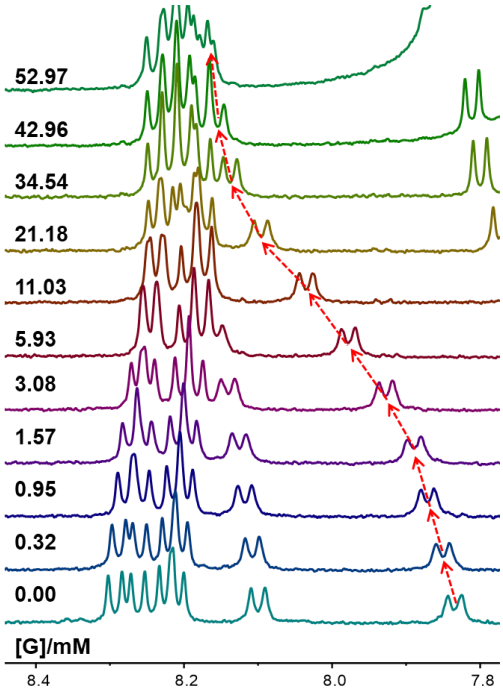

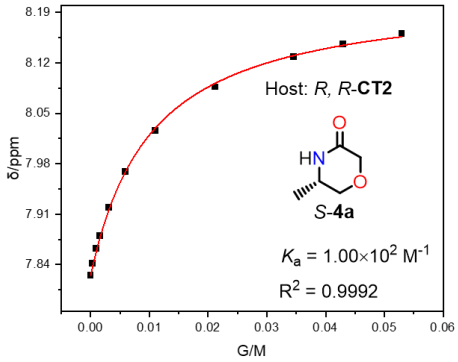

	K_a /M^{-1}	R^2
Titration-1	1.00×10^2	0.9992
Titration-2	0.83×10^2	0.9998
Titration-3	0.80×10^2	0.9998
Average	90 ± 1	

Figure *S42*. *Left*: Partial ^{1}H NMR spectra (500 MHz, Toluene-d$_8$, 298 K) of *R,R*-**CT2** (0.5 mM) titrated by *S*-**4a**. From bottom to top, the concentration range of 1 is 0 ~ 52.97 mM. *Right*: Nonlinear curve fitting for the complexation between *R,R*-**CT2** and *S*-**4a** based on the NMR data.

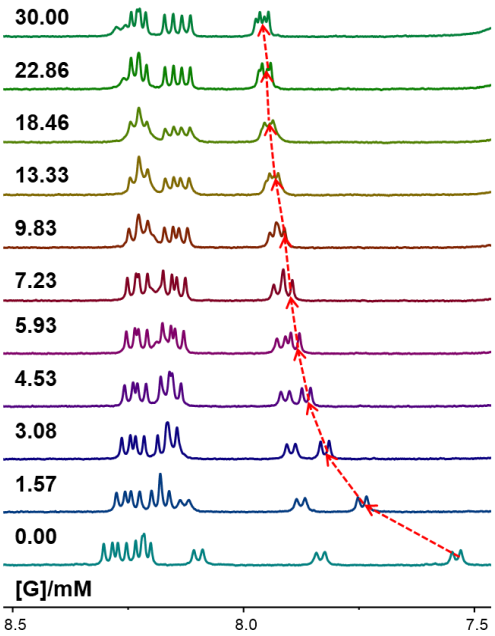

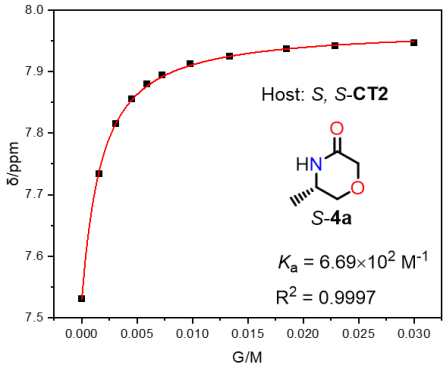

	K_a /M^{-1}	R^2
Titration-1	6.69×10^2	0.9997
Titration-2	6.67×10^2	0.9993
Titration-3	6.54×10^2	0.9998
Average	$(6.6\pm0.1)\times10^2$	

Figure *S43*. *Left*: Partial ^{1}H NMR spectra (500 MHz, Toluene-d$_8$, 298 K) of *S,S*-**CT2** (0.5 mM) titrated by *S*-**4a**. From bottom to top, the concentration range of 1 is 0 ~ 30.00 mM. *Right*: Nonlinear curve fitting for the complexation between *S,S*-**CT2** and *S*-**4a** based on the NMR data.

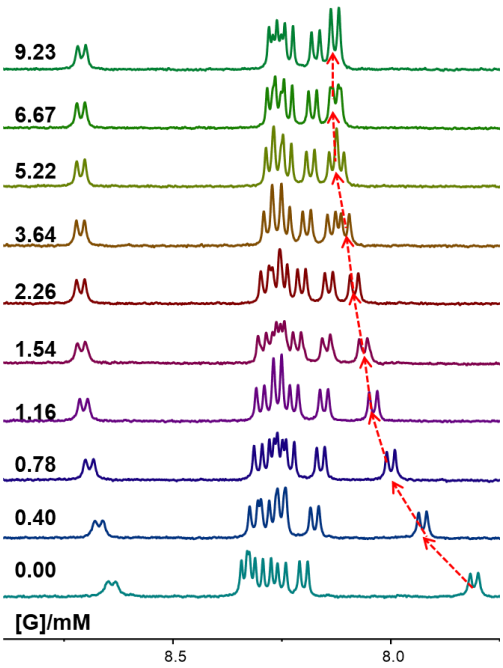

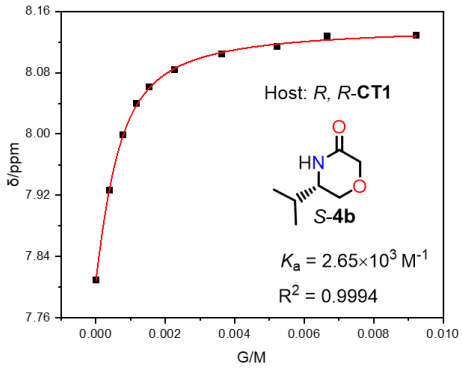

	K_a /M^{-1}	R^2
Titration-1	2.65×10^3	0.9994
Titration-2	3.01×10^3	0.9998
Titration-3	2.88×10^3	0.9986
Average	(2.8±0.1)×10^3	

Figure *S44*. *Left*: Partial ^{1}H NMR spectra (500 MHz, Toluene-d$_8$, 298 K) of *R,R*-**CT1** (0.5 mM) titrated by *S*-**4b**. From bottom to top, the concentration range of 1 is 0 ~ 9.23 mM. *Right*: Nonlinear curve fitting for the complexation between *R,R*-**CT1** and *S*-**4b** based on the NMR data.

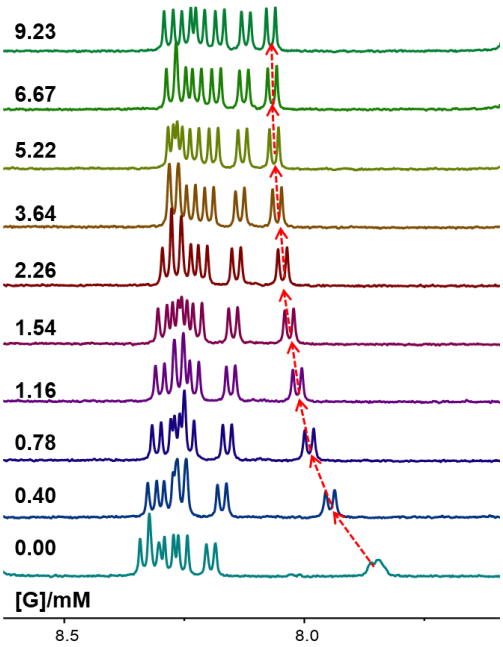

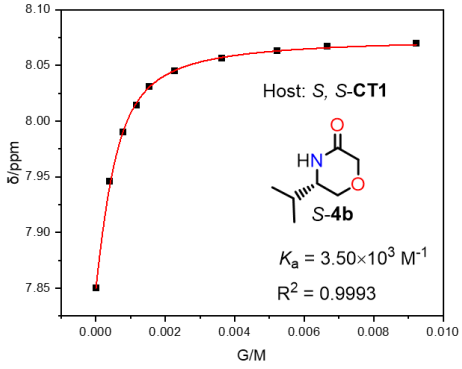

	K_a /M^{-1}	R^2
Titration-1	3.50×10^3	0.9993
Titration-2	2.81×10^3	0.9994
Titration-3	3.13×10^3	0.9998
Average	(3.1±0.3)×10^3	

Figure *S45*. *Left*: Partial ^{1}H NMR spectra (500 MHz, Toluene-d$_8$, 298 K) of *S,S*-**CT1** (0.5 mM) titrated by *S*-**4b**. From bottom to top, the concentration range of 1 is 0 ~ 9.23 mM. *Right*: Nonlinear curve fitting for the complexation between *S,S*-**CT1** and *S*-**4b** based on the NMR data.

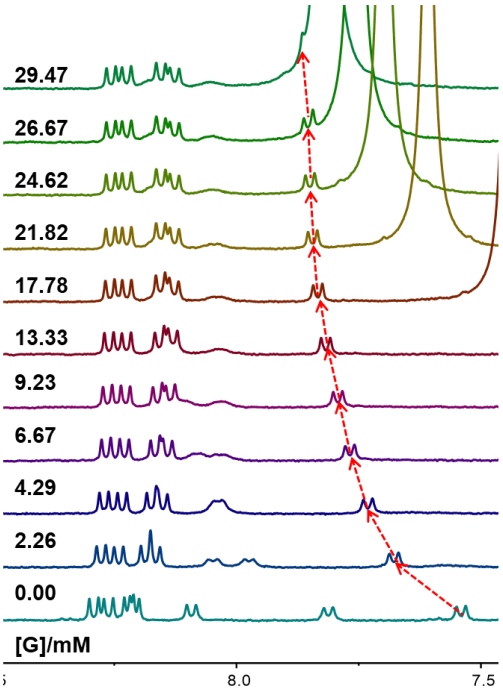

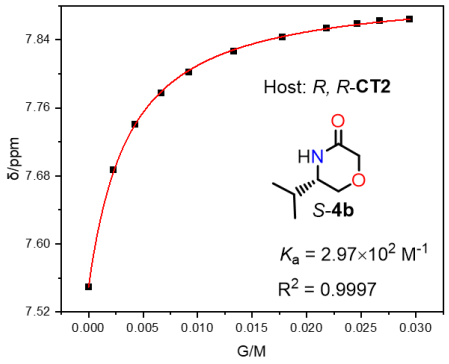

	K_a /M^{-1}	R^2
Titration-1	2.97×10^2	0.9997
Titration-2	4.17×10^2	0.9989
Titration-3	3.15×10^2	0.9995
Average	(3.4±0.5)×10^2	

Figure *S46*. *Left*: Partial ^{1}H NMR spectra (500 MHz, Toluene-d$_8$, 298 K) of *R,R*-**CT2** (0.5 mM) titrated by *S*-**4b**. From bottom to top, the concentration range of 1 is 0 ~ 29.47 mM. *Right*: Nonlinear curve fitting for the complexation between *R,R*-**CT2** and *S*-**4b** based on the NMR data.

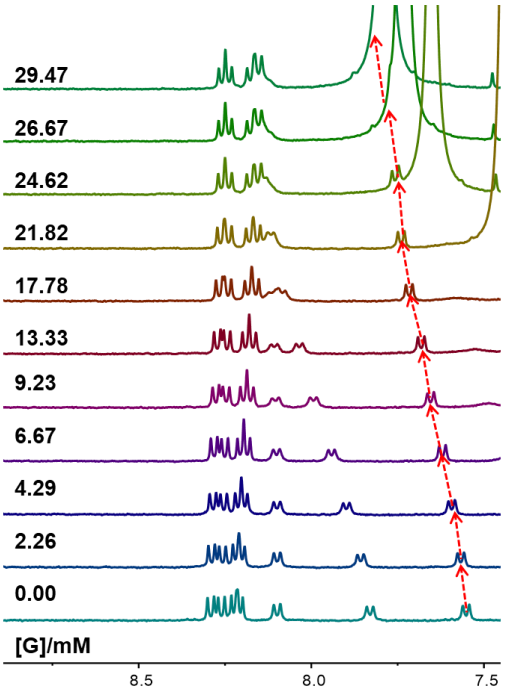

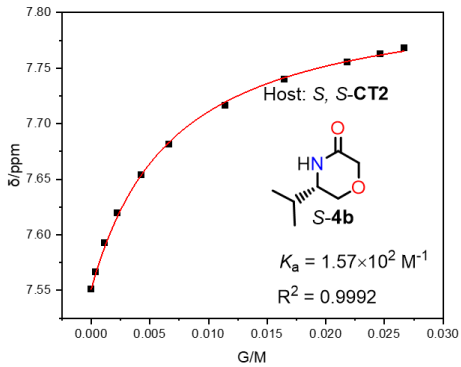

	K_a /M^{-1}	R^2
Titration-1	1.57×10^2	0.9992
Titration-2	1.72×10^2	0.9994
Titration-3	2.08×10^2	0.9998
Average	(1.8±0.2)×10^2	

Figure *S47*. *Left*: Partial ^{1}H NMR spectra (500 MHz, Toluene-d$_8$, 298 K) of *S,S*-**CT2** (0.5 mM) titrated by *S*-**4b**. From bottom to top, the concentration range of 1 is 0 ~ 29.47 mM. *Right*: Nonlinear curve fitting for the complexation between *S,S*-**CT2** and *S*-**4b** based on the NMR data.

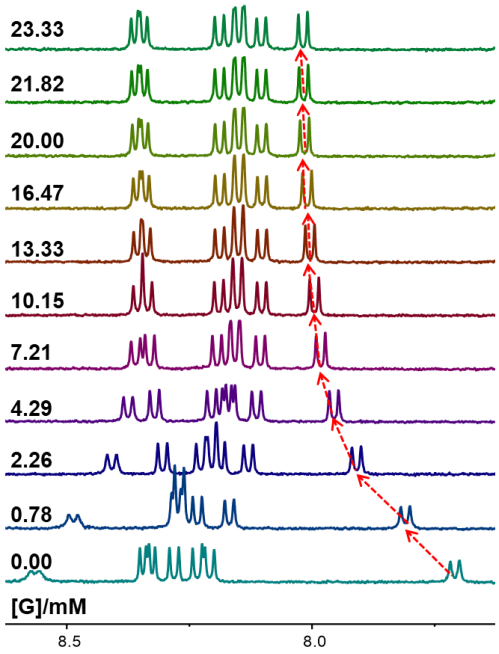

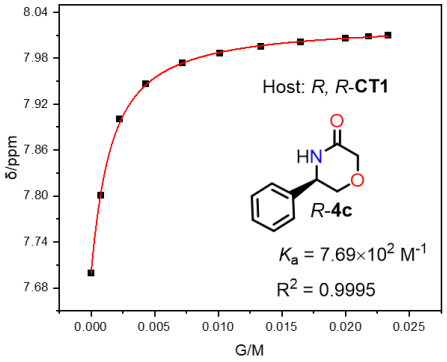

	K_a /M^{-1}	R^2
Titration-1	7.69×10^2	0.9995
Titration-2	8.63×10^2	0.9998
Titration-3	7.63×10^2	0.9993
Average	(8.0±0.4)×10^2	

Figure *S48*. *Left*: Partial ^{1}H NMR spectra (500 MHz, Toluene-d$_8$, 298 K) of *R,R*-**CT1** (0.5 mM) titrated by *R*-**4c**. From bottom to top, the concentration range of 1 is 0 ~ 23.33 mM. *Right*: Nonlinear curve fitting for the complexation between *R,R*-**CT1** and *R*-**4c** based on the NMR data.

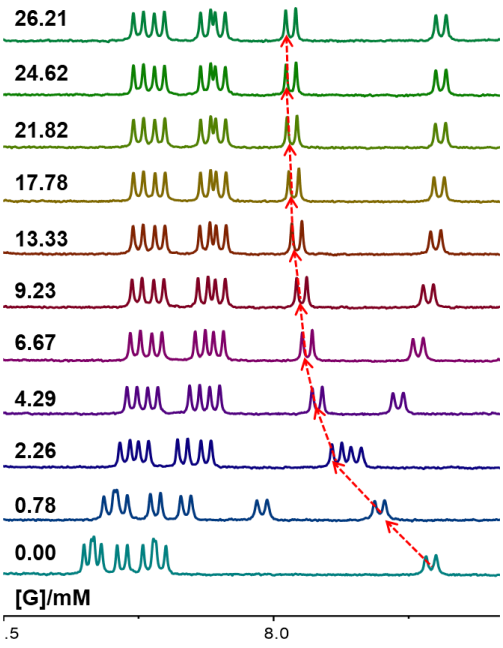

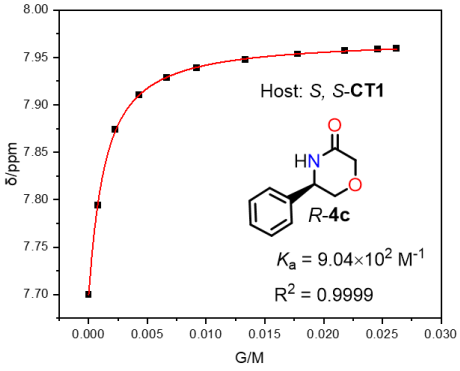

	K_a /M^{-1}	R^2
Titration-1	9.04×10^2	0.9999
Titration-2	8.89×10^2	0.9999
Titration-3	8.97×10^2	0.9999
Average	(9.0±0.1)×10^2	

Figure *S49*. *Left*: Partial ^{1}H NMR spectra (500 MHz, Toluene-d$_8$, 298 K) of *S,S*-**CT1** (0.5 mM) titrated by *R*-**4c**. From bottom to top, the concentration range of 1 is 0 ~ 26.21 mM. *Right*: Nonlinear curve fitting for the complexation between *S,S*-**CT1** and *R*-**4c** based on the NMR data.

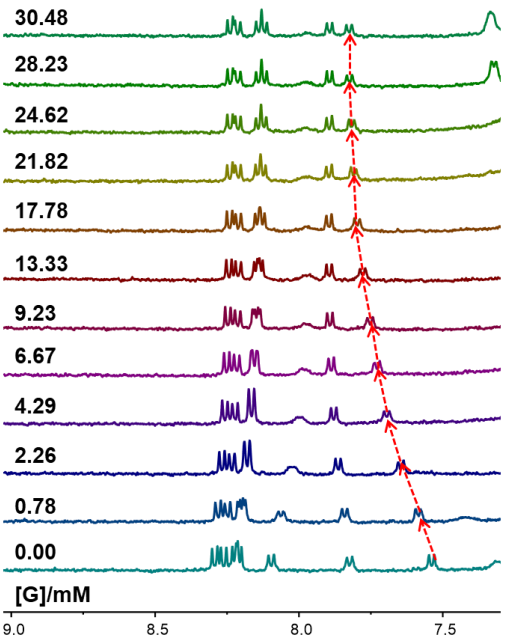

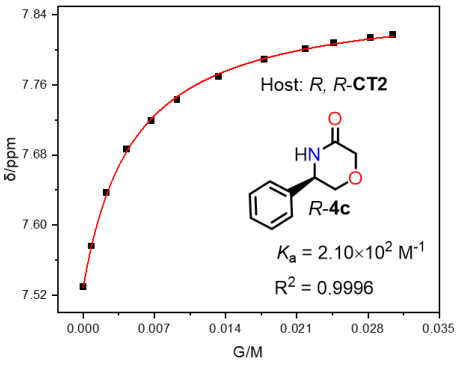

	K_a /M^{-1}	R^2
Titration-1	2.10×10^2	0.9996
Titration-2	2.09×10^2	0.9995
Titration-3	2.19×10^2	0.9995
Average	$(2.1\pm0.1)\times10^2$	

Figure *S50*. *Left*: Partial ^{1}H NMR spectra (500 MHz, Toluene-d$_8$, 298 K) of *R,R*-**CT2** (0.5 mM) titrated by *R*-**4c**. From bottom to top, the concentration range of 1 is 0 ~ 30.48 mM. *Right*: Nonlinear curve fitting for the complexation between *R,R*-**CT2** and *R*-**4c** based on the NMR data.

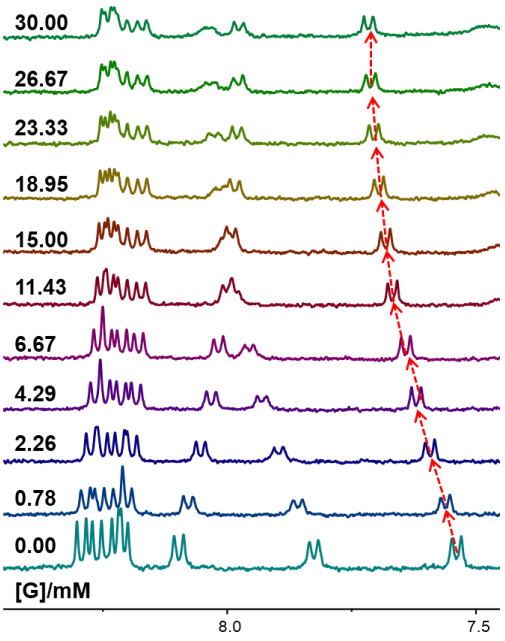

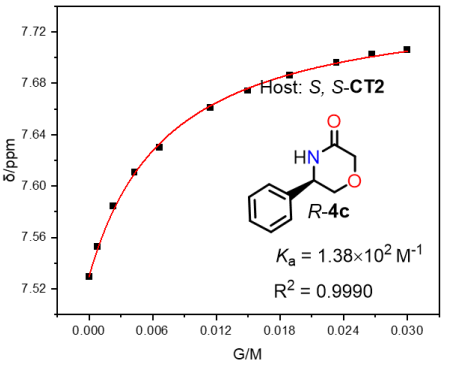

	K_a /M^{-1}	R^2
Titration-1	1.38×10^2	0.9990
Titration-2	1.58×10^2	0.9987
Titration-3	1.67×10^2	0.9998
Average	$(1.5\pm0.1)\times10^2$	

Figure *S51*. *Left*: Partial ^{1}H NMR spectra (500 MHz, Toluene-d$_8$, 298 K) of *S,S*-**CT2** (0.5 mM) titrated by *R*-**4c**. From bottom to top, the concentration range of 1 is 0 ~ 30.00 mM. *Right*: Nonlinear curve fitting for the complexation between *S,S*-**CT2** and *R*-**4c** based on the NMR data.

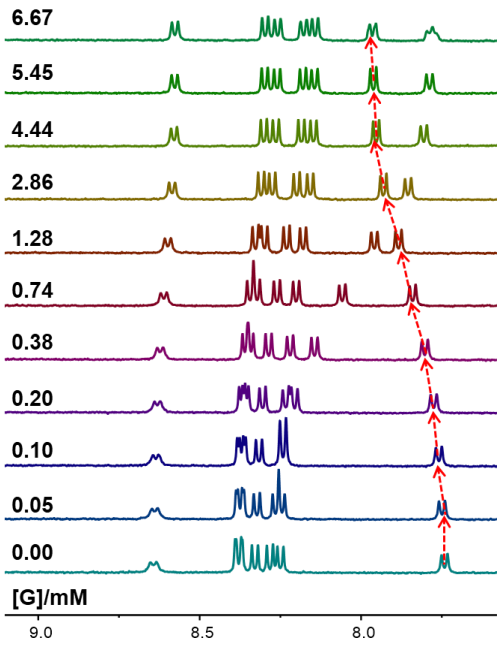

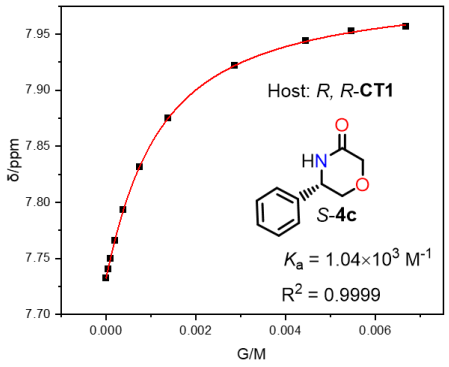

	K_a /M^{-1}	R^2
Titration-1	1.04×10^3	0.9999
Titration-2	1.09×10^3	0.9998
Titration-3	1.11×10^3	0.9998
Average	$(1.1\pm0.1)\times10^3$	

Figure *S52*. *Left*: Partial ^{1}H NMR spectra (500 MHz, Toluene-d$_8$, 298 K) of *R,R*-**CT1** (0.5 mM) titrated by *S*-**4c**. From bottom to top, the concentration range of 1 is 0 ~ 6.67 mM. *Right*: Nonlinear curve fitting for the complexation between *R,R*-**CT1** and *S*-**4c** based on the NMR data.

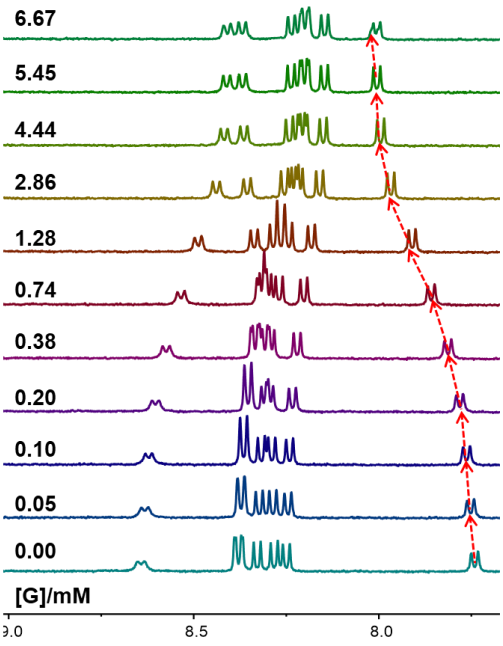

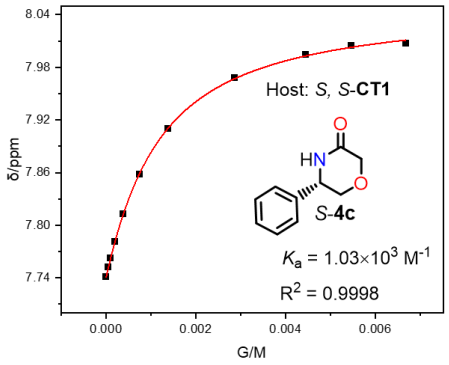

	K_a /M^{-1}	R^2
Titration-1	1.03×10^3	0.9998
Titration-2	1.19×10^3	0.9997
Titration-3	1.16×10^3	0.9998
Average	$(1.1\pm0.2)\times10^3$	

Figure *S53*. *Left*: Partial ^{1}H NMR spectra (500 MHz, Toluene-d$_8$, 298 K) of *S,S*-**CT1** (0.5 mM) titrated by *S*-**4c**. From bottom to top, the concentration range of 1 is 0 ~ 6.67 mM. *Right*: Nonlinear curve fitting for the complexation between *S,S*-**CT1** and *S*-**4c** based on the NMR data.

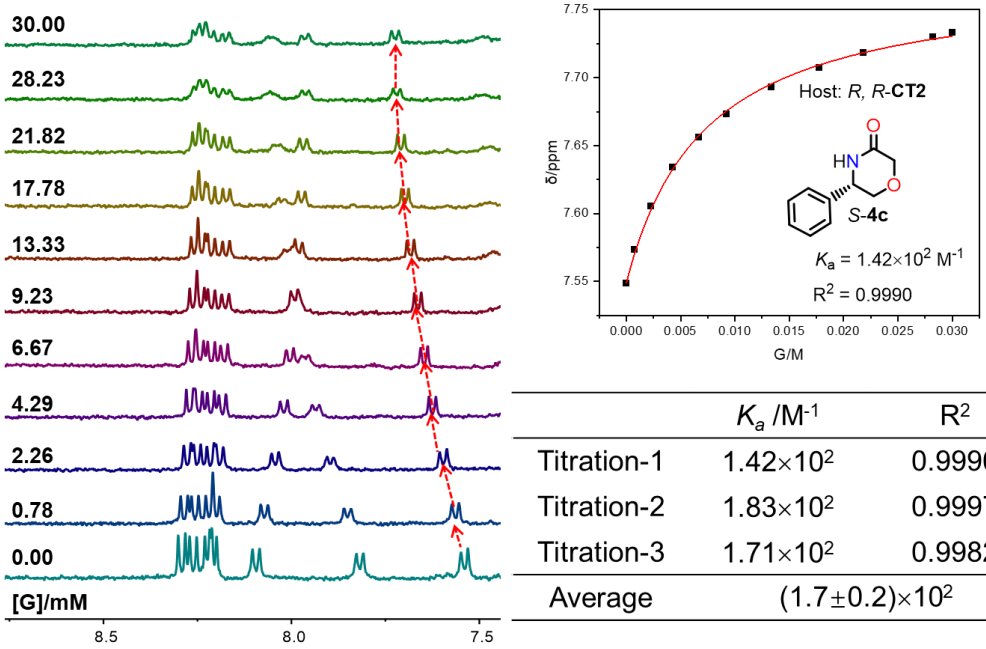

	K_a /M^{-1}	R^2
Titration-1	1.42×10^2	0.9990
Titration-2	1.83×10^2	0.9997
Titration-3	1.71×10^2	0.9982
Average	$(1.7\pm0.2)\times10^2$	

Figure *S54*. *Left*: Partial ^{1}H NMR spectra (500 MHz, Toluene-d$_8$, 298 K) of *R,R*-**CT2** (0.5 mM) titrated by *S*-**4c**. From bottom to top, the concentration range of 1 is 0 ~ 30.00 mM. *Right*: Nonlinear curve fitting for the complexation between *R,R*-**CT2** and *S*-**4c** based on the NMR data.

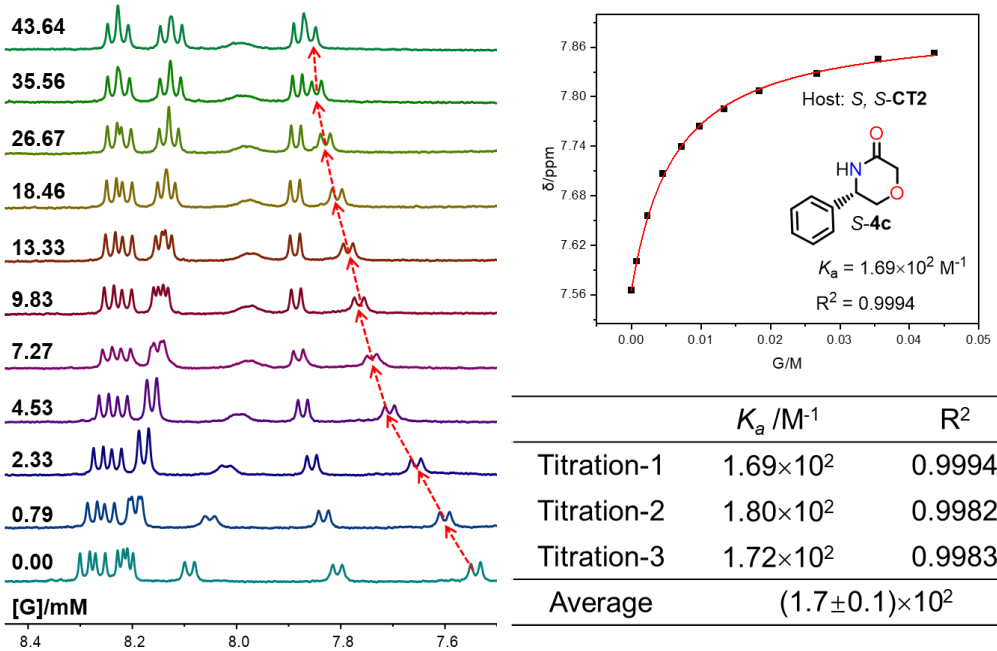

	K_a /M^{-1}	R^2
Titration-1	1.69×10^2	0.9994
Titration-2	1.80×10^2	0.9982
Titration-3	1.72×10^2	0.9983
Average	$(1.7\pm0.1)\times10^2$	

Figure *S55*. *Left*: Partial ^{1}H NMR spectra (500 MHz, Toluene-d$_8$, 298 K) of *S,S*-**CT2** (0.5 mM) titrated by *S*-**4c**. From bottom to top, the concentration range of 1 is 0 ~ 43.64 mM. *Right*: Nonlinear curve fitting for the complexation between *S,S*-**CT2** and *S*-**4c** based on the NMR data.

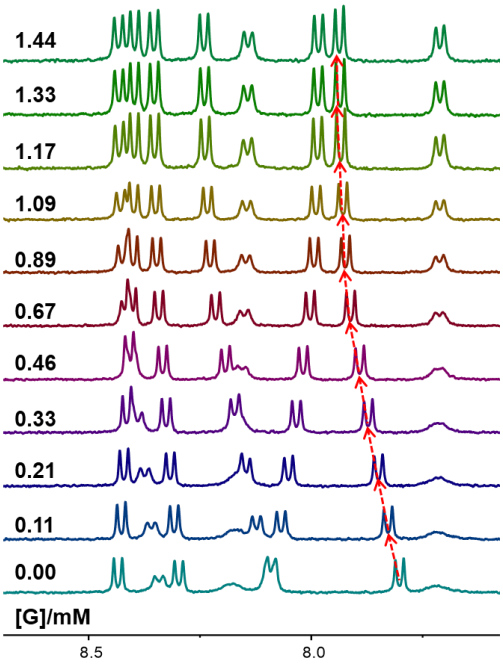

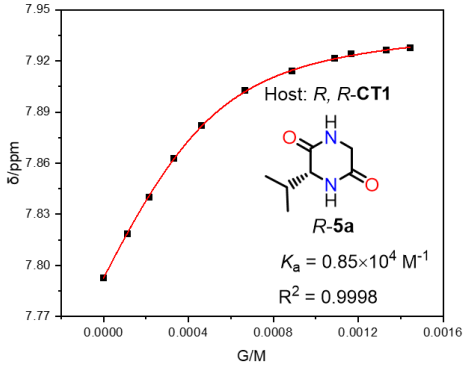

	K_a /M^{-1}	R^2
Titration-1	0.85×10^4	0.9998
Titration-2	1.09×10^4	0.9998
Titration-3	1.02×10^4	0.9999
Average	(1.0±0.1)×10^4	

Figure *S56*. *Left*: Partial ^{1}H NMR spectra (500 MHz, $CDCl_3$, 298 K) of *R,R*-**CT1** (0.5 mM) titrated by *R*-**5a**. From bottom to top, the concentration range of 1 is 0 ~ 1.44 mM. *Right*: Nonlinear curve fitting for the complexation between *R,R*-**CT1** and *R*-**5a** based on the NMR data.

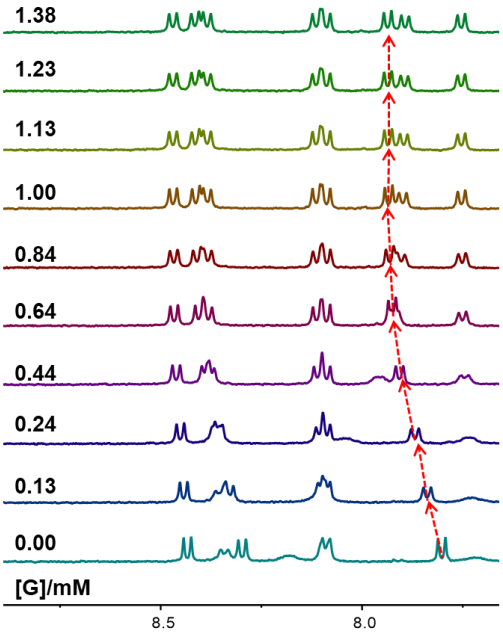

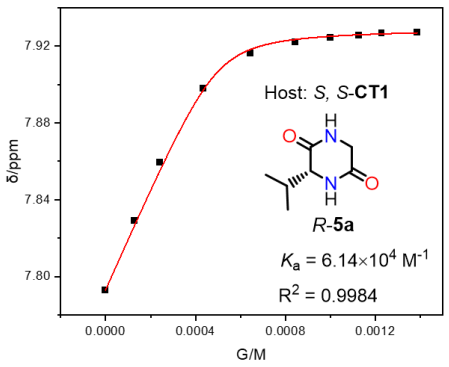

	K_a /M^{-1}	R^2
Titration-1	6.14×10^4	0.9984
Titration-2	5.43×10^4	0.9992
Titration-3	5.13×10^4	0.9992
Average	(5.6±0.4)×10^4	

Figure *S57*. *Left*: Partial ^{1}H NMR spectra (500 MHz, $CDCl_3$, 298 K) of *S,S*-**CT1** (0.5 mM) titrated by *R*-**5a**. From bottom to top, the concentration range of 1 is 0 ~ 1.38 mM. *Right*: Nonlinear curve fitting for the complexation between *S,S*-**CT1** and *R*-**5a** based on the NMR data.

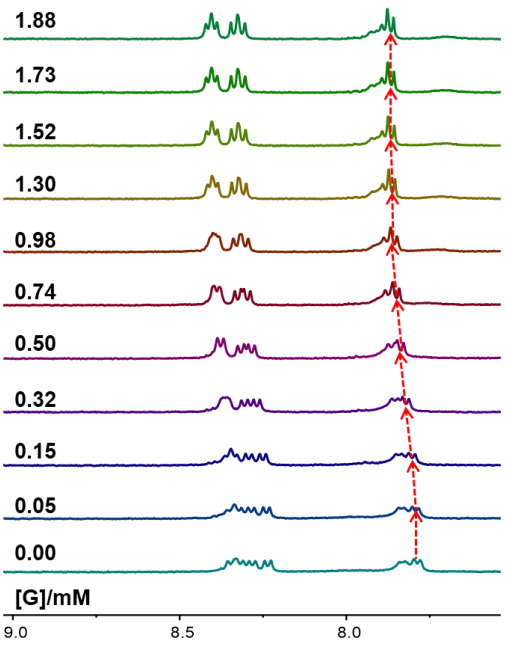

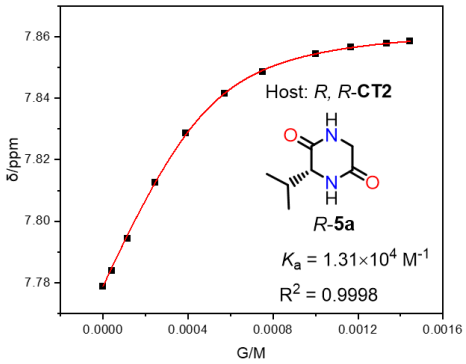

	K_a /M^{-1}	R^2
Titration-1	1.31×10^4	0.9998
Titration-2	1.74×10^4	0.9996
Titration-3	1.50×10^4	0.9996
Average	$(1.5\pm0.2)\times10^4$	

Figure *S58*. *Left*: Partial ^{1}H NMR spectra (500 MHz, $CDCl_3$, 298 K) of *R,R*-**CT2** (0.5 mM) titrated by *R*-**5a**. From bottom to top, the concentration range of 1 is 0 ~ 1.88 mM. *Right*: Nonlinear curve fitting for the complexation between *R,R*-**CT2** and *R*-**5a** based on the NMR data.

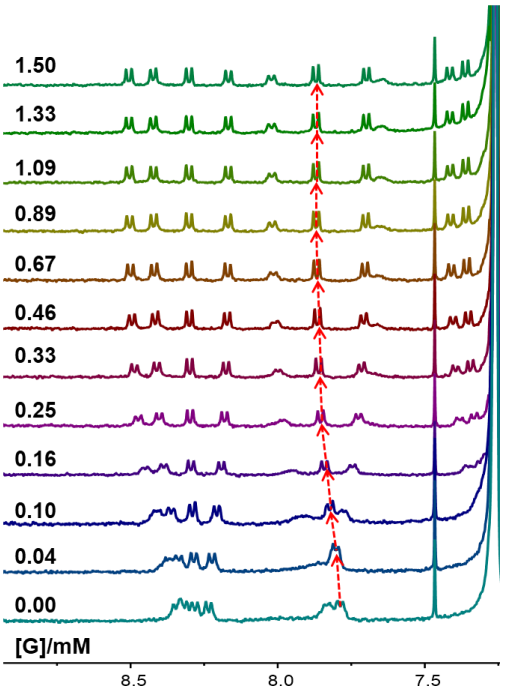

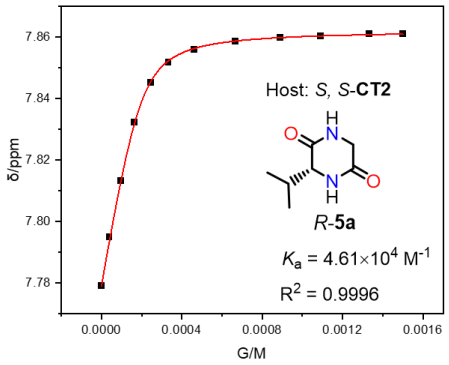

	K_a /M^{-1}	R^2
Titration-1	4.61×10^4	0.9996
Titration-2	4.35×10^4	0.9992
Titration-3	4.82×10^4	0.9999
Average	$(4.6\pm0.2)\times10^4$	

Figure *S59*. *Left*: Partial ^{1}H NMR spectra (500 MHz, $CDCl_3$, 298 K) of *S,S*-**CT2** (0.5 mM) titrated by *R*-**5a**. From bottom to top, the concentration range of 1 is 0 ~ 1.50 mM. *Right*: Nonlinear curve fitting for the complexation between *S,S*-**CT2** and *R*-**5a** based on the NMR data.

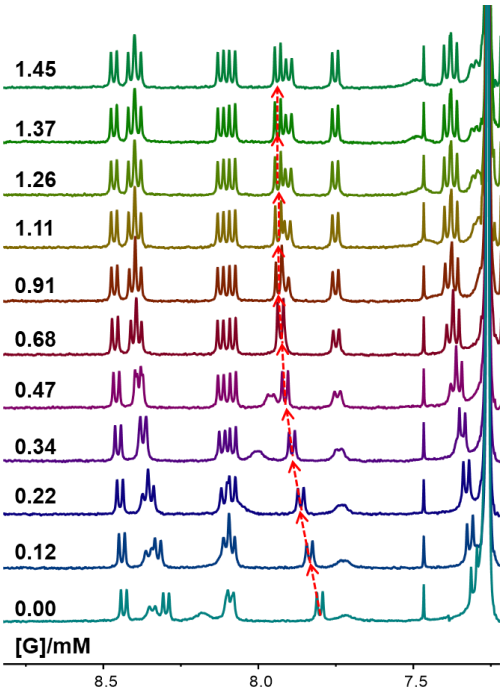

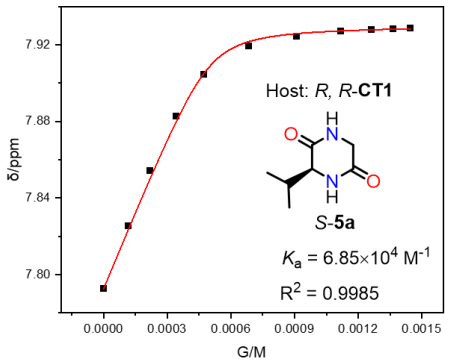

	K_a /M^{-1}	R^2
Titration-1	6.85×10^4	0.9985
Titration-2	6.34×10^4	0.9977
Titration-3	6.97×10^4	0.9974
Average	(6.7±0.3)×10^4	

Figure *S60*. *Left*: Partial ^{1}H NMR spectra (500 MHz, $CDCl_3$, 298 K) of *R,R*-**CT1** (0.5 mM) titrated by *S*-**5a**. From bottom to top, the concentration range of 1 is 0 ~ 1.45 mM. *Right*: Nonlinear curve fitting for the complexation between *R,R*-**CT1** and *S*-**5a** based on the NMR data.

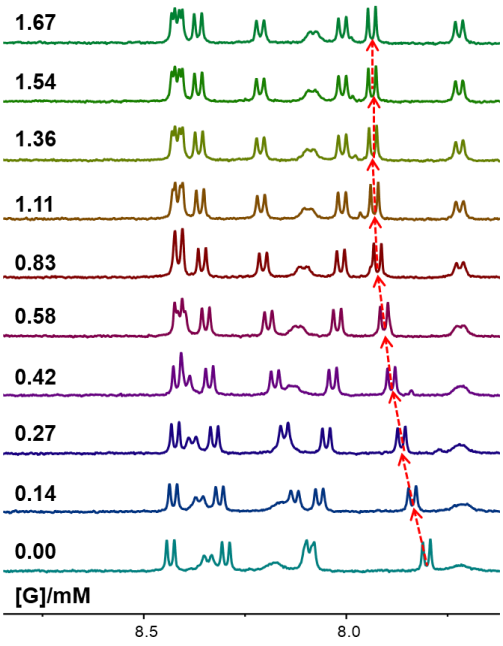

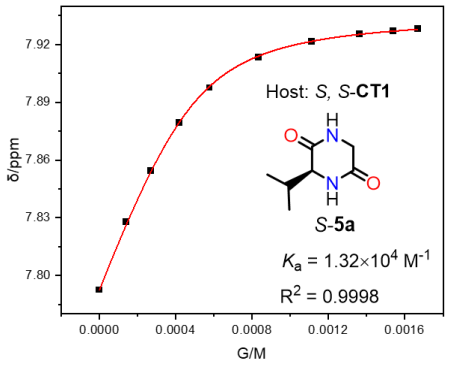

	K_a /M^{-1}	R^2
Titration-1	1.32×10^4	0.9998
Titration-2	1.45×10^4	0.9997
Titration-3	1.02×10^4	0.9999
Average	(1.3±0.2)×10^4	

Figure *S61*. *Left*: Partial ^{1}H NMR spectra (500 MHz, $CDCl_3$, 298 K) of *S,S*-**CT1** (0.5 mM) titrated by *S*-**5a**. From bottom to top, the concentration range of 1 is 0 ~ 1.45 mM. *Right*: Nonlinear curve fitting for the complexation between *S,S*-**CT1** and *S*-**5a** based on the NMR data.

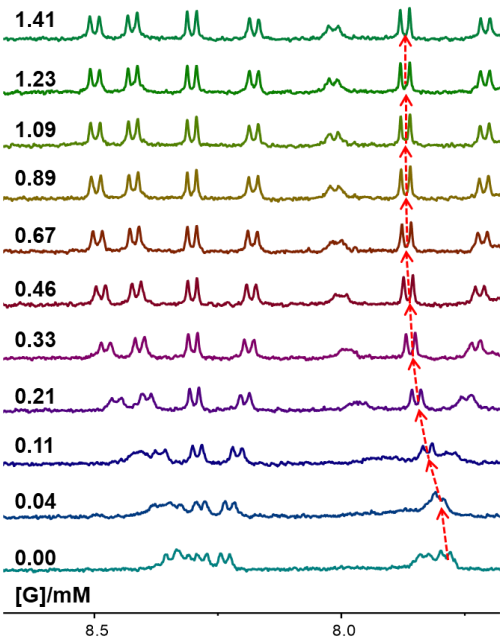

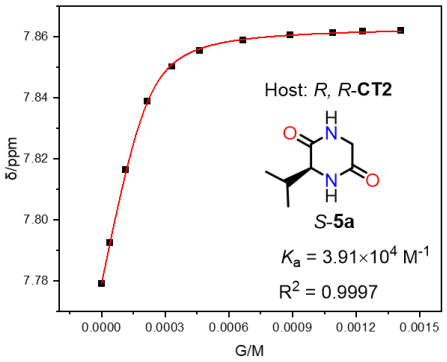

	K_a /M^{-1}	R^2
Titration-1	3.91×10^4	0.9997
Titration-2	4.33×10^4	0.9995
Titration-3	4.46×10^4	0.9980
Average	(4.2±0.2)×10^4	

Figure *S62*. *Left*: Partial ^{1}H NMR spectra (500 MHz, $CDCl_3$, 298 K) of *R,R*-**CT2** (0.5 mM) titrated by *S*-**5a**. From bottom to top, the concentration range of 1 is 0 ~ 40.00 mM. *Right*: Nonlinear curve fitting for the complexation between *R,R*-**CT2** and *S*-**5a** based on the NMR data.

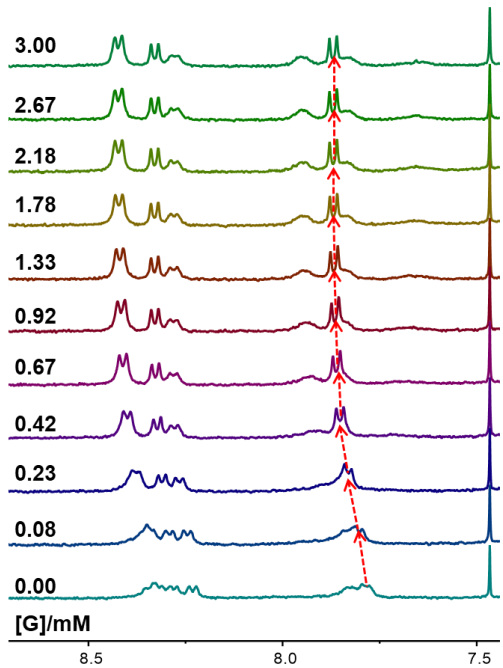

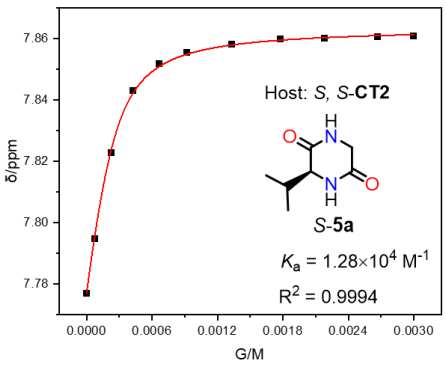

	K_a /M^{-1}	R^2
Titration-1	1.28×10^4	0.9994
Titration-2	1.14×10^4	0.9997
Titration-3	1.17×10^4	0.9997
Average	(1.2±0.1)×10^4	

Figure *S63*. *Left*: Partial ^{1}H NMR spectra (500 MHz, $CDCl_3$, 298 K) of *S,S*-**CT2** (0.5 mM) titrated by *S*-**5a**. From bottom to top, the concentration range of 1 is 0 ~ 3.00 mM. *Right*: Nonlinear curve fitting for the complexation between *S,S*-**CT2** and *S*-**5a** based on the NMR data.

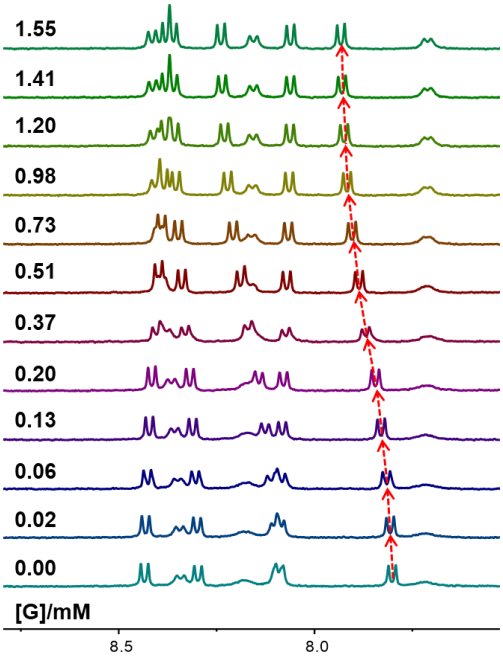

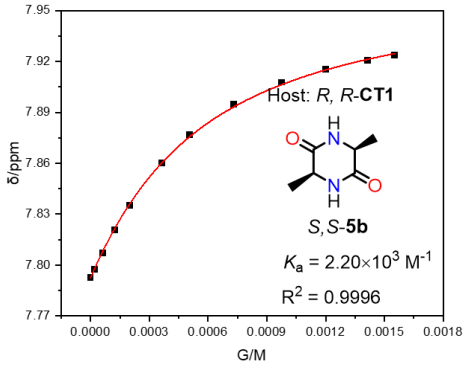

	K_a /M^{-1}	R^2
Titration-1	2.20×10^3	0.9996
Titration-2	2.61×10^3	0.9999
Titration-3	2.18×10^3	0.9994
Average	(2.3±0.2)×10^3	

Figure *S64*. *Left*: Partial ^{1}H NMR spectra (500 MHz, $CDCl_3$, 298 K) of *R,R*-**CT1** (0.5 mM) titrated by *R,R*-**5b**. From bottom to top, the concentration range of 1 is 0 ~ 1.55 mM. *Right*: Nonlinear curve fitting for the complexation between *R,R*-**CT1** and *R,R*-**5b** based on the NMR data.

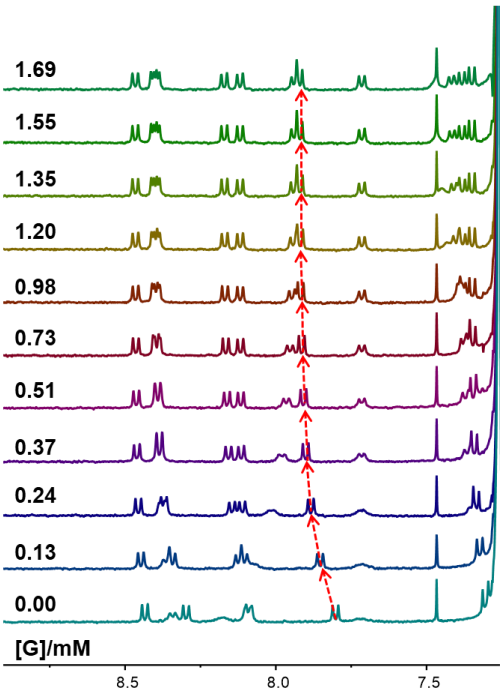

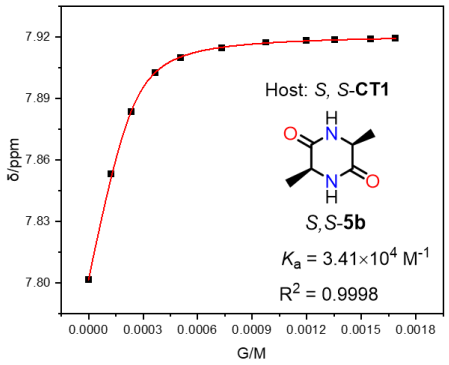

	K_a /M^{-1}	R^2
Titration-1	3.41×10^4	0.9998
Titration-2	4.05×10^4	0.9991
Titration-3	4.27×10^4	0.9986
Average	(3.9±0.4)×10^4	

Figure *S65*. *Left*: Partial ^{1}H NMR spectra (500 MHz, $CDCl_3$, 298 K) of *S,S*-**CT1** (0.5 mM) titrated by *R,R*-**5b**. From bottom to top, the concentration range of 1 is 0 ~ 1.69 mM. *Right*: Nonlinear curve fitting for the complexation between *S,S*-**CT1** and *R,R*-**5b** based on the NMR data.

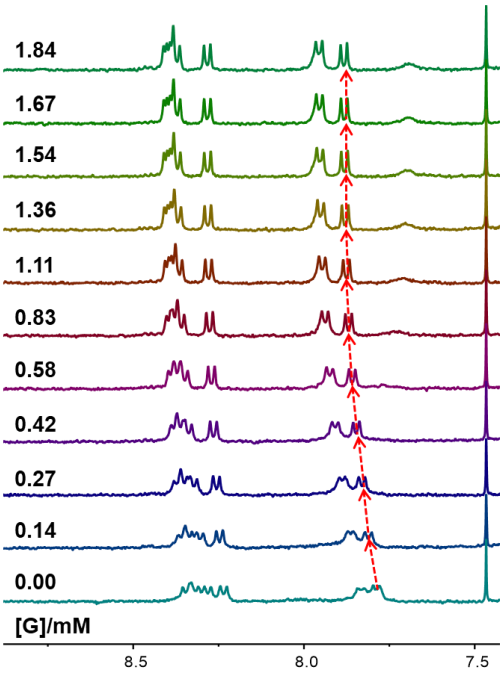

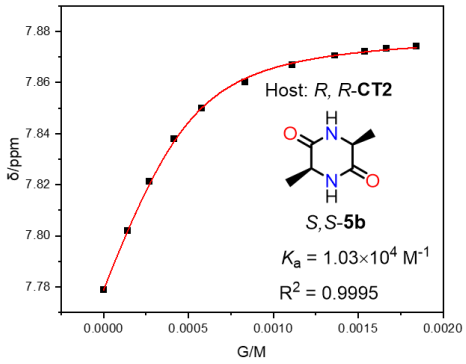

	K_a /M^{-1}	R^2
Titration-1	1.03×10^4	0.9995
Titration-2	0.96×10^4	0.9998
Titration-3	0.93×10^4	0.9995
Average	(1.0±0.1)×10^4	

Figure *S66*. *Left*: Partial ^{1}H NMR spectra (500 MHz, $CDCl_3$, 298 K) of *R,R*-**CT2** (0.5 mM) titrated by *R,R*-**5b**. From bottom to top, the concentration range of 1 is 0 ~ 1.84 mM. *Right*: Nonlinear curve fitting for the complexation between *R,R*-**CT2** and *R,R*-**5b** based on the NMR data.

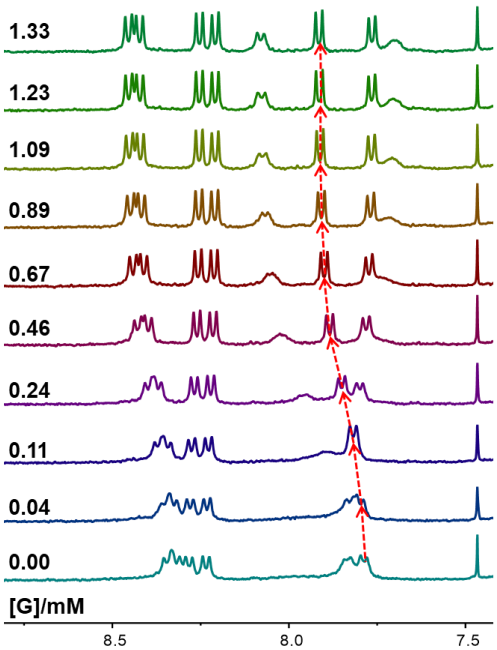

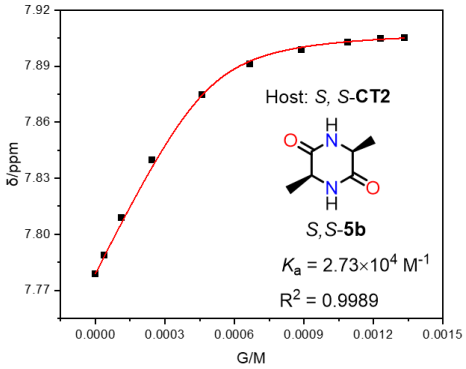

	K_a /M^{-1}	R^2
Titration-1	2.73×10^4	0.9989
Titration-2	3.01×10^4	0.9992
Titration-3	3.30×10^4	0.9981
Average	(3.0±0.2)×10^4	

Figure *S67*. *Left*: Partial ^{1}H NMR spectra (500 MHz, $CDCl_3$, 298 K) of *S,S*-**CT2** (0.5 mM) titrated by *S,S*-**5b**. From bottom to top, the concentration range of 1 is 0 ~ 1.33 mM. *Right*: Nonlinear curve fitting for the complexation between *S,S*-**CT2** and *S,S*-**5b** based on the NMR data.

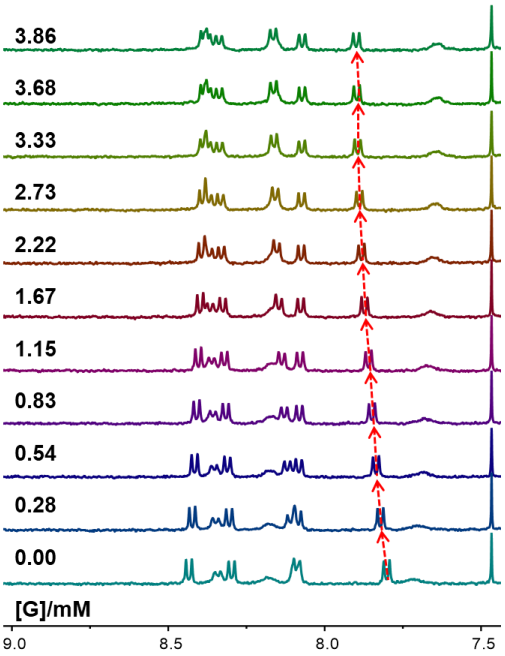

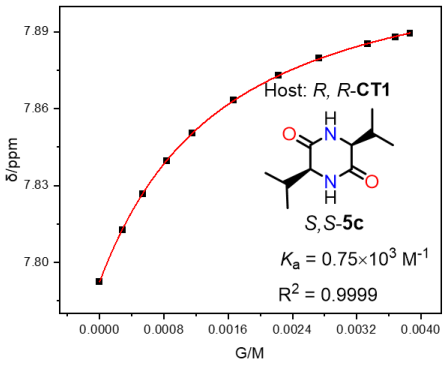

	K_a /M^{-1}	R^2
Titration-1	0.75×10^3	0.9999
Titration-2	0.83×10^3	0.9992
Titration-3	1.03×10^3	0.9999
Average	$(8.7\pm1.1)\times10^2$	

Figure *S68*. *Left*: Partial ^{1}H NMR spectra (500 MHz, $CDCl_3$, 298 K) of *R,R*-**CT1** (0.5 mM) titrated by *S,S*-**5c**. From bottom to top, the concentration range of 1 is 0 ~ 3.86 mM. *Right*: Nonlinear curve fitting for the complexation between *R,R*-**CT1** and *R,R*-**5c** based on the NMR data.

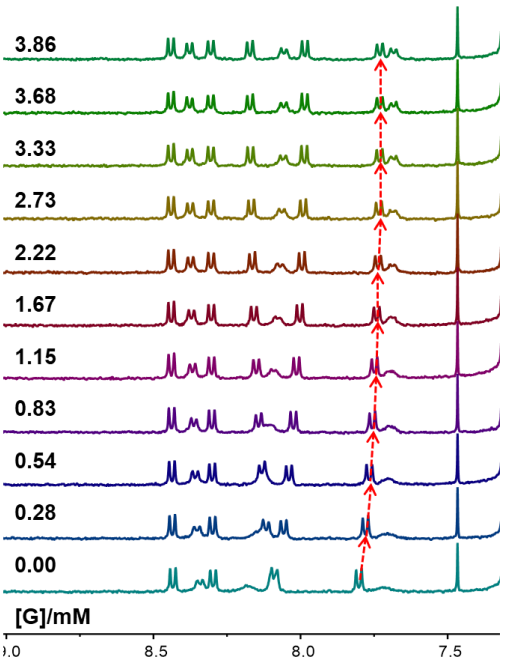

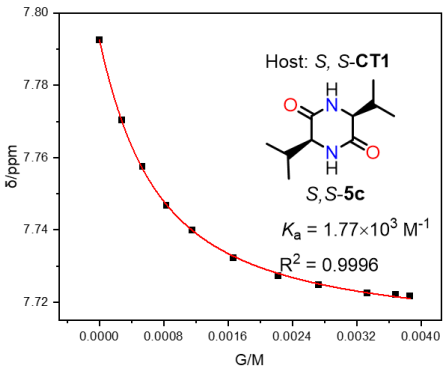

	K_a /M^{-1}	R^2
Titration-1	1.77×10^3	0.9996
Titration-2	1.87×10^3	0.9999
Titration-3	1.88×10^3	0.9999
Average	$(1.8\pm0.1)\times10^3$	

Figure *S69*. *Left*: Partial ^{1}H NMR spectra (500 MHz, $CDCl_3$, 298 K) of *S,S*-**CT1** (0.5 mM) titrated by *S,S*-**5c**. From bottom to top, the concentration range of 1 is 0 ~ 3.86 mM. *Right*: Nonlinear curve fitting for the complexation between *S,S*-**CT1** and *S,S*-**5c** based on the NMR data.

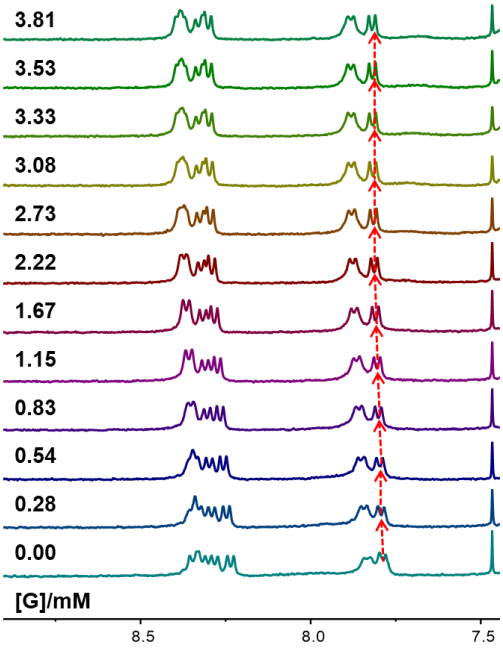

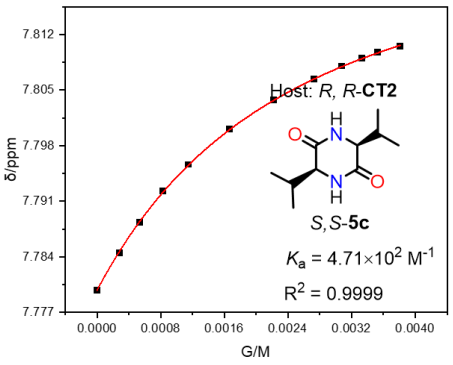

	K_a /M^{-1}	R^2
Titration-1	4.71×10^2	0.9999
Titration-2	5.41×10^2	0.9992
Titration-3	4.93×10^2	0.9994
Average	(5.0±0.3)×10^2	

Figure *S70*. *Left*: Partial ^{1}H NMR spectra (500 MHz, $CDCl_3$, 298 K) of *R,R*-**CT2** (0.5 mM) titrated by *S,S*-**5c**. From bottom to top, the concentration range of 1 is 0 ~ 3.81 mM. *Right*: Nonlinear curve fitting for the complexation between *R,R*-**CT2** and *S,S*-**5c** based on the NMR data.

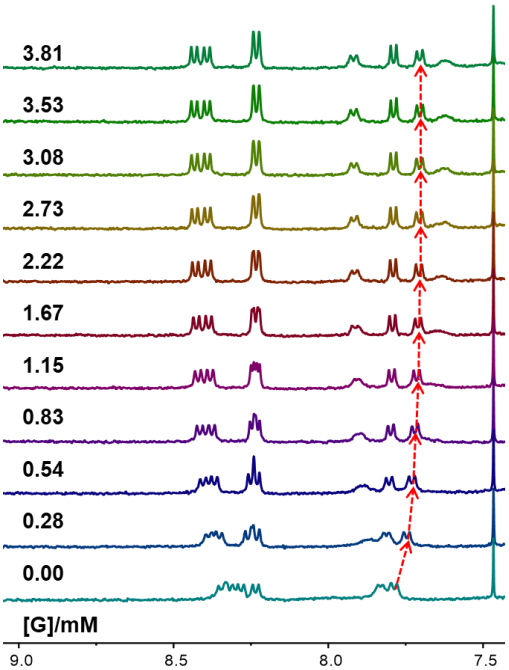

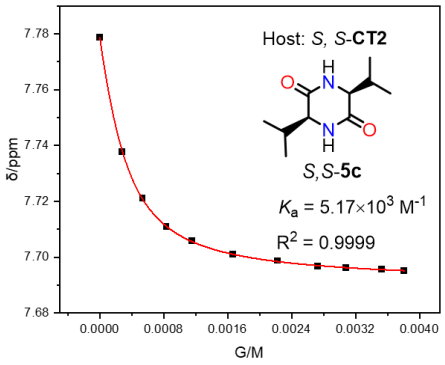

	K_a /M^{-1}	R^2
Titration-1	5.17×10^3	0.9999
Titration-2	5.95×10^3	0.9990
Titration-3	5.03×10^3	0.9994
Average	(5.4±0.4)×10^3	

Figure *S71*. *Left*: Partial ^{1}H NMR spectra (500 MHz, $CDCl_3$, 298 K) of *S,S*-**CT2** (0.5 mM) titrated by *S,S*-**5c**. From bottom to top, the concentration range of 1 is 0 ~ 3.81 mM. *Right*: Nonlinear curve fitting for the complexation between *S,S*-**CT2** and *S,S*-**5c** based on the NMR data.

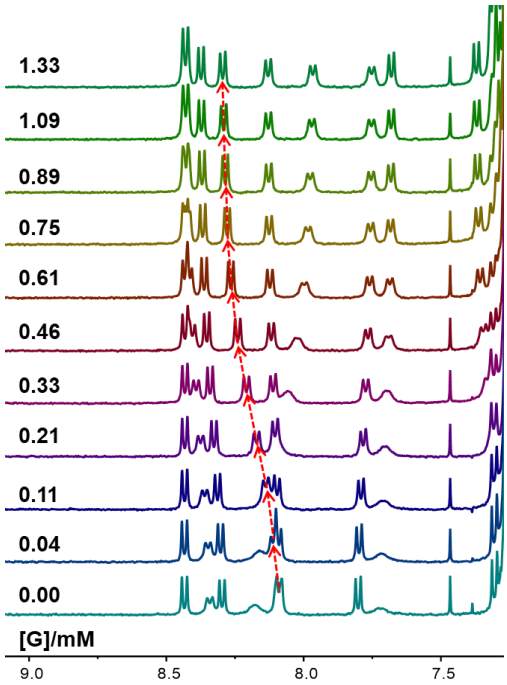

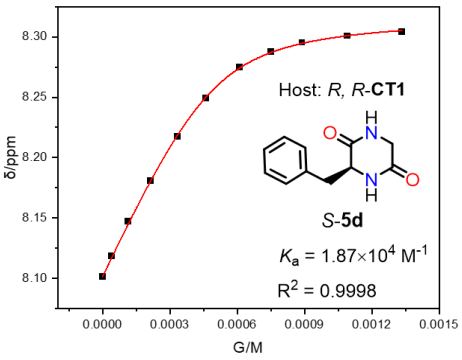

	K_a /M^{-1}	R^2
Titration-1	1.87×10^4	0.9998
Titration-2	1.42×10^4	0.9999
Titration-3	1.47×10^4	0.9999
Average	(1.6±0.2)×10^4	

Figure *S72*. *Left*: Partial ^{1}H NMR spectra (500 MHz, $CDCl_3$, 298 K) of *R,R*-**CT1** (0.5 mM) titrated by *S*-**5d**. From bottom to top, the concentration range of 1 is 0 ~ 1.33 mM. *Right*: Nonlinear curve fitting for the complexation between *R,R*-**CT1** and *S*-**5d** based on the NMR data.

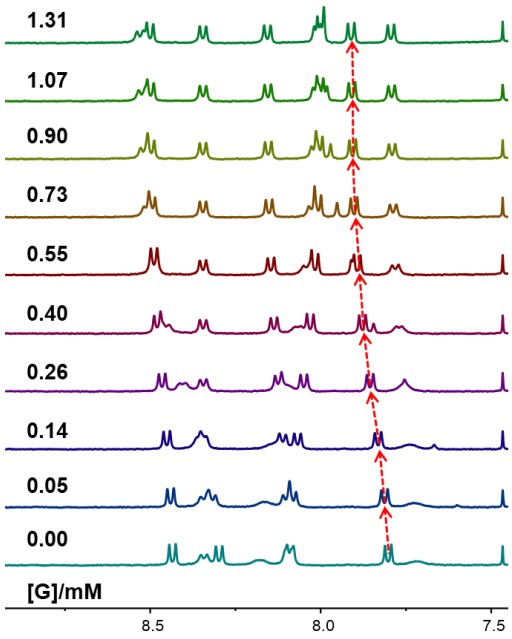

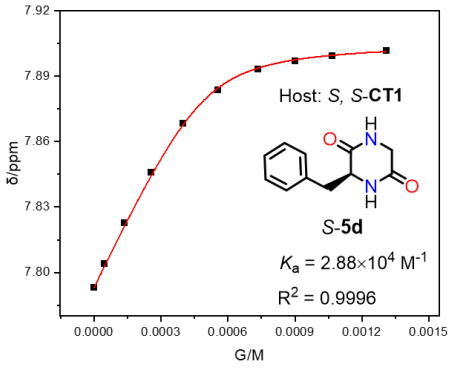

	K_a /M^{-1}	R^2
Titration-1	2.88×10^4	0.9996
Titration-2	3.15×10^4	0.9985
Titration-3	2.80×10^4	0.9990
Average	(2.9±0.1)×10^4	

Figure *S73*. *Left*: Partial ^{1}H NMR spectra (500 MHz, $CDCl_3$, 298 K) of *S,S*-**CT1** (0.5 mM) titrated by *S*-**5d**. From bottom to top, the concentration range of 1 is 0 ~ 1.31 mM. *Right*: Nonlinear curve fitting for the complexation between *S,S*-**CT1** and *S*-**5d** based on the NMR data.

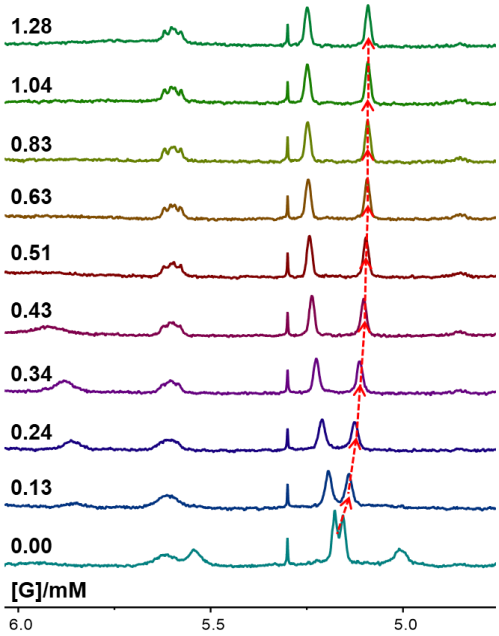

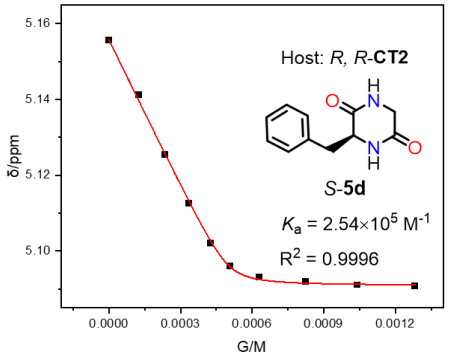

	K_a /M^{-1}	R^2
Titration-1	2.54×10^5	0.9993
Titration-2	2.47×10^5	0.9991
Titration-3	1.96×10^5	0.9995
Average	(2.3±0.3)×10^5	

Figure *S74*. *Left*: Partial ^{1}H NMR spectra (500 MHz, $CDCl_3$, 298 K) of *R,R*-**CT2** (0.5 mM) titrated by *S*-**5d**. From bottom to top, the concentration range of 1 is 0 ~ 1.28 mM. *Right*: Nonlinear curve fitting for the complexation between *R,R*-**CT2** and *S*-**5d** based on the NMR data.

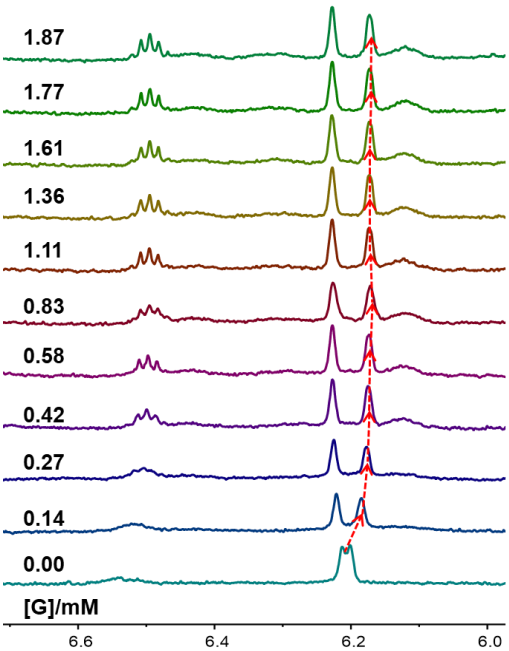

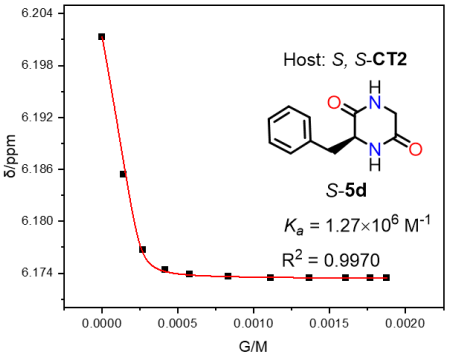

	K_a /M^{-1}	R^2
Titration-1	1.27×10^6	0.9970
Titration-2	1.54×10^6	0.9951
Titration-3	1.25×10^6	0.9961
Average	(1.4±0.1)×10^6	

Figure *S75*. *Left*: Partial ^{1}H NMR spectra (500 MHz, $CDCl_3$, 298 K) of *S,S*-**CT2** (0.5 mM) titrated by *S*-**5d**. From bottom to top, the concentration range of 1 is 0 ~ 1.87 mM. *Right*: Nonlinear curve fitting for the complexation between *S,S*-**CT2** and *S*-**5d** based on the NMR data.

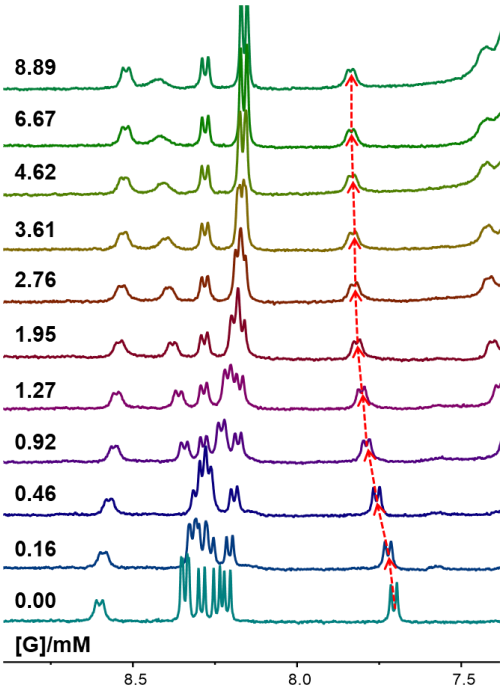

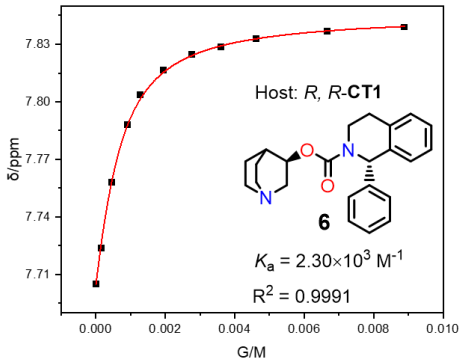

	K_a /M^{-1}	R^2
Titration-1	2.30×10^3	0.9991
Titration-2	2.29×10^3	0.9982
Titration-3	1.89×10^3	0.9987
Average	(2.2±0.2)×10^3	

Figure *S76*. *Left*: Partial ^{1}H NMR spectra (500 MHz, Toluene-d$_8$, 298 K) of *R,R*-**CT1** (0.5 mM) titrated by **6**. From bottom to top, the concentration range of 1 is 0 ~ 8.89 mM. *Right*: Nonlinear curve fitting for the complexation between *R,R*-**CT1** and **6** based on the NMR data.

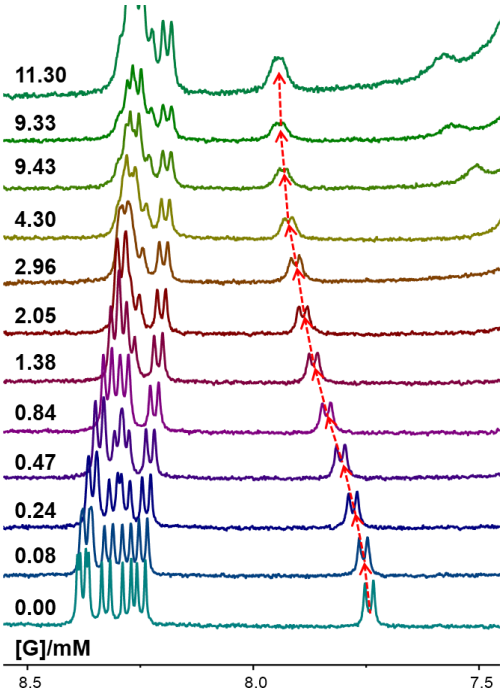

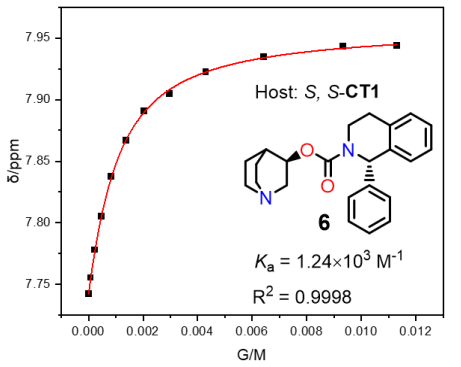

	K_a /M^{-1}	R^2
Titration-1	1.24×10^3	0.9998
Titration-2	1.01×10^3	0.9997
Titration-3	0.91×10^3	0.9994
Average	(1.1±0.1)×10^3	

Figure *S77*. *Left*: Partial ^{1}H NMR spectra (500 MHz, Toluene-d$_8$, 298 K) of *S,S*-**CT1** (0.5 mM) titrated by **6**. From bottom to top, the concentration range of 1 is 0 ~ 11.30 mM. *Right*: Nonlinear curve fitting for the complexation between *S,S*-**CT1** and **6** based on the NMR data.

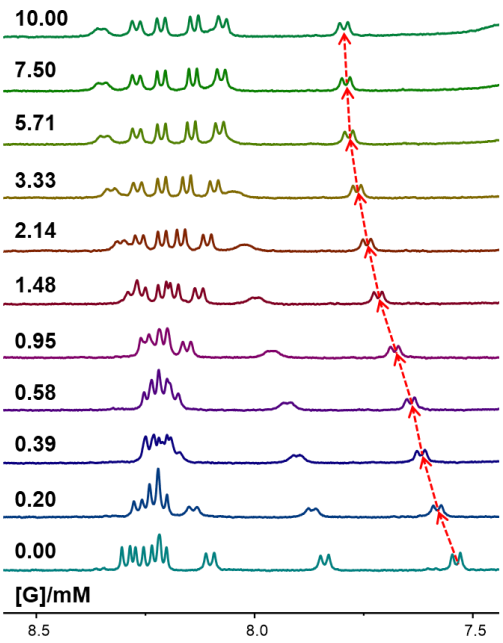

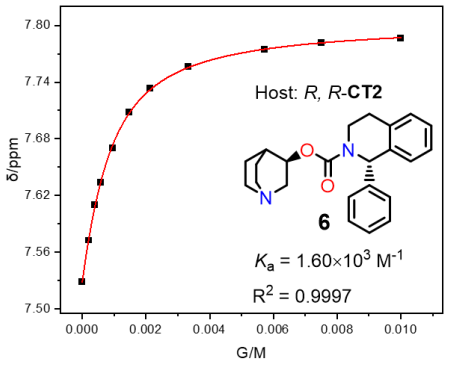

	K_a /M^{-1}	R^2
Titration-1	1.60×10^3	0.9997
Titration-2	1.91×10^3	0.9975
Titration-3	1.69×10^3	0.9990
Average	(1.7±0.1)×10^3	

Figure *S78*. *Left*: Partial ^{1}H NMR spectra (500 MHz, Toluene-d$_8$, 298 K) of *R,R*-**CT2** (0.5 mM) titrated by **6**. From bottom to top, the concentration range of 1 is 0 ~ 10.00 mM. *Right*: Nonlinear curve fitting for the complexation between *R,R*-**CT2** and **6** based on the NMR data.

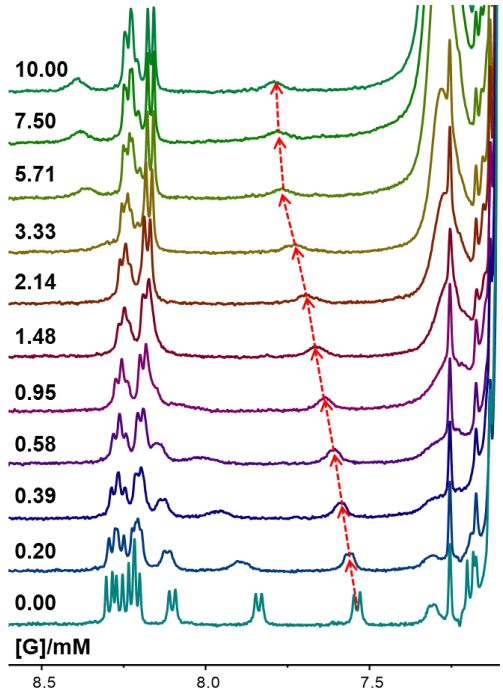

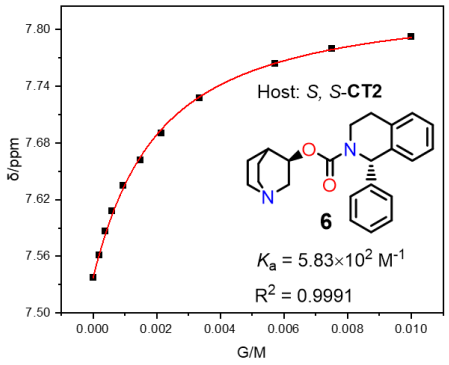

	K_a /M^{-1}	R^2
Titration-1	5.83×10^2	0.9991
Titration-2	4.50×10^2	0.9980
Titration-3	5.88×10^2	0.9987
Average	(5.4±0.6)×10^2	

Figure *S79*. *Left*: Partial ^{1}H NMR spectra (500 MHz, Toluene-d$_8$, 298 K) of *S,S*-**CT2** (0.5 mM) titrated by **6**. From bottom to top, the concentration range of 1 is 0 ~ 10.00 mM. *Right*: Nonlinear curve fitting for the complexation between *S,S*-**CT2** and **6** based on the NMR data.

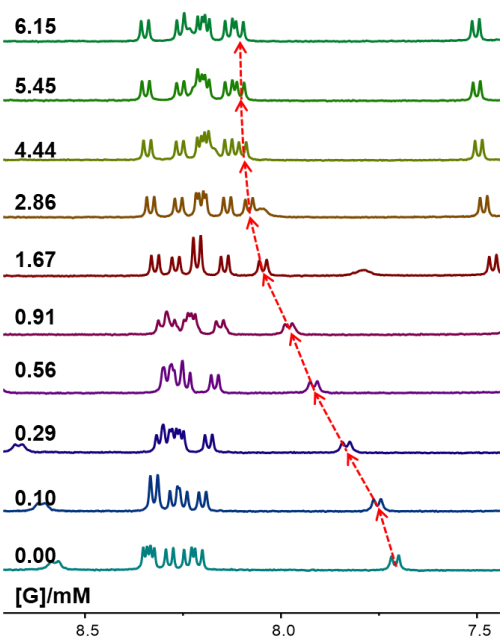

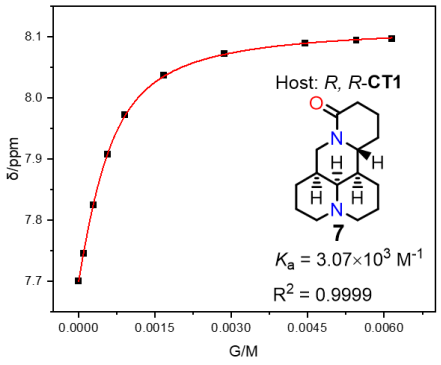

	K_a /M^{-1}	R^2
Titration-1	3.07×10^3	0.9999
Titration-2	3.03×10^3	0.9996
Titration-3	3.12×10^3	0.9999
Average	(3.1±0.1)×10^3	

Figure *S80*. *Left*: Partial ^{1}H NMR spectra (500 MHz, Toluene-d$_8$, 298 K) of *R,R*-**CT1** (0.5 mM) titrated by **7**. From bottom to top, the concentration range of 1 is 0 ~ 6.15 mM. *Right*: Nonlinear curve fitting for the complexation between *R,R*-**CT1** and **7** based on the NMR data.

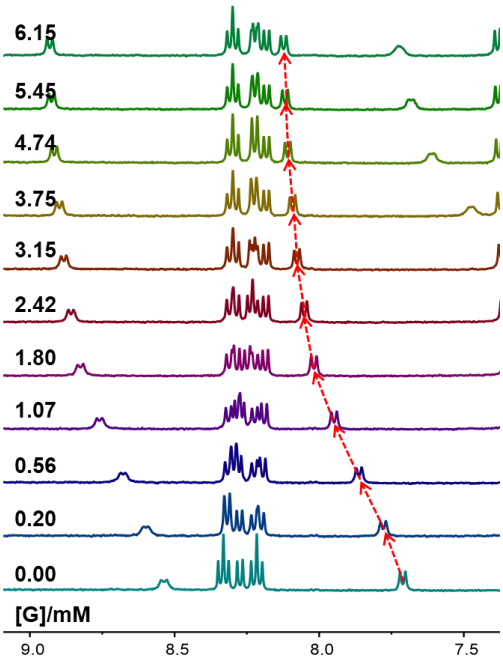

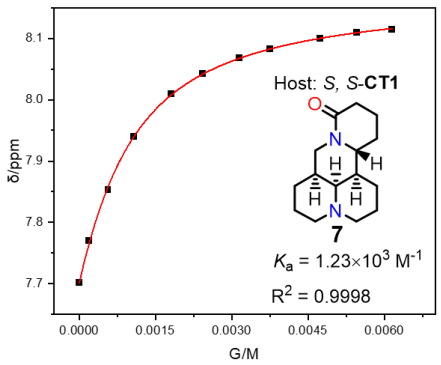

	K_a /M^{-1}	R^2
Titration-1	1.23×10^3	0.9998
Titration-2	1.13×10^3	0.9999
Titration-3	1.10×10^3	0.9999
Average	(1.2±0.1)×10^3	

Figure *S81*. *Left*: Partial ^{1}H NMR spectra (500 MHz, Toluene-d$_8$, 298 K) of *S,S*-**CT1** (0.5 mM) titrated by **7**. From bottom to top, the concentration range of 1 is 0 ~ 6.15 mM. *Right*: Nonlinear curve fitting for the complexation between *S,S*-**CT1** and **7** based on the NMR data.

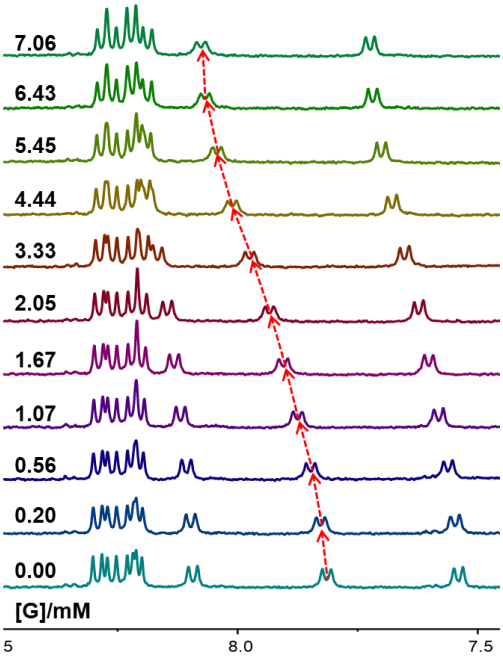

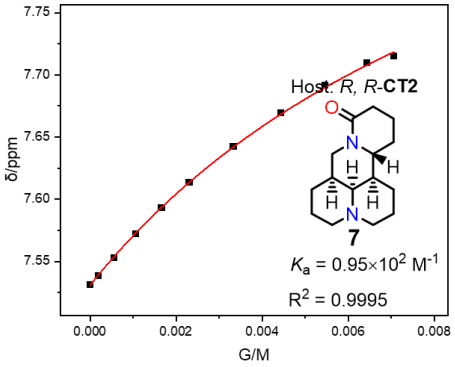

	K_a /M^{-1}	R^2
Titration-1	0.95×10^2	0.9995
Titration-2	0.88×10^2	0.9997
Titration-3	0.90×10^2	0.9995
Average	91±3	

Figure *S82*. *Left*: Partial ^{1}H NMR spectra (500 MHz, Toluene-d$_8$, 298 K) of *R,R*-**CT2** (0.5 mM) titrated by **7**. From bottom to top, the concentration range of 1 is 0 ~ 7.06 mM. *Right*: Nonlinear curve fitting for the complexation between *R,R*-**CT2** and **7** based on the NMR data.

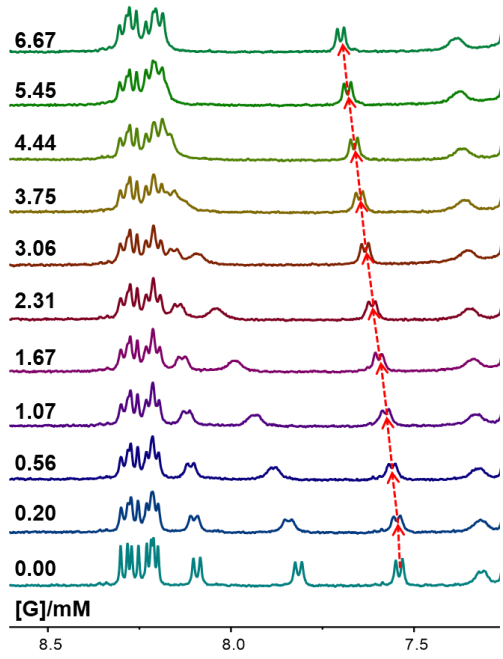

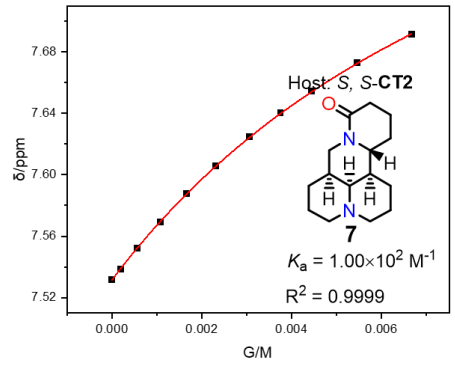

	K_a /M^{-1}	R^2
Titration-1	1.00×10^2	0.9999
Titration-2	0.91×10^2	0.9998
Titration-3	1.05×10^2	0.9995
Average	99±6	

Figure *S83*. *Left*: Partial ^{1}H NMR spectra (500 MHz, Toluene-d$_8$, 298 K) of *S,S*-**CT2** (0.5 mM) titrated by **7**. From bottom to top, the concentration range of 1 is 0 ~ 6.67 mM. *Right*: Nonlinear curve fitting for the complexation between *S,S*-**CT2** and **7** based on the NMR data.

9. X-Ray Single Crystallography

- Suitable single crystals of *R,R*-**CT2** and *S,S*-**CT2** were successfully obtained by slow evaporation of their saturated solutions in CH_2Cl_2 and acetone mixed solution.
- Suitable single crystals of *R*-**5a**@*S,S*-**CT2** and *S*-**5a**@*S,S*-**CT2** were successfully obtained by slow evaporation of their saturated solutions of CH_2Cl_2 and toluene.
- Suitable single crystals of *R,R*-**5b**@*S,S*-**CT2** were successfully obtained by slow evaporation of its saturated solution of CH_2Cl_2 and toluene.
- Suitable single crystals of *S,S*-**5c**@*S,S*-**CT2** were obtained by slow evaporation of their saturated solutions in CH_2Cl_2 and toluene mixed solution. Single crystal of 2**Toluene**@*S,S*-**CT2** was obtained by slow evaporation of *R,R*-**5c** and *S,S*-**CT2** saturated solutions in CH_2Cl_2 and toluene mixed solution.

Single crystal X-ray data were collected on a Bruker D8 VENTURE with Cu Kα radiation (λ = 1.54178 Å) at 100 K. The structures were solved by intrinsic phasing methods (SHELXT) and refined by full-matrix least-squares F^2 using SHELXL[5] in the OLEX2 program package.[6] All non-hydrogen atoms were refined with anisotropic thermal parameters and the hydrogen atoms were fixed at calculated positions and refined by a riding mode. SQUEEZE routine implemented on PLATON[7] was used to remove electron densities corresponding to disordered solvent molecules in the crystal data.

Table *S1*: Crystal data and structure refinement for *R,R*-**CT2**•2Acetone, *S,S*-**CT2**•2Acetone, *R*-**5a**@*S,S*-**CT2**, *S*-**5a**@*S,S*-**CT2**, *S,S*-**5c**@*S,S*-**CT2**, 2**Toluene**@*R,R*-**CT2**, *S,S*-**5b**@*R,R*-**CT2** complex

entry	*R,R*-**CT2**•2Acetone	*S,S*-**CT2**•2Acetone	*R*-**5a**@*S,S*-**CT2**	*S*-**5a**@*S,S*-**CT2**	*S,S*-**5c**@*S,S*-**CT2**	2**Toluene**@*R,R*-**CT2**	*S,S*-**5b**@*R,R*-**CT2**
Moiety formula	$C_{70}H_{76}N_4O_8S_2$, 2(C_3H_6O)	$C_{70}H_{76}N_4O_8S_2$, 2(C_3H_6O)	$C_{70}H_{76}N_4O_8S_2$, $C_7H_{12}N_2O_2$	$C_{70}H_{76}N_4O_8S_2$, C_7 H_{12} N_2 O_2	$C_{70}H_{76}N_4O_8S_2$, $C_{10}H_{18}N_2O_2$	$C_{70}H_{76}N_4O_8S_2$, 2(C_7H_8)	$C_{70}H_{76}N_4O_8S_2$, $C_6H_{10}N_2O_2$
Empirical formula	$C_{76}H_{88}N_4O_{10}S_2$	$C_{76}H_{88}N_4O_{10}S_2$	$C_{77}H_{88}N_6O_{10}S_2$	$C_{77}H_{88}N_6O_{10}S_2$	$C_{80}H_{94}N_6O_{10}S_2$	$C_{84}H_{92}N_4O_8S_2$	$C_{76}H_{86}N_6O_{10}S_2$
Formula weight	1281.62	1281.62	1321.65	1321.65	1363.73	1349.73	1307.62
Temperature/K	100.00	100.0	100.00	100.00	100.00	100.00	100.00
Crystal system	monoclinic	monoclinic	monoclinic	monoclinic	monoclinic	monoclinic	monoclinic
Space group	*P* 2_1	*P* 2_1 m	*P* 2_1	*P* 2_1	*C* 2	*P* 2_1	*P* 2_1
a/Å	11.0602(7)	11.0817(2)	10.9618(3)	10.9865(7)	23.956(3)	11.2491(4)	10.9839(5)
b/Å	17.0046(10)	16.9944(3)	17.1073(5)	17.1302(10)	19.291(2)	17.1295(6)	17.0968(7)
c/Å	18.2098(11)	18.2004(4)	18.2899(5)	18.2901(11)	21.304(2)	18.1480(6)	18.3330(7)
α/°	90	90	90	90	90	90	90
β/°	96.018(2)	96.0600(10)	97.5270(10)	97.639(2)	101.666(5)	96.0400(10)	96.456(2)
γ/°	90	90	90	90	90	90	90
Volume/Å^3	3405.9(4)	3408.47(11)	3400.29(17)	3411.7(4)	9641.6(19)	3477.6(2)	3420.9(2)
Z	2	2	2	2	4	2	2
ρ_{calc}g/cm^3	1.250	1.249	1.291	1.287	0.939	1.289	1.269
μ/mm^{-1}	1.207	1.207	0.802	0.799	0.573	0.772	0.791
F(000)	1368	1368	1408.0	1408	2912.0	1440.0	1392
Reflections collected	34293	44107	94883	89085	94043	126724	58696
Independent reflections	9728[R_{int}=0.0240, R_{sigma}=0.0265]	9900[R_{int}=0.0294, R_{sigma}=0.0244]	16806[R_{int} =0.0593, R_{sigma}= 0.0471]	16304[R_{int}=0.0479, R_{sigma} = 0.0420]	19634[R_{int}=0.0483,R_{sigma}= 0.0417]	20967[R_{int}=0.0564,R_{sigma}= 0.0415]	13776[R_{int}=0.0545,R_{sigma}=0.0530]
Data/restraints/parameters	9728/14/862	9900/1/851	16806/1966/895	16304/172/865	19634/234/881	20967/1/896	13776/866/64
Goodness-of-fit on F^2	1.051	1.028	1.088	1.061	1.265	1.099	1.084
Final R indexes [I>=2σ(I)]	R_1 =0.0295 wR_2 = 0.0746	R_1 = 0.0293 wR_2 = 0.0754	R_1 = 0.0493, wR_2 = 0.1309	R_1 = 0.0488, wR_2 = 0.1387	R_1 = 0.0988, wR_2 = 0.2693	R_1 = 0.0497, wR_2 = 0.1309	R_1 = 0.0793, wR_2 = 0.2344
Final R indexes [all data]	R_1 =0.0300 wR_2 = 0.0749	R_1 = 0.0312, wR_2 = 0.0768	R_1 = 0.0543, wR_2 = 0.1340	R_1 =0.0508, wR_2 = 0.1442	R_1 = 0.1081, wR_2 = 0.2857	R_1 = 0.0513, wR_2 = 0.1319	R_1 = 0.0875, wR_2 = 0.2420
CCDC number	2247175	2247230	2247191	2247223	2247283	2247282	2247244

R,R-**CT2**•2Acetone

Alert level B:

THETM01_ALERT_3_B The value of sine(theta_max)/wavelength is less than 0.575. Calculated sin(theta_max)/wavelength = 0.5580.

Response: The crystal has too weak diffraction to obtain high resolution data.

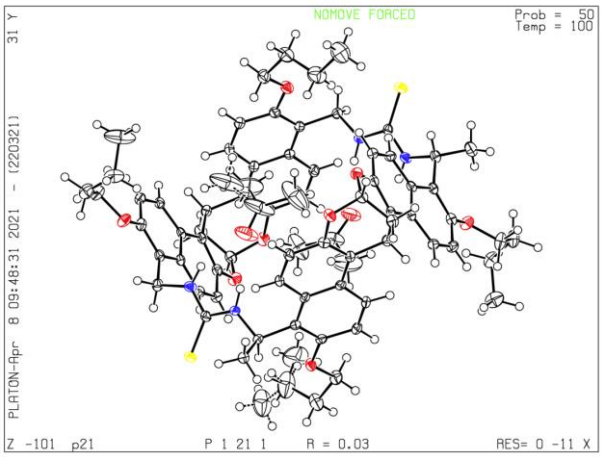

Crystal structure of *R,R*-**CT2**•2Acetone.

S,S-**CT2**•2Acetone

Alert level B:

THETM01_ALERT_3_B The value of sine(theta_max)/wavelength is less than 0.575. Calculated sin(theta_max)/wavelength = 0.5595.

Response: The crystal has too weak diffraction to obtain high resolution data.

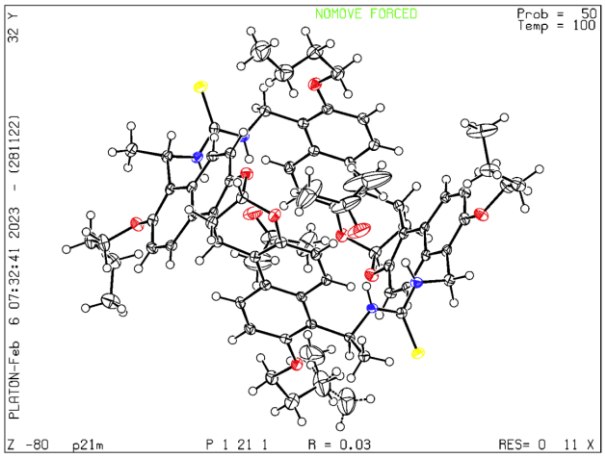

Crystal structure of *S,S*-**CT2**•2Acetone.

R-**5a**@*S,S*-**CT2**

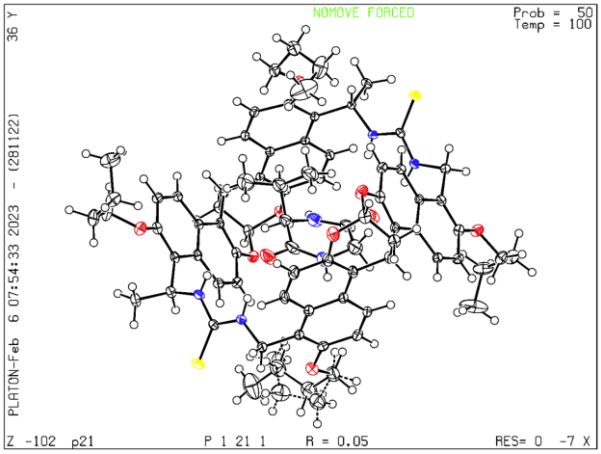

Crystal structure of *R*-**5a**@*S,S*-**CT2**.

S-**5a**@*S,S*-**CT2**

Alert level B:

PLAT220_ALERT_2_B NonSolvent Resd 1 C Ueq(max)/Ueq(min) Range 10.0 Ratio.
PLAT242_ALERT_2_B Low 'MainMol' Ueq as Compared to Neighbors of C1 Check.
PLAT934_ALERT_3_B Number of (Iobs-Icalc)/Sigma(W) > 10 Outliers .. 8 Check.
Response: The crystal has too weak diffraction to obtain high resolution data.

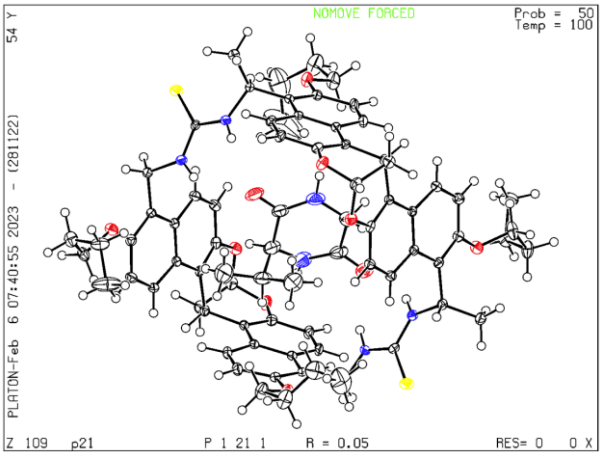

Crystal structure of *S*-**5a**@*S,S*-**CT2**.

S,S-**5b**@*R,R*-**CT2**

Alert level B:

PLAT097_ALERT_2_B Large Reported Max. (Positive) Residual Density 1.69 eA-3
PLAT220_ALERT_2_B NonSolvent Resd 1 C Ueq(max)/Ueq(min) Range 7.5 Ratio
Response: The crystal has too weak diffraction to obtain high resolution data.

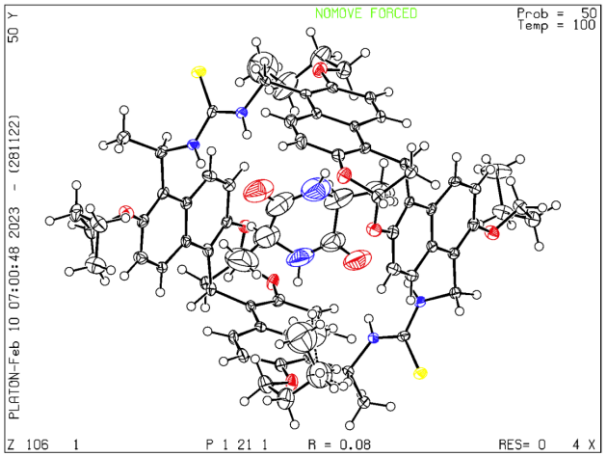

Crystal structure of *S,S*-**5b**@*R,R*-**CT2**.

S,S-**5c** @*S,S*-**CT2**

Alert level B:

PLAT213_ALERT_2_B Atom C014 has ADP max/min Ratio ..... 4.7 prolat
PLAT213_ALERT_2_B Atom C01C has ADP max/min Ratio ..... 4.2 prolat
PLAT220_ALERT_2_B NonSolvent Resd 1 C Ueq(max)/Ueq(min) Range 7.7 Ratio
PLAT230_ALERT_2_B Hirshfeld Test Diff for O00B --C031 . 14.0 s.u.
PLAT230_ALERT_2_B Hirshfeld Test Diff for C00T --C01Q . 12.0 s.u.
PLAT230_ALERT_2_B Hirshfeld Test Diff for C017 --C01I . 11.2 s.u.
PLAT230_ALERT_2_B Hirshfeld Test Diff for C02G --C033 . 11.0 s.u.
PLAT340_ALERT_3_B Low Bond Precision on C-C Bonds ..... 0.01054 Ang.
PLAT934_ALERT_3_B Number of (Iobs-Icalc)/Sigma(W) > 10 Outliers .. 2 Check
Response: The crystal has too weak diffraction to obtain high resolution data.

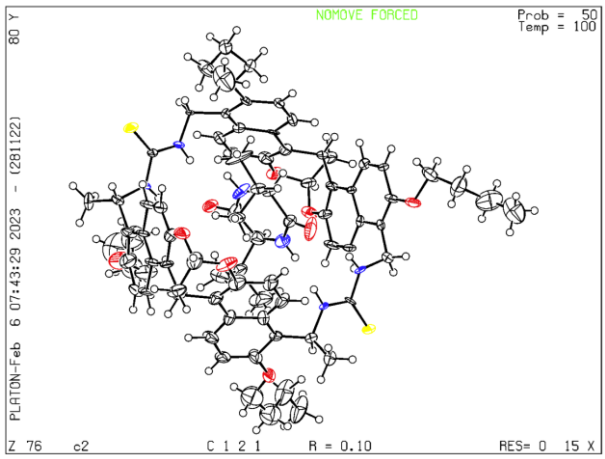

Crystal structure of *S,S*-**5c** @*S,S*-**CT2**.

2**Toluene**@*R*,*R*-**CT2**

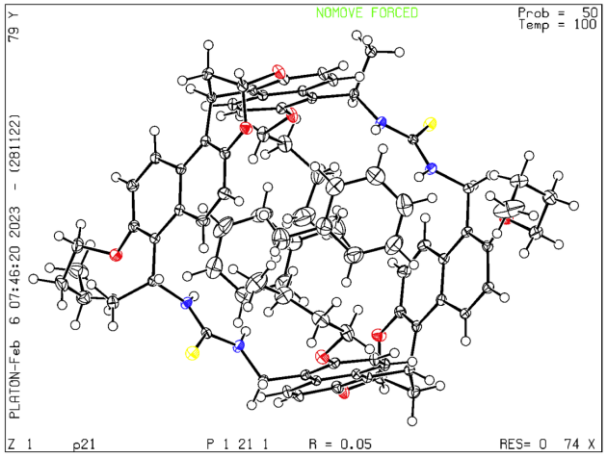

Crystal structure of 2**Toluene**@*R*,*R*-**CT2**

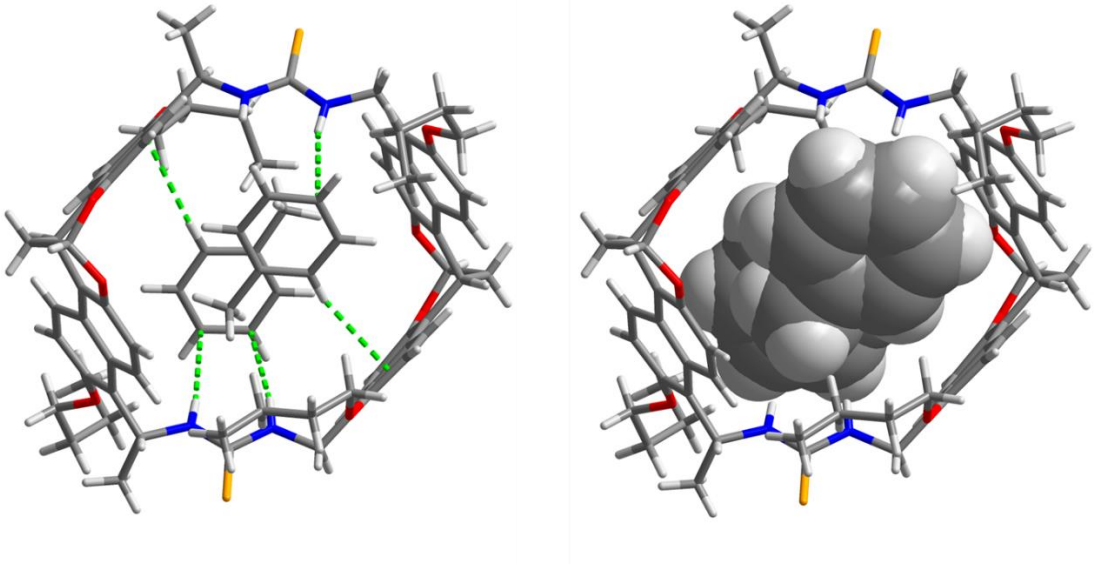

Figure *S84*. Crystal structure of 2**Toluene**@*R*,*R*-**CT2**, noncovalent interaction including hydrogen bonding, NH-π and ArH-π are marked with green dash lines.

10. Variable Temperature ^{1}H NMR Experiments

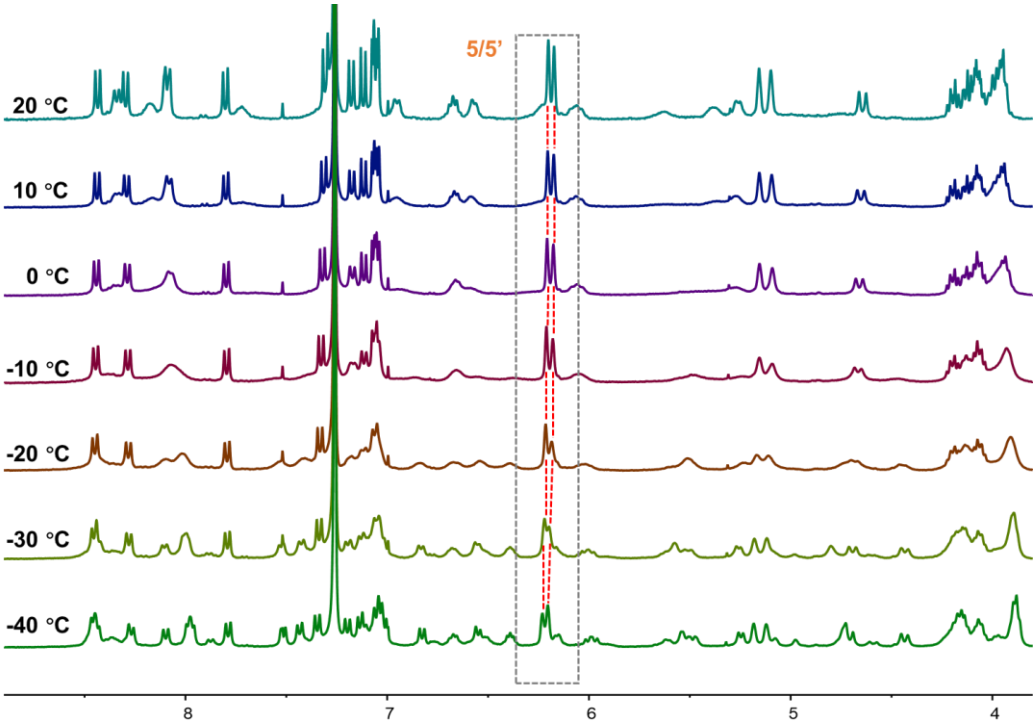

Figure *S85*. Variable-temperature ^{1}H NMR spectra of *S,S*-**CT1**, the temperature decreased from 20 °C to -40 °C (500 MHz, $CDCl_3$, 0.5 mM, 298 K).

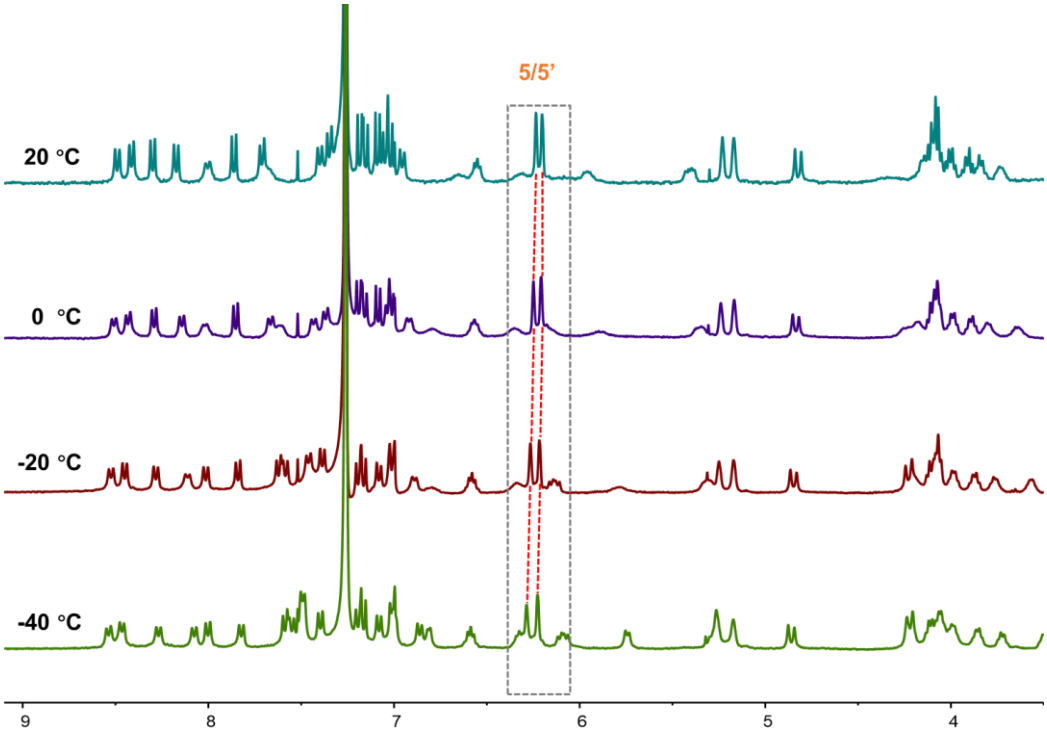

Figure *S86*. Variable-temperature ^{1}H NMR spectra of *R*-**5a**@*S,S*-**CT1**, the temperature decreased from 20 °C to -40 °C (500 MHz, $CDCl_3$, 0.5 mM, 298 K).

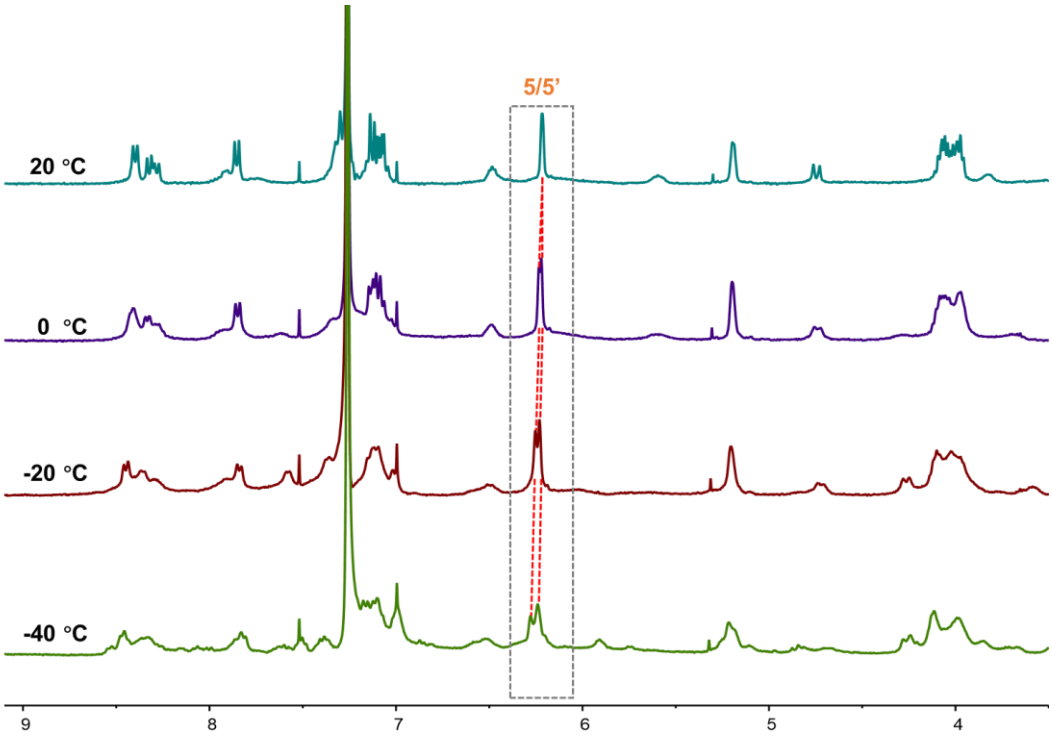

Figure *S87*. Variable-temperature ^{1}H NMR spectra of *S*-**5a**@*S,S*-**CT1**, the temperature decreased from 20 °C to -40 °C (500 MHz, $CDCl_3$, 0.5 mM, 298 K).

11. CD Spectra of Chiral Hosts Interact with Guests

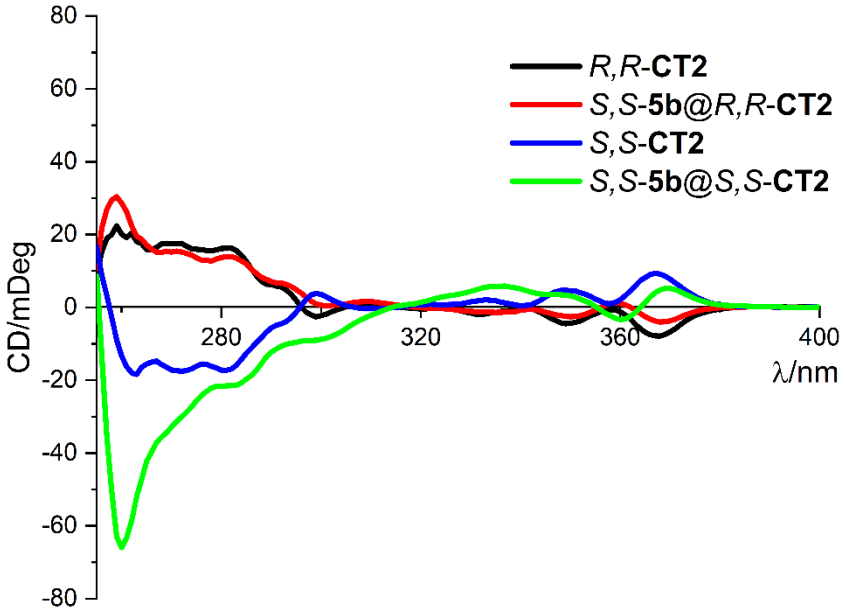

Figure *S88*. CD spectra of **CT2** with *S,S*-**5b** under saturated binding (25 μM in dichloroethane, 25 °C).

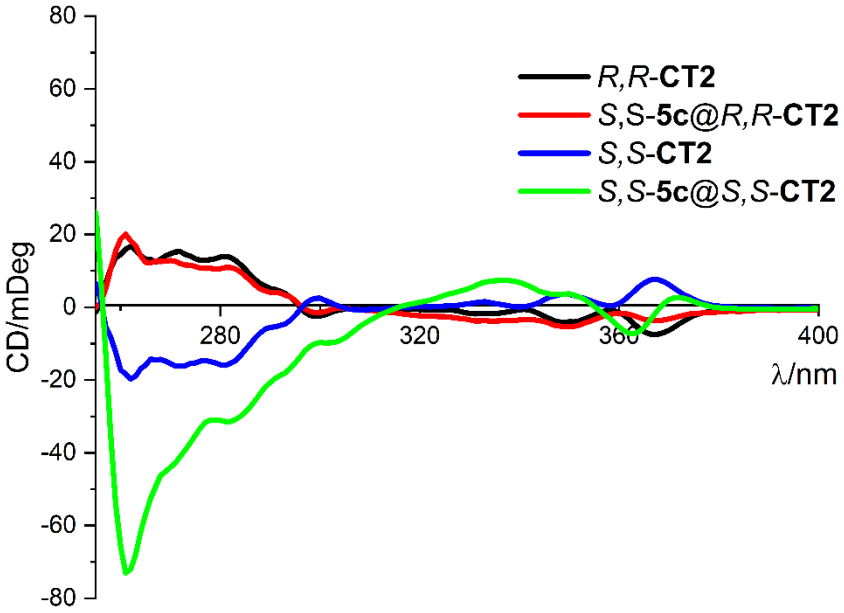

Figure *S89*. CD spectra of **CT2** with *S,S*-**5c** (25 μM in dichloroethane, 25 °C) under saturated binding.

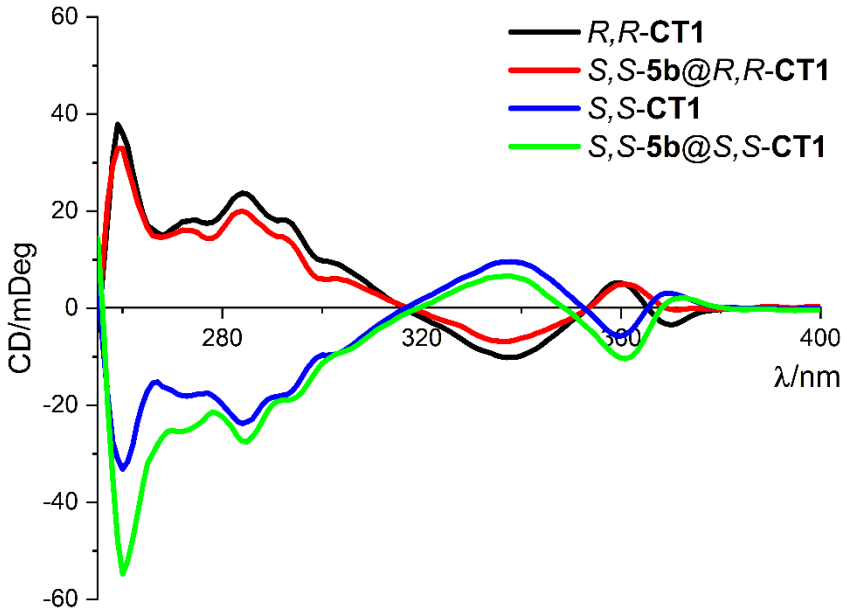

Figure *S90*. CD spectra of **CT1** with *S,S*-**5b** under saturated binding (25 μM in dichloroethane, 25 °C).

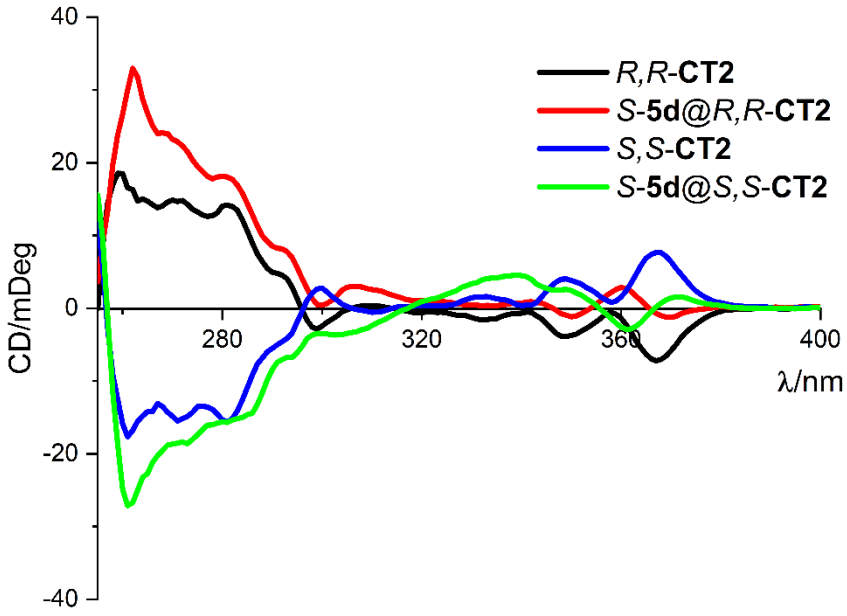

Figure *S91*. CD spectra of **CT2** with *S*-**5d** under saturated binding (25 μM in dichloroethane, 25 °C).

12. Computational Data

Geometry optimizations were performed with Gaussian 16 software package,[8] using the M06-2x/def2-svp[9] method, by considering the solvent effects (PCM, $CHCl_3$)[3] without applying any geometry constraints (C1 symmetry). Frequency calculations were then conducted at the same computational level to confirm the nature of all located stationary points and to obtain the thermal correction to Gibbs free energy and enthalpy. Single point energy in $CHCl_3$ was calculated with Gaussian 16 software package using the M062x/ma-def2-tzvpp method[9]. The total Gibbs free energy of the complex is the addition of single point energy and the thermal correction to Gibbs free energy (ZPE+$\Delta G_{0\rightarrow T}$). IGM analysis[10] was carried out with Multiwfn 3.8 (dev) program[11] and visualized by the VMD 1.9.3 program.[12] (set isovalue = 0.008)

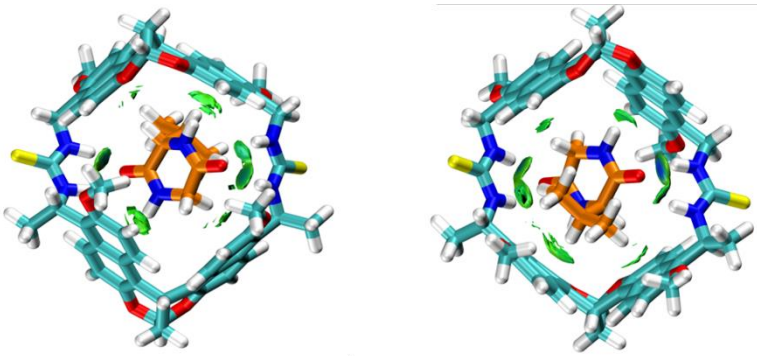

S-**5a**@*S,S*-**CT2**
0 kJ/mol

R-**5a**@*S,S*-**CT2**
-1.73 kJ/mol

Figure *S92*. IGM analysis. Energy minimized structures obtained by DFT (M06-2x/def2-svp) calculations with the PCM solution model in chloroform at 298 K. The single crystal structure of *S*-**5a**@*S,S*-**CT2** and *R*-**5a**@*S,S*-**CT2** were used as an initial guess for SCF. The relative Gibbs free energy (ZPE+$\Delta G_{0\rightarrow T}$) is shown (M06-2x/ma-def2-tzvpp). *R*-**5a**@*S,S*-**CT2** is more stable than *S*-**5a**@*S,S*-**CT2** by -1.73 kJ/mol, which qualitatively agrees with the results of ^{1}H NMR titration.

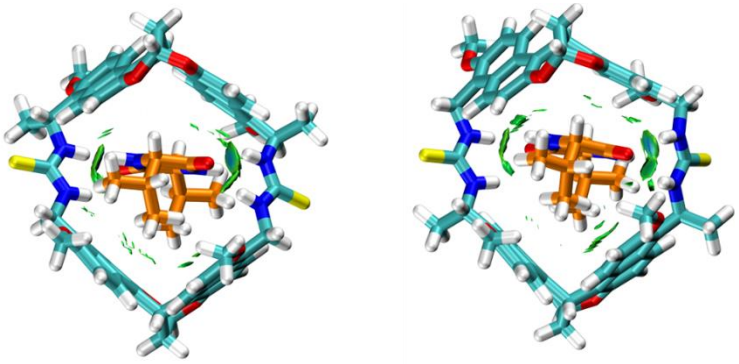

S,S-**5c**@*R,R*-**CT2**
0 kJ/mol

S,S-**5c**@*S,S*-**CT2**
-5.87 kJ/mol

Figure *S93*. IGM analysis. Energy minimized structures obtained by DFT (M06-2x/def2-svp) calculations with the PCM solution model in chloroform at 298 K. The relative Gibbs free energy (ZPE+$\Delta G_{0\rightarrow T}$) is shown (M06-2x/ma-def2-tzvpp). *S,S*-**5c**@*S,S*-**CT2** is more stable than *S,S*-**5c**@*R,R*-**CT2** by -5.87 kJ/mol, which qualitatively agrees with the results of ^{1}H NMR titration.

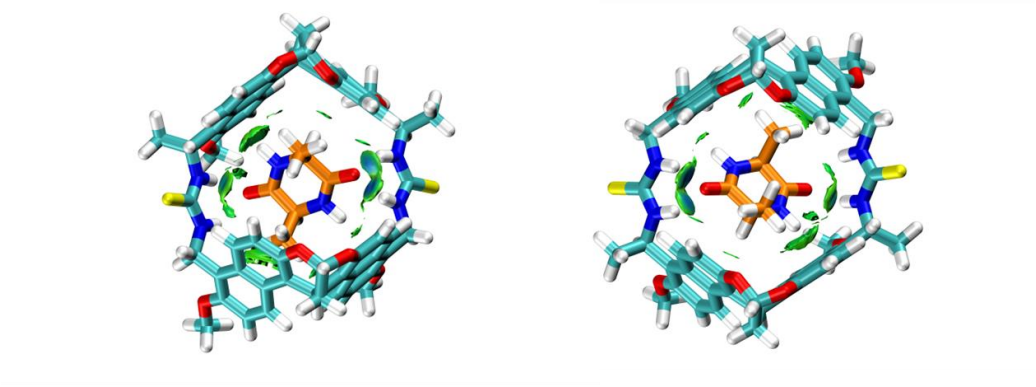

S,S-**5b**@*R,R*-**CT2**
0 kJ/mol

S,S-**5b**@*S,S*-**CT2**
-1.69 kJ/mol

Figure *S94*. IGM analysis. Energy minimized structures obtained by DFT (M06-2x/def2-svp) calculations with the PCM solution model in chloroform at 298 K. The relative Gibbs free energy (ZPE+$\Delta G_{0\rightarrow T}$) is shown (M06-2x/ma-def2-tzvpp). *S,S*-**5b**@*S,S*-**CT2** is more stable than *S,S*-**5b**@*R,R*-**CT2** by -1.69 kJ/mol, which qualitatively agrees with the results of ^{1}H NMR titration.

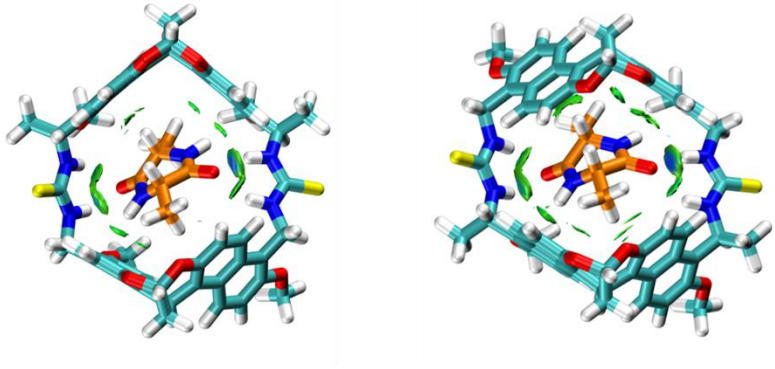

S,S-**5b**@*R,R*-**CT1**
0 kJ/mol

S,S-**5b**@*S,S*-**CT1**
-10.50 kJ/mol

Figure *S95*. IGM analysis. Energy minimized structures obtained by DFT (M06-2x/def2-svp) calculations with the PCM solution model in chloroform at 298 K. The relative Gibbs free energy (ZPE+$\Delta G_{0\rightarrow T}$) is shown (M06-2x/ma-def2-tzvpp). *S,S*-**5b**@*S,S*-**CT1** is more stable than *S,S*-**5b**@*R,R*-**CT1** by -10.50 kJ/mol, which qualitatively agrees with the results of ^{1}H NMR titration.

Table *S2*: Thermodynamic parameters of all calculated structures (298 K) Gibbs free energy (ZPE + $G_{0\rightarrow T}$) and enthalpy (ZPE + $H_{0\rightarrow T}$) are obtained after thermal correction.

	ΔG	***ΔH***	***-TΔS***
R-**5a**@*S,S*-**CT2** S-**5a**@*S,S*-**CT2**	**-1.81**	**-3.13**	**1.32**
S,S-**5b**@*S,S*-**CT1** *S,S*-**5b**@*R,R*-**CT1**	**-10.58**	**-12.00**	**1.42**
S,S-**5b**@*S,S*-**CT2** *S,S*-**5b**@*R,R*-**CT2**	**-1.69**	**-0.65**	**-1.04**
S,S-**5c**@*S,S*-**CT2** *S,S*-**5c**@*R,R*-**CT2**	**-5.86**	**-8.12**	**2.26**

References

[1] G. Huang, Z. He, C. X. Cai, F. Pan, D. Yang, K. Rissanen, W. Jiang, *Chem. Commun.* **2015**, *51*, 15490-15493.

[2] a) Hariharan, P. C.; Pople, J. A. Accuracy of AH Nequilibrium Geometries by Single Determinant Molecular Orbital Theory. *Molecular Physics* **1974**, *27*, 209-214. b) Petersson, G. A.; Bennett, A.; Tensfeldt, T. G.; Laham, Al, M. A.; Shirley, W. A.; Mantzaris, J. A Complete Basis Set Model Chemistry. I. the Total Energies of Closed-Shell Atoms and Hydrides of the First-Row Elements. *J. Chem. Phys.* **1988**, *89*, 2193-2218. c) Grimme, S.; Antony, J.; Ehrlich, S.; Krieg, H. A Consistent and Accurate Ab Initio Parametrization of Density Functional Dispersion Correction (DFT-D) for the 94 Elements H-Pu. *J. Chem. Phys.* **2010**, *132*, 154104. d) Grimme, S.; Ehrlich, S.; Goerigk, L. Effect of the Damping Function in Dispersion Corrected Density Functional Theory. *J. Comput. Chem.* **2011**, *32*, 1456-1465.

[3] a) E. Cances, B. Mennucci, J. Tomasi, *J. Chem. Phys.* **1997**, *107*, 3032. b) B. Mennucci, J. Tomasi, *J. Chem. Phys.* **1997**, *106*, 5151.

[4] D.-S. Guo, V. D. Uzunova, X. Su, Y. Liu and W. M. Nau, *Chem. Sci.* **2011**, *2*, 1722-1734.

[5] G. M. Sheldrick, *Acta Cryst.* **2015**, *C71*, 3-8.

[6] O. V. Dolomanov, L. J. Bourhis, R. J. Gildea, J. A. K. Howard, H. Puschmann, *J. Appl. Cryst.* **2009**, *42*, 339-341.

[7] A. L. Spek, *Acta Crystallorgr.* **2015**, *C71*, 9-18.

[8] Gaussian 16, Revision A.03, M. J. Frisch, G. W. Trucks, H. B. Schlegel, G. E. Scuseria, M. A. Robb, J. R. Cheeseman, G. Scalmani, V. Barone, G. A. Petersson, H. Nakatsuji, X. Li, M. Caricato, A. V. *Marenich*, J. Bloino, B. G. Janesko, R. Gomperts, B. Mennucci, H. P. Hratchian, J. V. Ortiz, A. F. Izmaylov, J. L. Sonnenberg, D. Williams-Young, F. Ding, F. Lipparini, F. Egidi, J. Goings, B. Peng, A. Petrone, T. Henderson, D. Ranasinghe, V. G. Zakrzewski, J. Gao, N. Rega, G. Zheng, W. Liang, M. Hada, M. Ehara, K. Toyota, R. Fukuda, J. Hasegawa, M. Ishida, T. Nakajima, Y. Honda, O. Kitao, H. Nakai, T. Vreven, K. Throssell, J. A. Montgomery, Jr., J. E. Peralta, F. Ogliaro, M. J. Bearpark, J. J. Heyd, E. N. Brothers, K. N. Kudin, V. N. Staroverov, T. A. Keith, R. Kobayashi, J. Normand, K. Raghavachari, A. P. Rendell, J. C. Burant, S. S. Iyengar, J. Tomasi, M. Cossi, J. M. Millam, M. Klene, C. Adamo, R. Cammi, J. W. Ochterski, R. L. Martin, K. Morokuma, O. Farkas, J. B. Foresman, and D. J. Fox, Gaussian, Inc., Wallingford CT, **2016**.

[9] a) Zhao and Truhlar, *Theor. Chem. Account* **2008**, *120*, 215-241. b) F. Weigend, R. Ahlrichs, *Phys. Chem. Chem. Phys.* **2005**, *7*, 3297.

[10] C. Lefebvre, G. Rubez, H. Khartabil, J.-C. Boisson, J. Contreras-García, E. Hénon, *Phys. Chem. Chem. Phys.* **2017**, *19*, 17928.
[11] a) T. Lu, F. Chen, *J. Comput. Chem.* **2012**, *33,* 580−592. b) J. Zhang, T. Lu, *Phys. Chem. Chem. Phys.* **2021**, *23*, 20323-20328.
[12] W. Humphrey, A. Dalke, K. Schulten, *J. Mol. Graph. Model.* **1996**, *14,* 33-38.